Quantum Noise Reduction in Semiconductor Lasers Using Dispersive Optical Feedback

Thesis by
John E. Kitching

In Partial Fulfillment of the Requirements
for the Degree of
Doctor of Philosophy

California Institute of Technology
Pasadena, California

1995

(Defended May 16, 1995)

Acknowledgments

I would like to express my deep gratitude to my advisor, Professor Amnon Yariv, for his support during these last five years. The environment he creates in his group is, in my experience, unsurpassed in generating ideas and excitement over a large spectrum of subjects from the most basic physics to technological invention. The freedom to pursue a wide range of possible research topics and his confidence in my abilities to carry out independent research were valued highly. While working in his group has never been easy, it has always been interesting and often rewarding.

Many thanks also go to Professor Yaakov Shevy who supervised the project in its initial stages and who has since provided irreplaceable input and suggestions on a great many aspects of the work. His attention to detail and rigorous standards are greatly appreciated. I also acknowledge the three students who have worked with me on the project in its various stages: John Iannelli, Richard Boyd and Dan Provenzano. Their ideas, suggestions and hard work improved the project enormously and are all appreciated. I would like to acknowledge financial support from NSERC Canada and from the California Institute of Technology.

I would also like to thank the fellow students with whom I have shared many questions and resulting lengthy discussions. These include Ali Shakouri, Bill Marshall, Dr. Thomas Schrans, John O'Brien and Randy Salvatore. Someday we'll figure it all out! Thanks also to the many administrative and technical personnel at Caltech who have helped make things run smoothly and efficiently.

Thanks also to my parents for their support, understanding and for putting things in perspective. Finally, I would like to thank Rebecca for her love and patience. Even from a thousand miles away, you have helped made the last five years a thoroughly enjoyable experience.

Quantum Noise Reduction in Semiconductor Lasers Using Dispersive Optical Feedback

by

John E. Kitching

In Partial Fulfillment of the
Requirements for the Degree of
Doctor of Philosophy

Abstract

This thesis describes the phase and amplitude noise properties of semiconductor lasers subjected to weak, dispersive optical feedback. In the first half, experiments demonstrating reductions in the laser frequency noise power spectrum and spectral linewidth by several orders of magnitude are presented. Weak optical feedback is applied to the laser by an external cavity containing an atomic vapor. The presence of the vapor adds to the dispersion of the cavity and simultaneously locks the laser to a fixed frequency reference. The role of 1/f frequency noise in limiting the effectiveness of this linewidth reduction technique is investigated and 1/f noise is found to be the dominant contribution to the linewidth under strong optical feedback conditions.

An electronic feedback scheme utilizing FM sideband locking is then implemented alongside the optical feedback, and an additional reduction in the low frequency 1/f frequency noise power spectrum by over two orders of magnitude is obtained. With both systems operating simultaneously, the spectral linewidth is narrowed from its free-running value of about 20 MHz to 1.4 kHz. Excellent absolute frequency stability is also achieved.

In the second half, the effects of optical feedback on the quantum mechanical amplitude noise properties of the laser are examined. A fully quantum mechanical theory of amplitude

and phase noise for a semiconductor laser with weak optical feedback is developed, and the nature and limits of the noise reduction using this technique are established. Particular attention is given to the feedback-induced enhancement of the amplitude squeezing which can be obtained in a pump-suppressed semiconductor laser: an improvement in the squeezing by 3 dB is predicted under moderate pumping. Somewhat larger noise reductions are expected when the laser is operating closer to threshold. Measurements performed on a laser biased close to threshold are then described and a reduction in the low frequency amplitude noise power spectrum by 7 dB is obtained.

An experimental investigation of the effects of optical feedback on the amplitude squeezing in a semiconductor laser is then discussed. The low frequency squeezing in a room-temperature device is increased from 3% below the standard quantum limit (SQL) under free-running conditions to 19% below the SQL with optimal feedback. The experimental results are found to agree poorly with the single-mode model and a multi-mode model including the effects of asymmetrical cross-mode non-linear gain is developed to explain the discrepancy. Finally, further experimental investigation into the generation of amplitude squeezed light is presented using a commercial laser with no intentional external modifications. Squeezing as large as 29% below the SQL is measured using a balanced homodyne detector with the laser operating near room temperature, corresponding to 41% below the SQL at the output facet of the laser.

Contents

List of Figures

List of Tables

Chapter 1

Introduction

1.1 Introduction

Since the earliest days of laser oscillators, noise issues have been an important consideration from both a basic science viewpoint and the design aspect. Certain limits, such as the Schawlow-Townes linewidth [1,2] and the shot noise limit were recognized early on as being fundamental to many types of lasers. Semiconductor lasers, in particular, have been useful devices for studying the quantum noise properties of lasers in general. Due to their small mode volume, low facet reflectivity and phase-amplitude coupling, free-running semiconductor lasers typically have linewidths of several megahertz which are dominated by fundamental noise sources such as spontaneous emission into the lasing mode. In addition, semiconductor laser cavities have relatively large cavity bandwidths with the result that the noise at frequencies of up to tens of GHz is determined mainly by the dynamics of the gain medium and its interaction with the optical field.

In recent years, advances in the understanding of these fundamental noise properties have pushed semiconductor laser performance beyond what was once thought to be basic limitations for both linewidth and amplitude noise. The discovery of the importance of phase-amplitude coupling in semiconductor lasers [3,4] has led to useful schemes for reducing both the laser spectral linewidth [5,6] and the amplitude

noise [5,7,8]. In addition, the understanding of the interaction of semiconductor lasers with their pumping circuits [9,10] has given rise to amplitude squeezed light sources capable of generating light which, when photodetected, exhibits a photocurrent noise power below the shot noise level. The ease with which such sources can be built and the large squeezing bandwidths which can be obtained make them an attractive tool for many applications. Other correlations between, for example, the junction voltage and the amplitude or phase noise, can also be used in conjunction with electronic feedback or feedforward to reduce the laser noise [11,12].

Due to the ubiquity of semiconductor diode lasers in commercial settings, applications of low-noise devices are many and varied. An advanced worldwide optical communications network will require narrow-linewidth, stable semiconductor lasers locked to frequency standards at 1.55 μm. Electronic and optical feedback systems are potentially important here to lock semiconductor lasers to atomic transitions. Atomic physicists are now turning to semiconductor lasers to replace large and expensive dye and solid state lasers currently used in many atomic physics experiments [13]. Optical feedback techniques are beginning to be used to generate the narrow linewidths and tunability required for experiments such as laser cooling and trapping of atoms. Portable, cheap frequency standards have been proposed using atoms trapped with semiconductor lasers [14]. Amplitude squeezed light may find use in certain precision measurements such as gravitational-wave detection [15] in which the shot noise is a crucial barrier to the observation of weak signals. In addition, optical communication schemes have been devised to take advantage of the noise redistribution which occurs in squeezed states in order to either increase transmission rates [16] or secure transmission secrecy [17].

Techniques for noise reduction in semiconductor lasers are many and varied (see [18] for a review of frequency stabilization techniques) but can be broadly classified into three basic methods: structural modifications, all-optical modifications and electronic feedback. Included in the structural modification group are brute-force

methods of noise reduction such as making longer lasers with better cold-cavity Q's. In addition, alterations in gain medium structure such as the use of quantum wells have been successful in the past in reducing the phase-amplitude coupling and hence the linewidth. Monolithic coupled cavity structures such as two or three-section DFB lasers have also exhibited reduced noise over simpler Fabry-Perot devices [19]. The goal here is to create low-noise devices at the fabrication stage which require little or no modification before being used in the application.

Related to structural modifications are optical feedback schemes. These are usually passive feedback systems which rely only on optical modifications to the initial laser structure such as external cavities or interferometers. Such techniques often can achieve much larger noise reduction than structural changes can, essentially because mode volumes which are orders of magnitude larger than those of solitary semiconductor lasers can be attained. The devices do become much larger, however, and the modifications are difficult to implement on a commercial level due to the usually high degree of complexity. Nevertheless, some of the narrowest spectral linewidths ever produced from diode lasers [20] have been generated in this way justifying the introduction of the additional complexity if very stable lasers are required.

The final method is that of electronic feedback. The idea here is to implement an active feedback system to stabilize the laser by measuring the noise and then changing the laser injection current to compensate. Electronic feedback can result in extremely large reductions in the noise at low frequencies but is difficult to implement at very high frequencies. As a result it is often used alongside one of the two previous schemes in order to enhance the low-frequency stability of the laser.

1.2 Outline of thesis

The work in this thesis concentrates mainly on the second method of noise reduction: optical feedback. In Chapter 2 the effects of optical feedback on the laser linewidth are

investigated. Particular attention is paid to the role of 1/f noise in the low frequency part of the frequency noise power spectrum both in how it is affected by the feedback and also in how it contributes to the laser's spectral linewidth. In Chapter 3 an electronic feedback scheme utilizing FM sideband locking is implemented along with the optical feedback to obtain very narrow linewidths. A linewidth of 1.4 kHz FWHM is obtained under optimum conditions.

In Chapter 4, the fully quantum mechanical theory of semiconductor laser noise in the presence of weak optical feedback is discussed. The quantum limits to the amplitude and frequency noise reduction which can be obtained with optical feedback are elucidated and predictions of an enhancement of the amplitude-squeezing in a pump-suppressed laser using optical feedback are made. The reduction of the "classical" amplitude noise with optical feedback is accomplished in Chapter 5. This experiment is done with the laser fairly close to threshold where the amplitude noise is large and the quantum nature of the optical field is not evident. Reductions in the amplitude noise by as much as 7 dB are demonstrated at an injection current of 1.5 times threshold.

An extension of the amplitude noise reduction into the quantum regime is then discussed in Chapters 6 and 7. These chapters describe an experimental demonstration of the enhancement of the amplitude squeezing in a pump-suppressed semiconductor laser using optical feedback. The noise is reduced to 19% below the standard quantum limit (SQL) under optimal feedback conditions. Poor agreement of the experimental results with the single-mode theory led to the development of a multi-mode theory including asymmetrical cross-mode non-linear gain saturation which is found to explain the measured data much better than does the single-mode theory. Finally, in Chapter 8 measurements of amplitude squeezing from a room temperature laser with no intentional external modifications are presented. Squeezing 29% below the SQL is obtained corresponding to 41% below the SQL at the facet of the laser. Improved side mode suppression seems a likely reason for the increased squeezing over previous

experiments.

Chapter 2

Linewidth and 1/f frequency noise reduction using optical feedback

2.1 Introduction

This chapter discusses linewidth reduction using optical feedback with emphasis on the effects of 1/f frequency noise. Section 2.2 reviews the fundamental origins of the semiconductor laser linewidth including the phasor model and phase-to-amplitude coupling. It also describes the basic idea behind linewidth reduction using optical feedback and dispersive loss. Finally, the basic experimental setup which is used in many of the experiments in this thesis is described and the preliminary results from this experiment summarized.

In Section 2.3, a more advanced theory of frequency noise in semiconductor lasers is outlined which includes the effects of a non-uniform frequency noise power spectrum. The linewidth generated from a spectrum containing not only the usual white noise but also 1/f noise at low frequencies is calculated and the changes induced by optical feedback on both the frequency noise power spectrum and the linewidth are described. It is found theoretically that optical feedback should be less effective in reducing the laser linewidth when 1/f noise dominates than when the linewidth is primarily generated by white noise.

Finally, in Section 2.4, experimental confirmation of the theoretical predictions

of Section 2.3 is presented. Both the frequency noise power spectrum and spectral linewidth are measured as a function of the feedback parameters yielding information on how the non-uniform noise spectrum affects the linewidth. It is seen that optical feedback is indeed considerably less effective at reducing the laser linewidth if 1/f noise is the dominant source of the frequency fluctuations than if white noise only is present. It is found that under strong feedback conditions, 1/f noise generates the largest contribution to the linewidth suggesting that electronic feedback could be a useful method for reducing the linewidth even further.

2.2 Frequency noise and linewidth reduction in semiconductor lasers

2.2.1 Origins of the semiconductor laser linewidth

The linewidth of a semiconductor laser can be understood by considering the phasor model [21]. In this model, the optical field is represented by a phasor of length $\sqrt{\bar{n}}$, where $\bar{n}$ is the number of energy quanta in the lasing mode, which rotates in the complex plain at the oscillation frequency, ω. Fluctuations in the optical field due to spontaneous emission are accounted for by the addition of vectors with length unity and random phase to the end of the field phasor. Such events occur at random times but with a mean rate equal to the rate of spontaneous emission into the mode and cause changes in both the length of the phasor (field amplitude) and its phase. The mean square fluctuation in the phase of the optical field after N spontaneous emission events occurring in time t can therefore be calculated using a random walk analysis to be [21]

$$\left\langle [\Delta\theta(N)]^2 \right\rangle = \frac{1}{2\bar{n}} \frac{n_{sp} t}{\tau_p} \tag{2.1}$$

where $n_{sp} = N_2/(N_2 - N_1)$ is the inversion parameter, N_2 is the number of atoms in the upper laser level, N_1 is the number of atoms in the lower laser level and τ_p is the

photon lifetime of the cold laser cavity. Under the assumption that the observation time is much longer that the time between the uncorrelated spontaneous emission events, the possible values of $\langle \Delta\theta^2 \rangle$ are Gaussian distributed and the field spectrum can be shown [22] to be Lorentzian with a FWHM

$$\Delta\nu_{ST} = \frac{n_{sp}}{4\pi\bar{n}t_c} = \frac{2\pi h\nu(\Delta\nu_{1/2})^2 n_{sp}}{P} \tag{2.2}$$

where $\Delta\nu_{1/2}$ is the cold cavity linewidth and P is the output power. For a typical semiconductor laser this linewidth is a few megahertz at milliwatt output powers. Thus, unlike most gas or solid state lasers where mirror vibrations and other technical noise sources obscure the quantum linewidth, a semiconductor laser's linewidth is dominated by the quantum mechanical process of spontaneous emission.

While this phase diffusion model of laser frequency noise accounts for the gross features of the noise behavior, it is incomplete in two ways. The first is that it is clearly a semi-classical theory: it does not treat the optical field as a quantum mechanical variable and therefore noise due to the discrete nature of light is not present. However, at frequencies below the cavity bandwidth the phase diffusion process usually contributes noise far in excess of the standard quantum limit (SQL) and therefore the quantum properties of the light can usually be ignored in this region. It should be noted, as will be described in Chapter 4, that the Heisenberg Uncertainty Principle which gives rise to the SQL does indeed generate the ultimate limit to linewidth reduction schemes and must be taken into account when determining the minimum possible linewidths.

Secondly, there is the issue of phase-to-amplitude coupling which occurs in semiconductor lasers as a result of the asymmetrical gain profile and non-zero resonant refractive index at the lasing wavelength. The first measurements of the spectral linewidth of semiconductor lasers [23] resulted in values 50 times larger than that predicted by the Schawlow-Townes expression, (2.2). Three years later, an explanation was proposed [3,4]: the asymmetrical gain profile in a semiconductor laser could

result in a large coupling of amplitude noise into the field phase generating excess phase noise and hence an increased linewidth. This explanation, while originally present in early theories of laser noise in general [24] and semiconductor laser noise in particular [25] had been ignored for many years before being proposed to explain the experimental results of Ref. [23].

The essence of the phase-amplitude coupling argument is as follows. For a typical gas or solid state laser, the gain profile and resonant refractive index are symmetrical as a function of frequency about their center frequencies. If the lasing frequency is close to the gain peak, fluctuations in the gain do not cause any substantial change in the refractive index seen by the internal optical field. For a semiconductor laser, however, the situation is very different. The gain profile in a semiconductor laser is asymmetrical, its shape produced at the low frequency end by the density of carrier states and at the high frequency end by the Fermi function cutoffs. Hence, the resonant refractive index at the gain peak is non-zero and changes with the gain as required by the Kramers-Kronig relations. Fluctuations in the gain, caused by spontaneous emission events into the lasing mode, are therefore coupled into the field phase resulting in excess phase noise.

This phase-amplitude coupling is described quantitatively by the linewidth enhancement factor or α-parameter defined by

$$\alpha = \frac{\partial \chi_r / \partial N_c}{\partial \chi_i / \partial N_c}. \tag{2.3}$$

where χ_r and χ_i are the real and imaginary parts of the optical susceptibility of the lasing medium and N_c is the carrier density. The numerical value of α depends to some extent on the type of laser but is typically 4-6 for bulk lasers [26] and about half that for quantum well lasers [27]. The existence of phase-amplitude coupling in semiconductor lasers results in several important consequences. One of these is that the excess phase noise generated because of the coupling results in an enhancement

of the spectral linewidth of the laser by a factor of $(1 + \alpha^2)$ resulting in a linewidth

$$\Delta\nu_0 = \Delta\nu_{ST}(1 + \alpha^2). \tag{2.4}$$

This factor of $(1 + \alpha^2)$ explains why measured linewidths of Fleming and Mooradian [23] were larger than those predicted by the phase diffusion model. The unity term in $1 + \alpha^2$ is due to the original phase fluctuations while the α^2 term is caused by the added noise due to the phase-amplitude coupling. Another consequence of phase-amplitude coupling is a correlation between the amplitude and phase fluctuations in the external field of the laser. The correlation between two quantities $x(t)$ and $y(t)$ can be described by the cross-correlation spectral density function

$$P_{xy}(\Omega) = \left[\int_{-\infty}^{\infty} \langle x(t)y(t+\tau)\rangle\, e^{i\Omega\tau} d\tau\right] / \sqrt{P_x(\Omega)P_y(\Omega)} \tag{2.5}$$

where $P_x(\Omega)$ and $P_y(\Omega)$ are the power spectral densities for the quantities x and y respectively. A semiclassical theory shows that the magnitude of this cross-correlation between amplitude and phase at low frequencies, $|P_{\Delta r\Delta\psi}(\Omega = 0)|$, is equal to $\alpha/\sqrt{1+\alpha^2}$ where $|P_{\Delta r\Delta\psi}(\Omega = 0)| = 1$ represents a perfect correlation. As α increases, the linewidth does likewise and the phase-amplitude correlation gets increasingly closer to unity as the fraction of phase noise uncorrelated with the field amplitude gets smaller.

The fully quantum mechanical theory (discussed in more detail in Chapter 4), which includes not only noise due to spontaneous emission into the lasing mode but also noise due to spontaneous emission into non-lasing modes, predicts a correlation of [11,28]

$$|P_{\Delta r\Delta\psi}(\Omega = 0)| = \frac{\alpha}{\sqrt{(1+\alpha^2)(1+R/2)}} \tag{2.6}$$

in a pump-suppressed laser where $R = i_L/i_{th} - 1$ is the pump rate, i_L, the injection current, and i_{th}, the threshold current of the laser. The additional term $R/2$ is due to the effect of spontaneous emission into non-lasing modes. This noise component

produces amplitude noise without a corresponding correlated component in the phase noise. Since this noise source dominates the laser amplitude noise at high pump rates (see Section 4.2.1), the amplitude-phase correlation decreases to zero as the injection current is increased far above threshold.

2.2.2 Linewidth reduction using optical feedback

Some of the earliest demonstrations of narrow linewidths in semiconductor lasers were obtained by using extended cavities [29,30,31]. In these experiments, one of the laser facets was anti-reflection coated and an external, high-reflectivity mirror positioned in front of the facet to reflect the output light back into the laser. The idea here was to increase the laser cavity mode volume and thus the Q, essentially making it like a conventional gas or solid-state laser with a semiconductor material providing the gain. Linewidths of around 10 kHz were obtained in this fashion, and this technique, often modified by using a diffraction grating rather than a mirror to reflect the light, remains a popular one for linewidth reduction accompanied by good tunability [13].

Weak optical feedback has been discussed as a method of reducing the linewidth of semiconductors since as early as 1980 when Lang and Kobayashi [32] performed a theoretical analysis of the subject. Several other theoretical papers [7,33,34,35,36,37, 38,39] have been written since then emphasizing different aspects of the problem. The basic mechanism for the linewidth reduction is illustrated in Figure 2-1. The figure shows a semiconductor laser with weak feedback from an external cavity which may contain some dispersive element such as a Fabry-Perot resonator or atomic vapor. The feedback field has some phase, ϕ_1, with respect to the internal field of the laser which depends on the frequency of the laser because of the phase delay induced by the feedback field's trip through the external cavity. Due to the presence of the feedback field, the internal laser field sees a slightly altered complex reflectivity at the laser facet which depends on the oscillation frequency. This frequency dependent loss has been modeled by substituting into the equation of motion for the optical field, a

frequency dependent photon lifetime [33,34,40,7] which accounts for the frequency dependence of the facet loss to first order in the frequency deviation. The photon lifetime is thus written

$$\frac{1}{\tau_{ph}} = \frac{1}{\tau_{ph}^{(0)}} + 2C\dot{\phi}(t) \tag{2.7}$$

where $\tau_{ph}^{(0)}$ is the original (frequency independent) photon lifetime, $\dot{\phi}(t)$ is the instantaneous frequency deviation of the internal optical field and C is a (possibly complex) constant. The real part of C represents a change in the loss rate caused by the presence of the optical field and the imaginary part represents a change in the round-trip phase shift. The relative magnitudes of $C_r = Re(C)$ and $C_i = Im(C)$ depend on the steady state phase deviation between the internal field and the feedback field as will be discussed in more detail below.

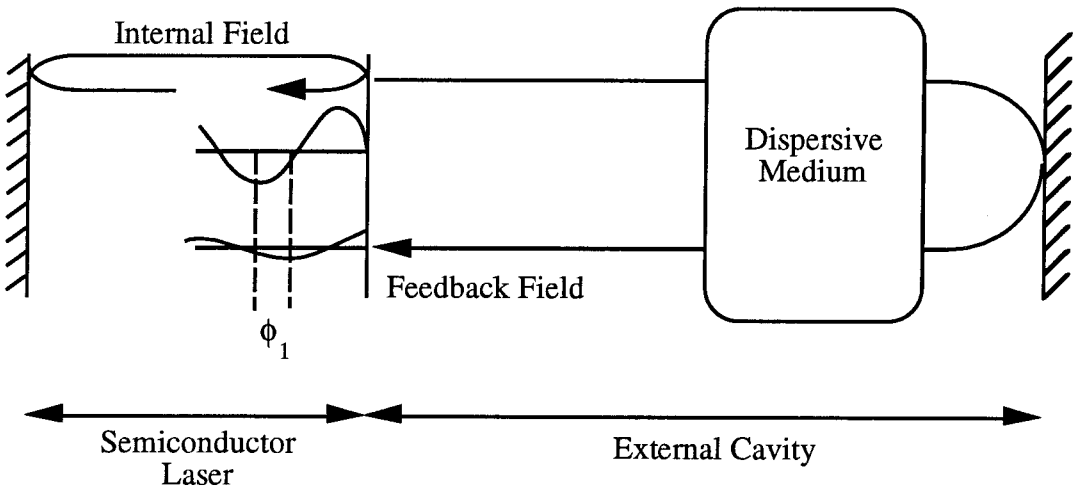

Figure 2-1: Schematic of optical feedback experiments.

The frequency noise of the laser can now be affected in two ways. The first way is direct compensation of frequency fluctuation through the feedback-induced phase shift of the internal field, represented by C_i. The second way is through the phase-amplitude coupling mechanism. The original frequency fluctuation $\Delta\omega$ produces a

change in the cavity loss rate, equal to $2C_r\Delta\omega$, which causes a small change in the gain (since the gain=loss condition must be satisfied) and therefore in the field intensity. Accompanying this change in gain is a change in the refractive index and hence a change in the oscillation frequency. If this change is in the opposite direction to the original fluctuation, negative feedback results, thereby reducing the frequency noise and spectral linewidth. The linewidth reduction via this path clearly relies on phase-amplitude coupling and hence depends on the α-parameter. The final result is that the linewidth under feedback conditions is given by [7,41]

$$\Delta\nu = \Delta\nu_0 \frac{1}{(1 + C_i + \alpha C_r)^2} \tag{2.8}$$

where $\Delta\nu_0$ is the linewidth under free-running conditions. It is clear from (2.8) that not only can the original enhancement of the linewidth caused by the phase-amplitude coupling be eliminated but that the linewidth can in fact be brought far below the original Schawlow-Townes limit if C is made large enough. It can also be seen that for the same coupling strength C, the noise reduction due to the phase-amplitude coupling mechanism (represented by C_r) can be substantially larger than the equivalent reduction from the direct compensation (represented by C_i) due to the factor of α multiplying the C_r term in (2.8).

It remains to determine how the parameters C_r and C_i depend on the feedback power, P_{fb}, and phase, $\phi_0 = \omega_0\tau + \phi_m$, where ω_0 is the steady-state oscillation frequency, ϕ_m is the phase shift at the external cavity mirror and $\tau = \tau_0 + \partial\phi\prime/\partial\omega$ is the propagation delay through the external cavity which includes not only the empty cavity delay τ_0 but also the group delay to the dispersive element $\partial\phi\prime/\partial\omega$. These can be shown to be given by [41]

$$C_r = -\kappa(\omega_0)\tau\sin(\phi_0) + \left.\frac{\partial\kappa}{\partial\omega}\right|_{\omega=\omega_0}\cos(\phi_0) \tag{2.9}$$

$$C_i = \kappa(\omega_0)\tau\cos(\phi_0) + \left.\frac{\partial\kappa}{\partial\omega}\right|_{\omega=\omega_0}\sin(\phi_0) \tag{2.10}$$

where

$$\kappa(\omega) = \frac{(1-r_c^2)}{(r_c\tau_c)}\sqrt{\frac{P_{fb}(\omega)}{P_{out}}} \tag{2.11}$$

is the feedback coupling rate, r_c is the facet field reflectivity, τ_c is the laser cavity round-trip delay time and where the feedback power is allowed to be a function of frequency in case the laser is not tuned to the peak of the resonant element. In the case of $\partial\kappa/\partial\omega = 0$, the relative strengths of C_r and C_i depend on the feedback phase $\phi_1 = \phi_0 mod 2\pi$. If the feedback field is exactly in phase with the internal field ($\phi_1 = 0$), then small changes in the phase of the feedback field generate changes in only the *phase* of the internal field and the corresponding noise reduction depends only on C_i ($C_r = 0$). If, on the other hand, the feedback field is $\pi/2$ out of phase with the internal field ($\phi_1 = \pi/2$), then changes in feedback field phase cause changes only in the *amplitude* of the internal field and the noise reduction depends only on the amplitude-phase coupling and C_r ($C_i = 0$).

Experimental demonstration of linewidth reduction has been performed by a number of groups. Large linewidth reductions were accomplished using weak feedback by Favre et al. [42] who measured narrowing by over two orders of magnitude using weak feedback from a single-mode fiber cavity. Dahmani et al. [5] have obtained a linewidth of 20 kHz using weak feedback from a Fabry-Perot optical cavity. The large dispersion of the optical cavity increased the value of C and therefore enhanced the linewidth reduction. In addition, the cavity served to stabilize the center frequency of the laser. The experiments described in Section 2.2.3, Chapter 2 and Chapter 3 are essentially extensions to this technique in which the dispersion from the optical cavity is replaced with dispersion from an atomic transition. Similar experiments using feedback from an atomic transition have also been performed by Lee and Campbell [43,44].

2.2.3 Basic experimental setup

The experimental setup described in this section is the basic setup used in most of the experiments discussed in this thesis. A detailed description of the feedback mechanism is given which will generally apply throughout the thesis. The experimental setup is shown in Figure 2-2. As described above, a semiconductor laser was weakly coupled to an external cavity formed by the laser front facet and an end mirror, M_1, located about 75 cm away. Inside the external cavity was placed a 6 cm cell containing Cesium (Cs) vapor. On either side of the cell were placed two crossed polarizers, the first (P_1, Figure 2-2) polarized along the direction of the output from the laser. Thus, when the laser was not tuned to the Cs D2 resonance at 852 nm, the crossed polarizers blocked all the light and no feedback was allowed back into the laser. However, when the laser was tuned to the Cs transition and an axial magnetic field was applied to the Cs cell using Helmholtz coils, Faraday rotation caused partial transmission of light through the polarizers allowing feedback into the laser [45]. Part of the light was coupled out of the cavity to one of several detection systems by beam splitter BS1 which served the additional purpose of reflecting part of the returning feedback beam into a photodetector, D_1, for a measurement of the feedback strength. A neutral density filter and PZT attached to the end mirror provided control of the feedback amplitude and phase.

The Cs resonance was used in two qualitatively different ways. If a magnetic field of around 50-100 Gauss was applied, a Doppler-broadened profile could be resolved. Figure 2-3 shows a typical feedback Faraday spectrum obtained by defocusing the feedback beam so it did not enter the laser, scanning the laser injection current (and therefore frequency) and detecting at D_1 in Figure 2-2. This is the feedback signal that the laser sees under these conditions. Two resonances can be seen, the centers separated by 9.2 GHz. The high frequency (low injection current) resonance corresponds to the $6s_{1/2}$ $(F = 4) \rightarrow 6p_{3/2}$ $(F = 5)$ transition and the low frequency resonance to the $6s_{1/2}$ $(F = 3) \rightarrow 6p_{3/2}$ $(F = 2)$ transition. The small dip in the

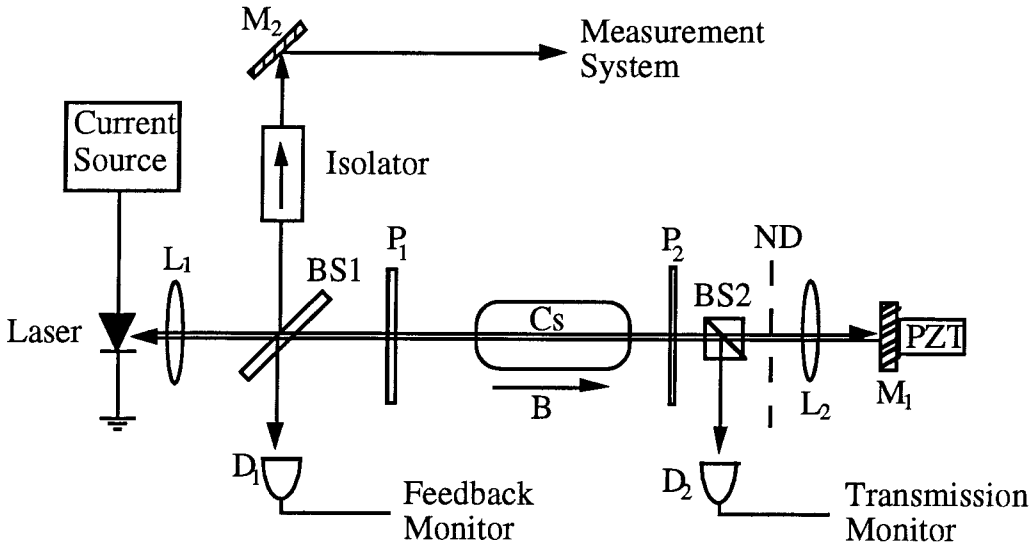

Figure 2-2: Basic experimental setup used in most of the experiments described in this thesis. L, lens; BS, beam splitter; P, polarizer; NP, neutral density filter; M, mirror; PZT, piezoelectric transducer; D, detector.

center of each resonance is due to the nature of the Faraday rotation: absorption at the line center reduces the transmission there slightly [46]. This type of transmission spectrum was used in the measurements of 1/f noise later in this chapter.

If the temperature of the Cs is increased, the shape of the transmission spectrum becomes substantially different. The density of atoms in the vapor goes up causing a much larger absorption near the line center and also a larger rotation of the field polarization in the wings of the transition. A typical transmission spectrum at a Cs temperature of $\approx 95°$ C is shown in Figure 2-4. Near-zero transmission near the center of each line is caused by the absorption. The three peaks which are seen on either side of each line center are caused by rotation of the polarization by 90°, 270° and 450° as the optical field moves toward the line center and experiences a stronger interaction with the atoms. Feedback using this type of transmission spectrum was used in the amplitude noise reduction experiments in Chapters 5 and 6. In these experiments the laser was tuned to the lowest frequency peak of the spectrum.

The second method of using the Cs transition was to obtain feedback from the

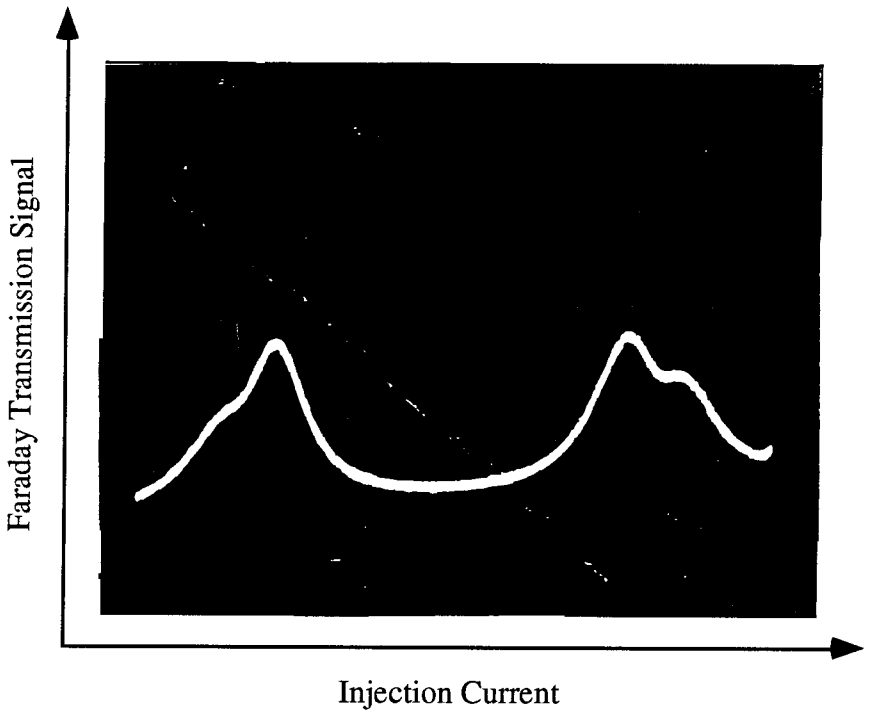

Figure 2-3: One-way transmission spectrum through the external cavity, measured at D_2 in Figure 2-2 with a Cs temperature of $\approx 50°$ C and an axial magnetic field of ≈ 50 G. The two peaks correspond to the two closed transitions of Cs near 852 nm and the slight dips in the center of each resonance are due to the slight absorption of the vapor near the line center.

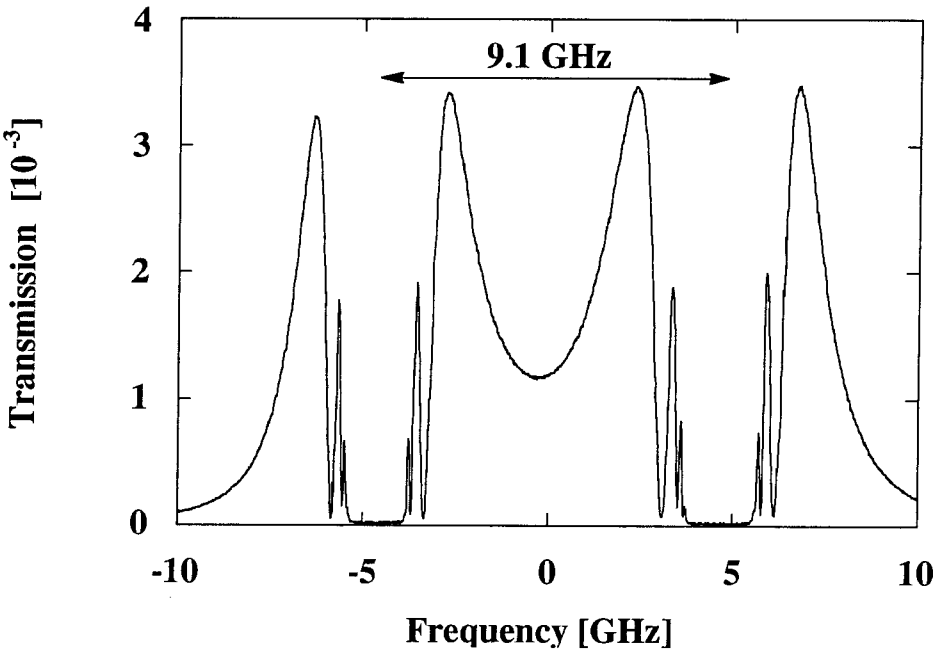

Figure 2-4: One-way transmission spectrum through the external cavity, measured at D_2 in Figure 2-2 with a Cs temperature of $\approx 95°$ C and an axial magnetic field of ≈ 50 G.

Doppler-free transition by using saturation spectroscopy [45]. With this configuration, it was possible to resolve the narrow, Doppler-free transition and as a result the Cs dispersion and thus the effect of the feedback was substantially stronger. When the magnetic field was reduced to about 1 Gauss, such a transition was indeed observed with a FWHM of about 16 MHz corresponding to a C larger by a factor of roughly 100 at the same feedback power level from the Doppler-broadened case. The shape of the Doppler-free line was not easy to measure since the spatially overlapping pump-probe configuration necessitated feedback into the laser; the light could not be blocked at the end mirror since the saturation spectroscopy required a return beam. Thus the Doppler-free signal could only be measured while the laser was locked to the line (i.e., with feedback) and since the feedback affected the lasing frequency, a clear picture of the frequency dependence of the feedback signal was difficult to obtain. Feedback from this Doppler-free transmission spectrum was used when large values of C were required in order to generate large linewidth reductions in this chapter and in Chapter 3.

This technique of using feedback incorporating an atomic resonance has an advantage over feedback from Fabry-Perot cavities or plain mirrors in that the laser locks to an absolutely stable frequency. Atomic transitions do not have substantial frequency drifts due to temperature changes and room vibrations as do optical cavities, and therefore much better low-frequency stability can typically be obtained using atoms. It should be noted, however, that although the absolute frequency stability obtained in the setup outlined above is expected to be good, Zeeman shifts in the atomic levels induced by the applied magnetic field make this particular system less effective as a frequency standard. Modifications on this scheme which do not use magnetic fields have been proposed [47] to get around this particular problem.

Frequency pulling and locking

One effect of the coupled cavity formation described in Section 2.2.3 is that the oscillation frequency is pulled from its free-running value to the coupled cavity resonance. This frequency of the laser with feedback, ω, has been calculated to be [38]

$$\omega = \omega_0 - \kappa\sqrt{1+\alpha^2}\sin(\omega\tau_0 + \phi\prime(\omega) + \arctan(\alpha)) \tag{2.12}$$

where ω_0 is the free-running lasing frequency. This transcendental equation can be solved by graphical means and one finds that as the feedback gets stronger, the laser tends to "lock" to a single frequency as the free-running laser frequency is varied (by varying the injection current, for example). This locking behavior can be seen in Figure 2-5. Figure 2-5(a) shows the Doppler-broadened transmission spectrum through the Cs and polarizers with the feedback blocked at the mirror (this is a single peak from Figure 2-4). Figure 2-5(b) shows the same transmission spectrum with the feedback now applied to the laser: a step-like structure can be seen as the laser scans over the line with the laser locking to only certain frequencies. The frequency chirp (variation of lasing frequency with injection current) is reduced within each locking unit.

Measurements such as the one shown in Figure 2-5 are one way to estimate the value of the Cs dispersion. The dispersion caused by the frequency-dependent refractive index in the vicinity of the resonance adds some additional group delay to intensity and phase fluctuations which propagate through the cavity. This delay is difficult to calculate exactly or measure directly and yet is an important parameter in the linewidth reduction expression. Equation (2.12) predicts that in the limit of strong feedback, the difference in free-running frequency between two successive "jumps" in the step-like structure should be equal to the cavity free-spectral range (FSR) which is just equal to the inverse of the cavity delay. Thus by measuring the dependence of the laser frequency on injection current both with and without feed-

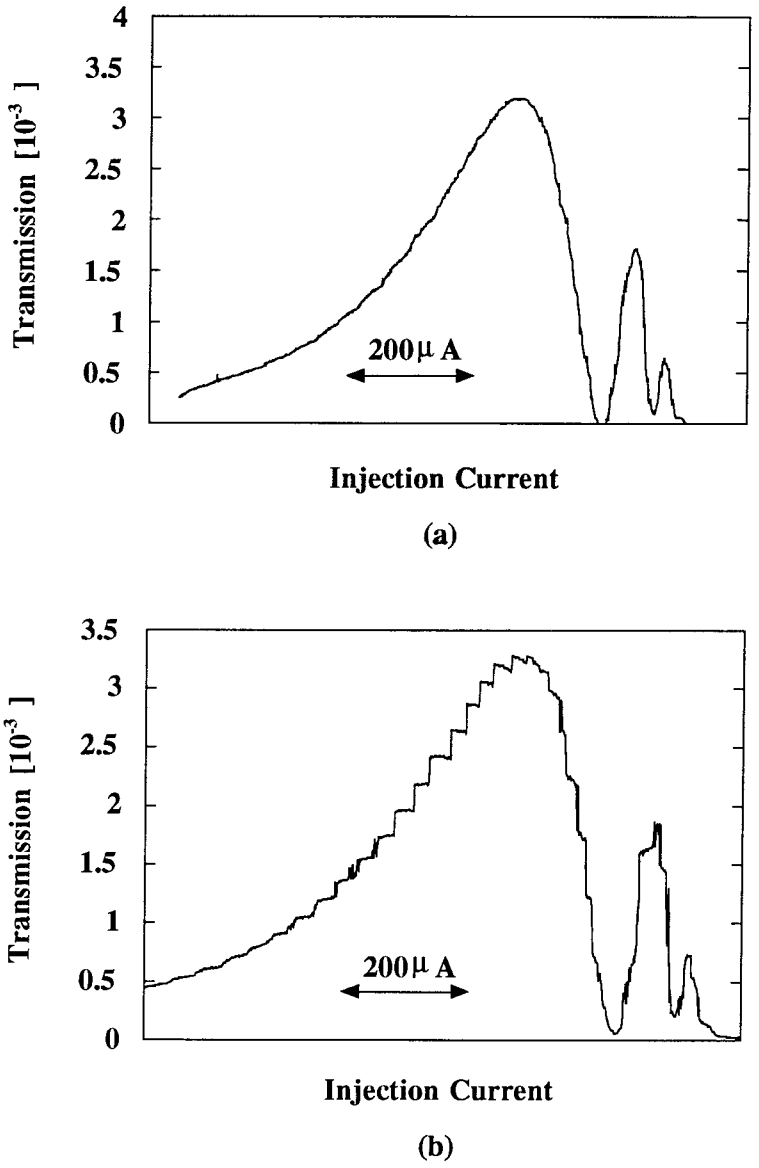

Figure 2-5: Locking behavior of the laser to the atomic transition. (a) The transmission spectrum measured at D_2 (Figure 2-2) as the laser injection current is scanned with the feedback blocked at the end mirror. (b) The same spectrum when the feedback is allowed back into the laser.

back, one can then calculate a value for the cavity delay. In cases where spurious optical feedback is a problem (see Chapter 6), the step-like structure on the spectrum can also be used to estimate the amount of feedback present.

The locking of the laser to the narrow, Doppler-free line was more difficult to observe directly since the locking range (of several hundred MHz) was typically much larger than the width of the transition. Evidence of the locking was observed by scanning the laser injection current and measuring the transmission through an external cell. When the laser locked to the narrow line, the frequency would remain almost constant over a large range of injection currents before the locking would cease as the unperturbed laser frequency moved too far from the atomic resonance frequency. One such absorption spectrum from an external cell is shown in Figure 2-6. The top trace in the figure shows the absorption of the external cell while the bottom trace shows the feedback signal as the injection current is scanned. When the locking occurs (non-zero feedback evident in the bottom trace), the laser frequency remains almost constant leading to a constant absorption (evident in the top trace) as the injection current is scanned.

Initial measurements

The initial experiment in which linewidth reduction was obtained using the method outlined above is described in Refs. [6] and [48]. It was found that large reductions in the semiconductor laser linewidth were indeed possible, the minimum linewidth obtained being 10 kHz. This represents a reduction by a factor of over 1000 from the free-running linewidth. Despite this initial success, two anomalous results were observed. The first was that the linewidth was not found to be reduced by factor of $(1 + C_i + \alpha C_r)^2$ as predicted by (2.8) but rather by a factor of only $(1 + C_i + \alpha C_r)$. Thus, although $1 + C_i + \alpha C_r$ was estimated to be 2000, the linewidth reduction was substantially less that the predicted value of about 10^6. The second result was that the lineshapes, measured using a delayed self-heterodyne system [21], were not found

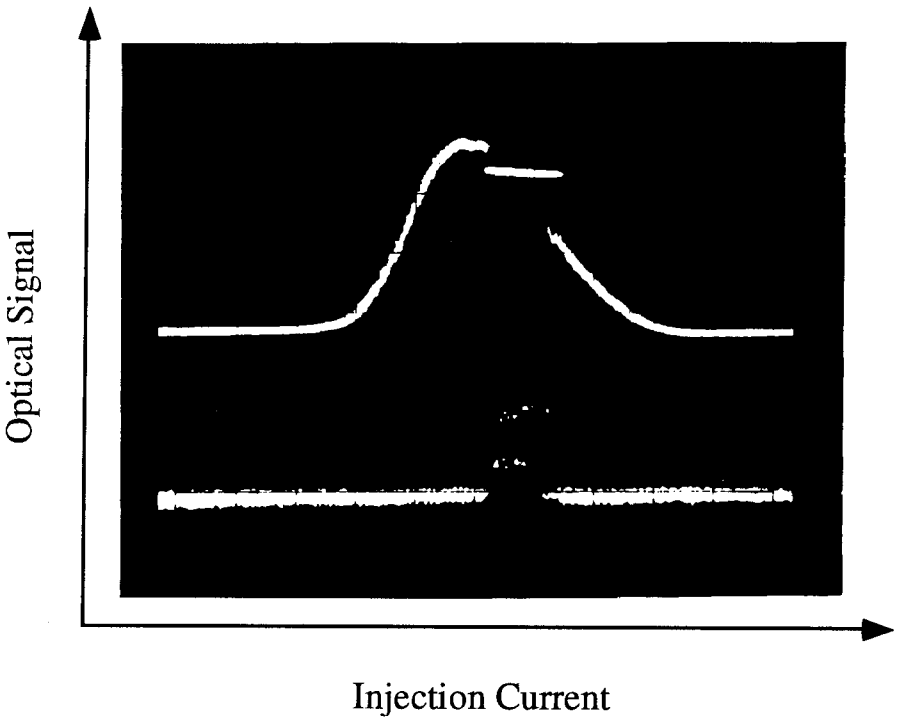

Figure 2-6: Absorption spectrum through an external Cs cell: evidence of frequency locking to the Doppler-free line. The upper trace shows the external cell absorption spectrum while the lower trace shows the feedback power.

to be Lorentzian in shape as the theory again predicts. Instead they were found to fit best with a Lorentzian to the power 3/2, a result found in other, similar experiments [49].

These deviations from the expected behavior can be explained by assuming the existence of 1/f noise in the low-frequency frequency noise spectrum of the laser. Sections 2.3 and 2.4 describe further investigations to verify this hypothesis and determine the effects of optical feedback on a non-uniform frequency noise spectrum.

2.3 Theory of 1/f frequency noise reduction

The experiment in Section 2.2.3 [6] produced two unexpected results: the laser self-heterodyne lineshape was found to be a Lorentzian to the power 3/2 rather than a Lorentzian and the linewidth as a function of feedback power was measured to be proportional to $1/C$ rather than the expected $1/C^2$. The explanation given was that 1/f noise was present in the low-frequency part of the frequency noise power spectrum. This and the following sections explore the presence and consequences of 1/f noise further.

1/f noise is defined as noise for which the power spectrum $S(\Omega)$ is proportional to the inverse of the angular frequency Ω at which the noise is measured. 1/f noise occurs in a surprising variety of physical systems [50,51,52] but the physical processes which give rise to such a spectrum are not generally known. The origin of 1/f noise in semiconductor lasers has been discussed by several authors and a number of possible mechanisms have been proposed. Included in these are noise due to the presence of longitudinal side modes [53] and noise due to event driven temperature fluctuations [54]. Conclusive experimental verification of which of these mechanisms is the most important has yet to be performed, however.

It is shown here that optical feedback provides an effective method for reducing both the white noise and the 1/f noise in the frequency noise spectrum of a semicon-

ductor laser. This section will review the basic theory of frequency noise reduction using optical feedback and show how feedback affects an arbitrary frequency noise spectrum. The field spectrum lineshape for a laser which exhibits both white and 1/f frequency noise will then be discussed, and the dependence of the field spectrum linewidth on optical feedback parameters will be derived.

The analysis is performed using a model of the laser in which it is assumed that the refractive index responds instantaneously to changes in the optical field intensity. This eliminates the carrier density from the rate equations making them simpler to solve, but the analysis is limited to frequencies below the inverse of the carrier stimulated lifetime (typically a few hundred MHz under normal operating conditions). Since the laser linewidth is dominated by the low-frequency (below $\approx$ 20 MHz) FM noise, the above assumption is justified in the following calculations of the linewidth.

As in Section 2.2.2, an internal dispersive loss and phase change are modeled by the introduction of a frequency-dependent photon lifetime as in (2.7). It is assumed that there is no time delay between a given frequency fluctuation and the correction due to optical feedback: the noise frequencies considered are small compared to the cavity FSR. This assumption is usually justified for calculations of the spectral linewidth of the laser since only the low-frequency part of the frequency noise power spectrum typically contributes to broadening the linewidth. Following the analysis in Ref. [7], the equations for the internal optical field $a(t) = [A_0 + \Delta A(t)]e^{i[\omega_m t + \phi(t)]}$ are then given by

$$\Delta\dot{A} + \omega_1 \Delta A + A_0 C_r \dot{\phi} = \frac{\Delta_i}{2\omega_m} \tag{2.13}$$

$$A_0(1 + C_i)\dot{\phi} - \alpha\omega_1 \Delta A = -\frac{\Delta_r}{2\omega_m} \tag{2.14}$$

where $\omega_1 = -A_0 \omega \chi_i^{(3)}/n^2$, and $\Delta(t) = \Delta_r(t) + i\Delta_i(t)$ is a Langevin noise term. Here ω is the laser oscillation frequency, n is the non-resonant refractive index and $\chi_i^{(3)}$ is the imaginary part of the third order non-linear susceptibility of the gain medium

($\chi = \chi^{(1)} + \chi^{(3)}|A_0|^2$). Since we assume from the outset that the phase noise will always be much larger than the SQL at the frequencies of interest, a semiclassical analysis is justified and a distinction between the internal and external optical fields need not be made.

Using Fourier transforms to solve the coupled equations, the solution for the Fourier transform of the phase variable $\tilde{\phi}(\Omega)$ in the limit $\Omega \ll \omega_1$ is

$$\tilde{\phi}(\Omega) = \frac{1}{2i\omega_m \Omega A_0} \frac{\alpha\tilde{\Delta}_i(\Omega) - \tilde{\Delta}_r(\Omega)}{1 + C_i + \alpha C_r} \tag{2.15}$$

From this, the frequency noise spectrum $S_{\dot{\phi}}(\Omega)$ can be quickly calculated to be

$$\begin{aligned} S_{\dot{\phi}}(\Omega) &= \lim_{T\to\infty} \frac{\langle \tilde{\dot{\phi}}_T(\Omega)\tilde{\dot{\phi}}_T^*(\Omega)\rangle}{T} \\ &= \Omega^2 \lim_{T\to\infty} \frac{\langle \tilde{\phi}_T(\Omega)\tilde{\phi}_T^*(\Omega)\rangle}{T} \\ &= \frac{S_{\dot{\phi}}^{(0)}(\Omega)}{Q^2} \end{aligned} \tag{2.16}$$

where $S_{\dot{\phi}}^{(0)}(\Omega)$ is the frequency noise spectrum with no optical feedback, T is the time interval over which the Fourier transform is taken and $Q = 1 + \alpha C_r + C_i$. This result agrees with those previously obtained by others [36,49,37,39].

For the case of a semiconductor laser coupled to an external cavity containing an element of dispersive loss, the field equation must be modified differently since the feedback field suffers a delay in traversing the cavity. However, as discussed in Section 2.2.2 and Ref. [41], the result of (2.16) is again recovered with $Q = 1+C_i+\alpha C_r$ now given by

$$\begin{aligned} Q = 1 &+ \sqrt{1+\alpha^2}\kappa(\omega)\left(\tau_0 + \frac{d\phi\prime}{d\omega}\right) \\ &\times \cos(\omega\tau_0 + \phi\prime(\omega) + \arctan(\alpha)) \\ &+ \sqrt{1+\alpha^2}\frac{d\kappa(\omega)}{d\omega}\sin(\omega\tau_0 + \phi\prime(\omega) + \arctan(\alpha)). \end{aligned} \tag{2.17}$$

It can be seen that even at low feedback levels, Q can be made very large by using a very sharp feature in the feedback system such that $d\phi\prime/d\omega$ and/or $d\kappa/d\omega$ is large. As mentioned in Section 2.2.3, Q has been found to be as large as 2000 for this system.

Unlike the corresponding noise reduction for amplitude fluctuations [7], the frequency noise reduction does not depend necessarily on a preexisting correlation between frequency and amplitude fluctuations. A given frequency fluctuation is first translated by the optical feedback into an amplitude fluctuation which then corrects for the original frequency fluctuation through the phase-to-amplitude coupling. The optical feedback therefore corrects for more than just the component of the frequency fluctuations which are correlated with the amplitude noise; it corrects for all frequency fluctuations, regardless of whether they are correlated or not. Thus, any frequency noise spectrum will be reduced by the same amount at all frequencies within the optical feedback bandwidth. In particular, both a white noise spectrum and a 1/f noise spectrum will be reduced by this same factor of $1/Q^2$.

In addition, the noise term $\Delta(t)$ may contain contributions from carrier fluctuations (pump fluctuations) and other, technical, noise sources as well as spontaneous emission. The carrier density and dipole moment typically both have large damping constants ($> 1GHz$) and so on sub-gigahertz time scales they can be assumed to follow the field variable adiabatically. These variables can then be eliminated from the equations and their noise terms combined with the spontaneous emission noise to form the $\Delta(t)$ in (2.13) and (2.14). It is shown below that optical feedback can reduce the frequency noise regardless of the exact form of the correlation function $\langle\Delta(t_1)\Delta(t_2)\rangle$. Therefore, this analysis applies equally well to 1/f noise of unknown origin as to white noise resulting from spontaneous emission [36].

The actual shape of the field spectrum is not easily evaluated analytically for a laser which has both white and 1/f noise. If the field phase $\phi(t)$ is assumed to be a stationary random variable obeying Gaussian statistics, the field power spectrum

$S_E(\Omega)$ is formally given in terms of the frequency noise power spectrum as [55]

$$S_E(\omega) = \int_{-\infty}^{\infty} exp\left[-\frac{1}{\pi}\int_{-\infty}^{\infty} \sin^2\left(\frac{\Omega\tau}{2}\right) S_{\dot{\phi}}(\Omega)\frac{d\Omega}{\Omega^2}\right] e^{i(\omega-\omega_m)\tau} d\tau \qquad (2.18)$$

where ω_m is the lasing frequency, $S_{\dot{\phi}}(\Omega)$ is the two-sided frequency noise spectrum in $(rad/s)^2/Hz$ and where the total noise power has been normalized to unity. For a white noise frequency spectrum, $S_{\dot{\phi}} = S_0$, the integral is easily evaluated resulting in the well known Lorentzian lineshape with a linewidth of $\Delta\omega_{W.N.} = S_0/2\pi$ FWHM.

For a 1/f noise spectrum, no closed form expression is known to exist for the field spectrum and approximations must be used. It has been shown that near the peak, the field spectrum can be approximated by a Gaussian profile [56]. However, numerical calculations indicate that this approximation breaks down in the wings, far from its center frequency [57]. Thus, another approximation is necessary to describe the behavior of the field spectrum away from the line center.

The 1/f frequency spectrum is given by $S_{\dot{\phi}}(\Omega) = \Omega_1^2/\Omega$ where Ω_1 measures the magnitude of the 1/f noise. To approximate the RHS of (2.18) for large ω, the integral is first written as

$$S_E(\omega) = \int_{-\infty}^{\infty} e^{-\frac{2}{\pi}f(\tau)} e^{i(\omega-\omega_m)\tau} d\tau \qquad (2.19)$$

with

$$f(\tau) = \int_{\omega_D}^{\infty} \frac{\Omega_1^2}{\Omega^3} \sin^2\left(\frac{\Omega\tau}{2}\right) d\Omega. \qquad (2.20)$$

Here ω_D is the low frequency detection limit either given by the reciprocal of the measurement time, or, in the case of a self-heterodyne measurement, approximately given by the reciprocal of the fiber delay time. If $(\omega - \omega_m)$ is large, a stationary phase argument can be used and the exponential expanded about the stationary point $\tau = 0$. In this case,

$$f(\tau) \approx \frac{\Omega_1^2\tau^2}{4} \ln\left(\frac{a}{\omega_D\tau}\right) \qquad (2.21)$$

where a is a constant related the high frequency limit of the detection system. Ex-

panding the exponential, we find

$$S_E(\omega) \approx 2\pi\delta(\omega-\omega_m) - \frac{\Omega_1^2}{2\pi}\frac{\partial^2}{\partial\omega^2}\int_{-\infty}^{\infty} \ln\left(\frac{\omega_D\tau}{a}\right) e^{i(\omega-\omega_m)\tau} d\tau. \tag{2.22}$$

After integrating by parts and then taking the principal value of the result, we find that

$$S_E(\omega) \approx 2\pi\delta(\omega-\omega_m) + \frac{\Omega_1^2}{(\omega-\omega_m)^3}. \tag{2.23}$$

This result is valid for $(\omega-\omega_m) \gg \Omega_1 \gg \omega_D$, i.e., in the wings of the field spectrum, and agrees with previously published results [58,49].

In order to fit data to this calculated spectrum, it is advantageous to have an approximation which does not diverge at the line center, ω_m. To this end, as in [49], the above field spectrum can again be approximated by a Lorentzian to the power 3/2, which behaves correctly at large frequencies and which is finite at the line center [58]. The resulting linewidth from the fitted spectrum can then be related to the 1/f noise level by writing

$$S_E^{(fit)}(\omega) = \frac{\pi(\Delta\omega_{1/f})^2}{[(\omega-\omega_m)^2 + (\Delta\omega_{1/f})^2]^{3/2}} \approx \frac{\pi(\Delta\omega_{1/f})^2}{(\omega-\omega_m)^3} \tag{2.24}$$

for $(\omega-\omega_m) \gg \Delta\omega$ and where the total noise power has again been normalized to unity. Comparing the two results (2.23) and (2.24), the width $\Delta\omega_{1/f}$ of the Lorentzian to the power 3/2 fit can be written in terms of the noise spectrum level

$$\Delta\omega_{1/f} = \frac{\Omega_1}{\sqrt{\pi}} = \sqrt{\frac{S_{\dot{\phi}}(1)}{\pi}}. \tag{2.25}$$

Thus we see that if the frequency noise spectrum is reduced by a factor of $1/Q^2$ as in (2.16), then the corresponding reduction in the linewidth is only $1/Q$ [49,37] due to the square root in (2.25). A similar result is found if a Gaussian approximation for the 1/f noise spectrum is used and, again, the linewidth of the corresponding field spectrum is found to be reduced by $1/Q$ [56].

The reason for this weaker dependence of the 1/f linewidth on optical feedback can be understood on a more intuitive level than the derivation above. For a reasonably flat frequency noise power spectrum, $S_{\dot{\phi}}(\Omega) = S_0\ [Hz^2/Hz]$, the dominant contribution to the linewidth comes from noise at frequencies below $\Omega = 2\pi S_0$. The reason for this is that very fast (high frequency) fluctuations in the lasing frequency cause relatively smaller changes in the rms field phase than do slower fluctuations of the same magnitude since the optical field spends less time at a different frequency and thus accumulates a smaller phase shift. Thus, as the frequency noise power spectrum is reduced, the most important contribution to the linewidth comes from progressively lower frequency parts of the frequency noise power spectrum. This is illustrated in Figure 2-7 where the solid lines (A, B and C) indicate three different frequency noise power levels and the dashed lines indicate the corresponding region of the frequency noise power spectrum which contributes significantly to the laser linewidth. If the frequency noise power spectrum is flat, then the average noise level in the important part of the noise spectrum is reduced by the same factor as the entire frequency noise spectrum, namely, $1/Q^2$.

If the frequency noise power spectrum has a 1/f dependence (see Figure 2-7b), however, then as the noise is reduced by the optical feedback, the important part of the spectrum shifts to lower frequencies where the average noise is *higher*. This higher noise level results in a smaller linewidth reduction when 1/f noise dominates the linewidth than when white noise is exclusively present.

If a self-heterodyne system is used to measure the linewidths, then the lineshape and linewidths will of course change. However, if the delay time of the measurement apparatus is considerably longer than the coherence time of the laser, then the noise in the two beams reaching the detector will have only a small degree of correlation. In this case the phase noise can be added incoherently and the self-heterodyne frequency noise power spectrum will be twice the real one. The white noise linewidth will therefore increase by a factor of 2 in the self-heterodyne measurement while the 1/f

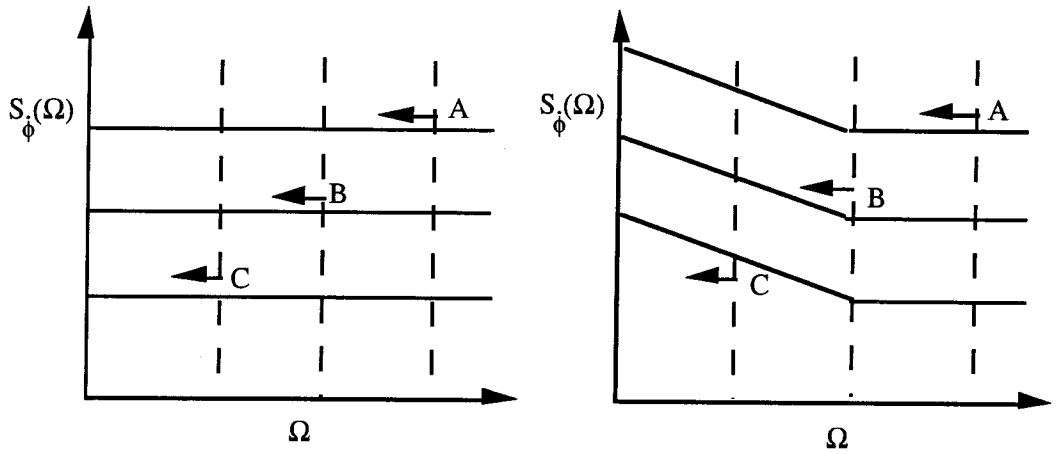

Figure 2-7: Intuitive explanation of why a linewidth generated by 1/f noise as in (b) is reduced less than one generated by white noise as in (a) when optical feedback is applied to the laser.

noise linewidth will increase by a factor of $\sqrt{2}$ [21].

If both white noise and 1/f noise are present, then the frequency noise spectrum can be written as $S_{\dot{\phi}}(\Omega) = S_0 + \Omega_1^2/\Omega$. The exponential in (2.18) then factors and the field spectrum becomes a convolution of the individual field spectra for the white noise and the 1/f noise. This convolution is discussed by Mercer [57] in the case that the Gaussian approximation can be used to represent the 1/f field spectrum. He found that a Gaussian profile is a good approximation to the 1/f field spectrum near the center but shows significant deviations in the wings. This resulting convolution is known as the plasma dispersion function or Voigt profile for which many approximation schemes exist making fitting experimental data fairly easy. However, if the white noise linewidth is very small compared to the 1/f noise linewidth, then the 1/f noise spectrum will dominate the combined spectrum even far from the peak. In this case the Gaussian approximation is no longer valid and the resulting Voigt profile no

longer accurately fits the lineshape.

In the experiments described in the next section, linewidths have been observed which correspond to both of the above cases. For low values of Q, it is found that the Voigt profile fits the experimental data very well. The white noise linewidth and the 1/f noise linewidth can be extracted from each spectrum by fitting the spectrum to a Voigt profile approximation. But for large values of Q, the white noise linewidth is reduced much more than the 1/f noise linewidth and the resulting field spectrum is given exclusively by a Lorentzian to the power 3/2. In this case, the 1/f noise linewidth can be extracted, but the white noise linewidth cannot be obtained since the contribution from the white noise is only seen far from the line center where it is obscured by system noise.

2.4 Measurements of 1/f frequency noise reduction using optical feedback

The experimental setup, shown in Figure 2-8, was mostly described in Section 2.2.3. A single mode index guided semiconductor laser (Hitachi HLP1400) was coupled through one facet to an external cavity which provided weak optical feedback for the laser via Faraday rotation in Cs vapor. The output coupling beamsplitter (BS in Figure 2-8) had a power reflection coefficient of 40%.

Two different values of the magnetic field were used in the experiment resulting in two different sets of feedback parameters. With a magnetic field of $\approx$ 50 Gauss applied to the Cs, the typical two-peaked Faraday transmission signal was produced (similar to Figure 2-3 but with a more pronounced absorption dip in the center resulting in two distinct peaks for each transition). The FWHM of each of the peaks in this case was 400 MHz and the maximum feedback power reentering the collimating lens was $2.2 \times 10^{-4} P_{out}$, where P_{out} is the total output power from the laser. It is expected that the actual feedback power entering the active region of the laser was somewhat

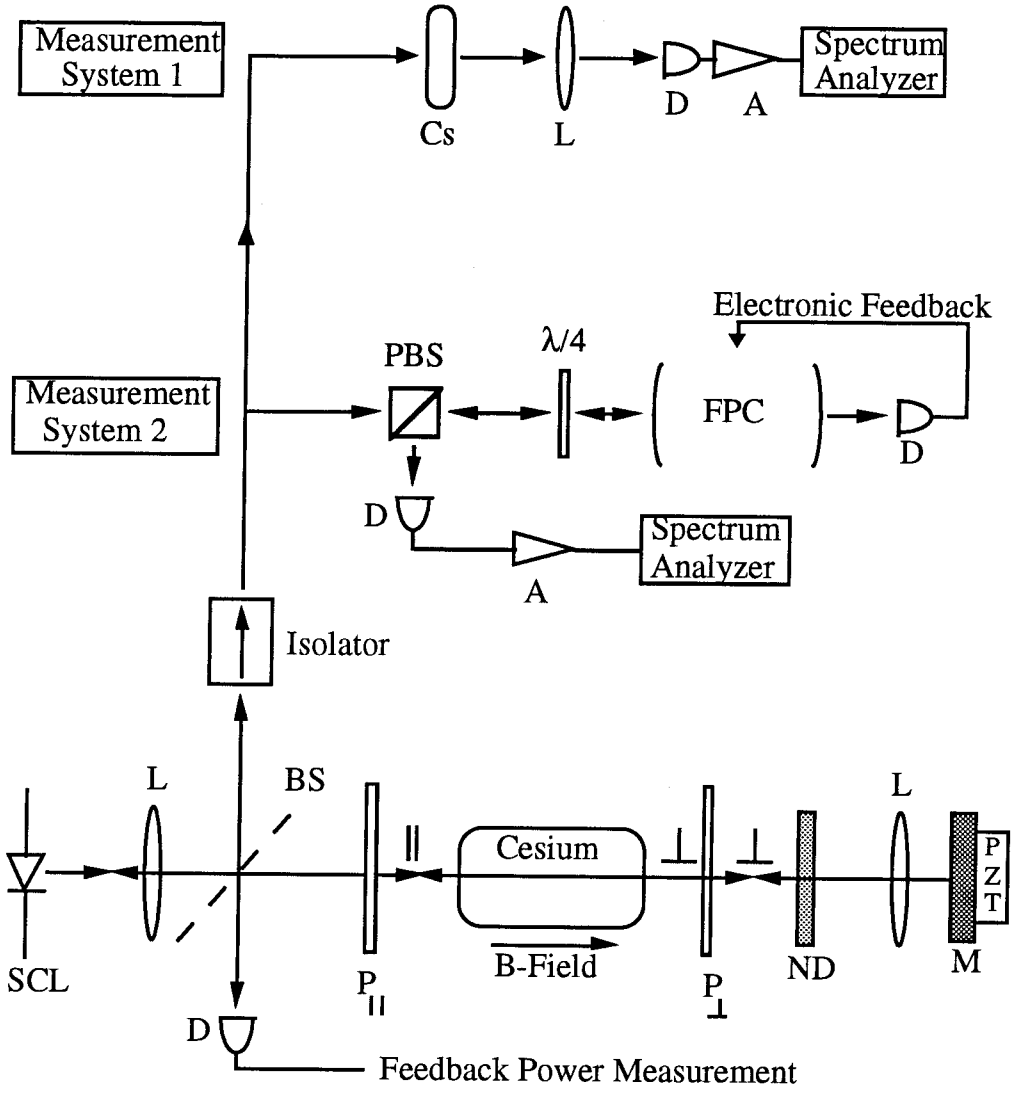

Figure 2-8: Experimental setup for measurements of 1/f noise. SCL, semiconductor laser; L, lens; BS, beam splitter; P, polarizer; ND, neutral density filter; M, mirror; PZT, piezoelectric transducer; D, detector; A, amplifier; $\lambda/4$, quarter-wave plate; FPC, Fabry-Perot cavity; Cs, Cesium cell.

d	$\Delta\nu_{W.N.}$	$\Delta\nu_{1/f}$	Q (Approx)
Free-running	30 ± 10 MHz	3 ± 1 MHz	1
Low-Q Line	220 kHz	205 kHz	14
High-Q Line	0.65 kHz	8 kHz	400

Table 2.1: Linewidths calculated form the measured frequency noise power spectra. For the free-running and low-Q line measurements, the 1/f cutoff frequency was 2 MHz. For the high-Q line, a different laser was used with a cutoff frequency of 300 kHz.

smaller due to coupling losses.

When the magnetic field was lowered to about 1 Gauss, the narrow Doppler-free resonance provided feedback to the laser. This transition had a FWHM of 16 MHz at our operating conditions and a maximum feedback power of $6.8 \times 10^{-5} P_{out}$ allowing much larger values of Q than were produced with the high field configuration due to the stronger frequency dependence.

In all measurements, the laser was tuned to the very top of the feedback line. Thus $d\kappa/d\omega$ was zero but both $d\phi\prime/d\omega$ and κ_0 were roughly maximized. From the linewidth reductions (see Table 2.1), Q was estimated to be about 15 for the high magnetic field (henceforth called the low Q) line and about 400 for the low magnetic field (high Q) line at maximum feedback levels. In order to fix the feedback phase to a known value, care was taken to ensure that there was no frequency pulling due to the feedback: before each measurement, the free running laser frequency was adjusted to be exactly equal to the frequency of the laser with feedback. Thus, from (2.12) it is found that $\omega\tau_0 + \phi\prime(\omega) + \arctan(\alpha) = 0$ which, when substituted into (2.17) results in a Q given by the simple expression $Q = 1 + \sqrt{1+\alpha^2}\kappa_0(\tau_0 + d\phi\prime/d\omega)$ where κ_0 is the maximum feedback coupling rate. An optical isolator was placed between the laser and the detector in order to reduce optical feedback from the detection system.

The frequency noise power spectrum of the laser was measured by translating the frequency fluctuations into intensity fluctuations using a frequency discriminator. The

discrimination was accomplished by tuning the laser onto the side of the transmission (or reflection) spectrum from a resonant element such as an Fabry-Perot optical cavity. Two different discriminators were used depending on the magnitude of the noise signal. The first discriminator was the absorption signal due to the Doppler broadened transition of an external Cs cell 3mm in length. The external cell was heated slightly so that the maximum power absorption at the peak of the line was 90%. The linewidth of the transition was 900 MHz FWHM. All measurements of the noise spectra of the free-running laser and of the laser with low Q feedback were made using this discriminator.

The second discriminator used was a confocal Fabry-Perot cavity (Tropel 240). The cavity had a free spectral range of 1.5 GHz and a finesse of 310 giving a linewidth of 4.8 MHz. The reflection mode from the cavity was used and the minimum reflected power at the line peak was 8% of the total power. The cavity was locked to the laser at frequencies below 1 kHz using a simple electronic servo. Low frequency stability was obtained in this fashion to about 10% of the peak transmission amplitude. This system was used for measurements of the noise power spectrum for the laser with high Q feedback.

The light exiting from each of these discriminators was focused on a high frequency detector (HP1400 PIN). The detector signal was then amplified and sent to an electronic spectrum analyzer for measurement of the noise spectrum. The spectrum could be measured from 1 kHz up to 2 MHz with the cavity and from 1 kHz to 50 MHz with the external Cs cell. The upper limit for the cavity was imposed by its photon lifetime and the other limits were imposed by electronics. Since the cavity locking scheme only operated below 1 kHz, the effect of this system on the noise measurements would have been minimal. While these discriminators provided a good way to measure changes in the frequency noise power spectrum induced by the optical feedback, the exact calibration of the system was difficult since it involved the propagation of electronic signals through a fairly complex measurement system. Linewidths

calculated with the measured frequency noise data did give reasonably close agreement with the (intrinsically calibrated) self-heterodyne measurements, however. In addition, the measurement of the relative change in the noise power should be considerably more accurate. Linewidths were measured using a self-heterodyne system with a 5 km fiber delay. The resolution of this system was limited to about 6 kHz.

2.5 Results

Figure 2-9 shows typical measured frequency noise power spectra $S_{\dot{\phi}}(\Omega)$ as a function of frequency Ω for the free running laser (no feedback) and the laser with feedback from the low Q line. The low frequency behavior was indeed 1/f and the frequency at which the 1/f noise becomes dominant, $\Omega_{1/f}$, did not change with the feedback level. From the spectra, the white noise and 1/f noise linewidths could be calculated for each case and are summarized in Table 2.1. From these linewidths it is estimated that the white noise should be the dominant linewidth for the free running laser, the 1/f noise should be the dominant linewidth when locked to the high Q line, and the laser locked to the low Q line should be somewhere in between. Under optimum conditions with the high Q line, reductions in the frequency noise spectrum by up to five orders of magnitude were observed. This reduction was uniform over the entire range of frequencies examined.

The dependence of the frequency noise spectrum on the feedback power when the laser was locked to the high Q line is shown in Figure 2-10. By changing the neutral density filter in the external cavity, the feedback power, and hence Q, could be varied by over an order of magnitude. Since Q is expected to be at least 10 in magnitude, the unity term in (2.17) can be neglected at the level of accuracy of the measurements. Since the laser was tuned to the line peak, $\partial\kappa/\partial\omega \approx 0$ and Q is found to be proportional to κ_0 which is in turn proportional to the square root of the feedback power. The laser current for these measurements was 94 mA and $\Omega_{1/f}$ was

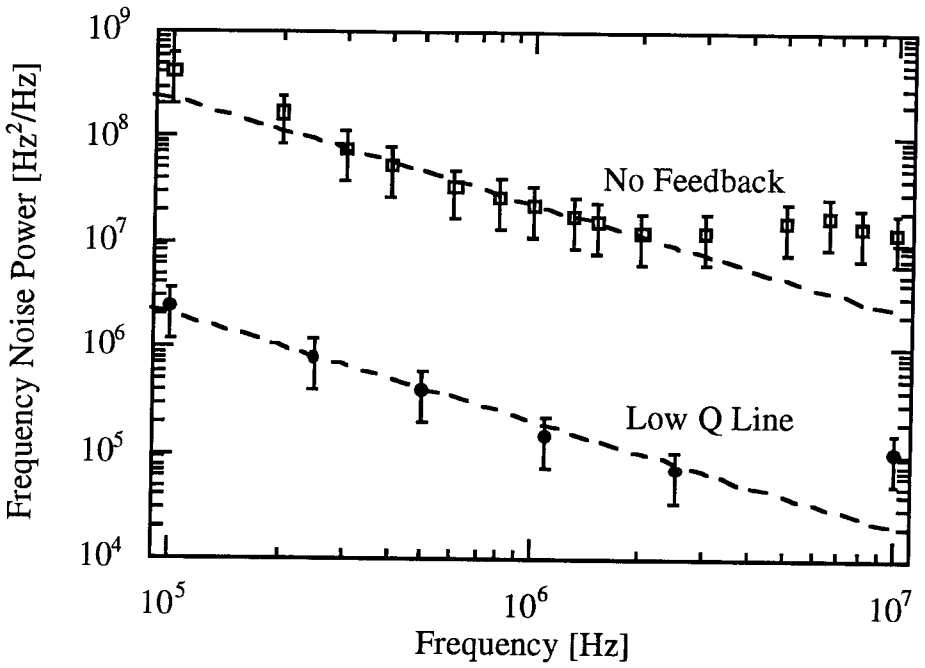

(a)

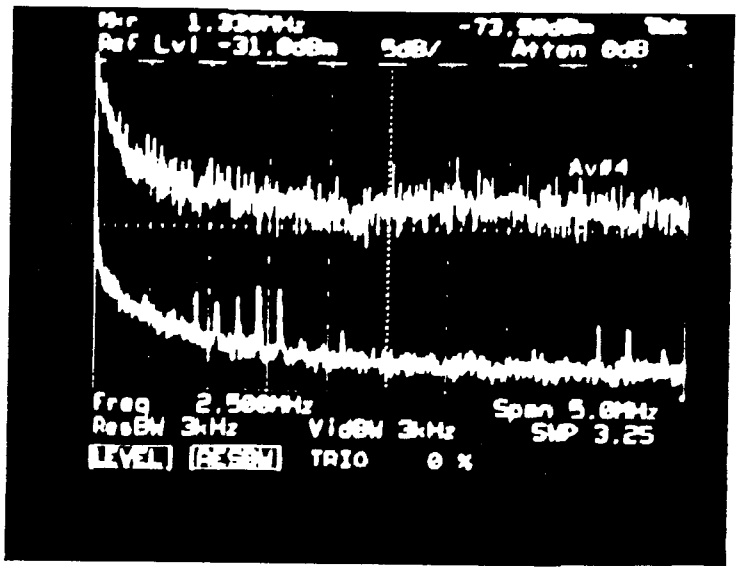

(b)

Figure 2-9: (a) Frequency noise power spectrum for the free-running laser and for the laser when locked to the low-Q line. (b) A spectrum analyzer trace showing the continuous frequency noise power spectrum between DC and 5 MHz without (upper trace) and with (lower trace) optical feedback from the low-Q line.

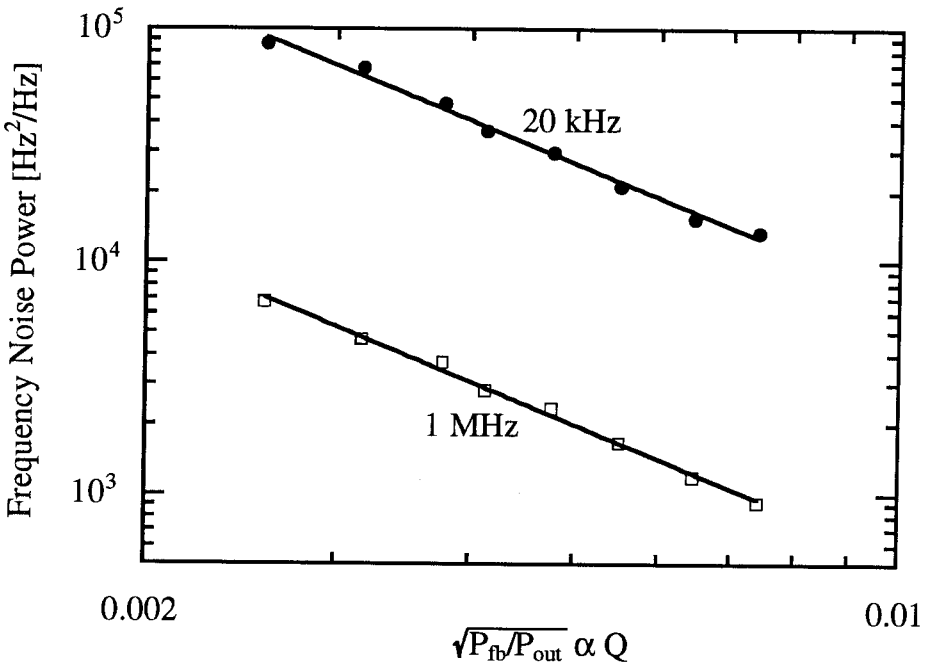

Figure 2-10: Reduction of the laser frequency noise power spectrum as a function of the feedback level for the Doppler-free Cs line. The 1/f cutoff frequency is 300 kHz so the two frequencies measured determine the entire frequency noise spectrum. The power law fits show a $1/Q^2$ dependence.

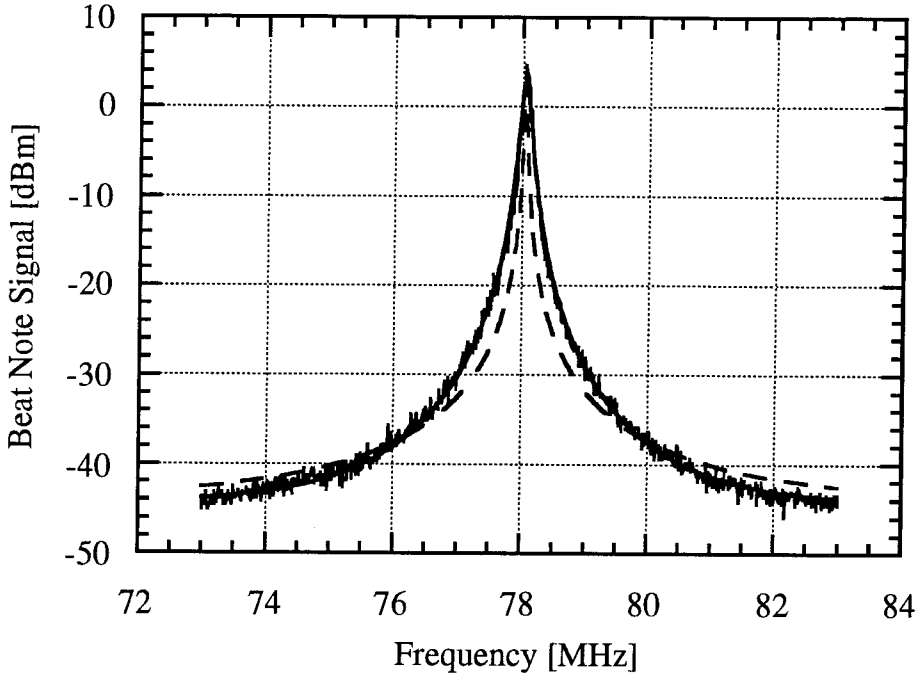

Figure 2-11: A typical self-heterodyne beatnote field spectrum for the laser locked to the high-Q line. The solid line is a fit to a Lorentzian to the power 3/2 indicating that the entire spectrum is dominated by 1/f noise. The broken line is a fit to a Lorentzian spectrum for comparison.

measured to be 300 kHz. The noise power was measured at 20 kHz and 1 MHz for each value of the feedback power and is shown in Figure 2-10. It is found from the slope of the line that $S_{\dot{\phi}}(\Omega) \propto Q^{(-1.95\pm0.1)}$ in agreement with (2.16).

When the linewidth was measured, it was found that the lineshape shown in Figure 2-11 was proportianal to a Lorentzian to the power 3/2 suggesting (according to the discussion of the previous section) that 1/f noise dominated the entire field spectrum. This is, of course, expected since at large values of Q, the white noise linewidth should be very much smaller than the 1/f noise linewidth and should therefore be difficult to observe in the field spectrum. The calculation of the linewidths from the noise spectrum shown in Table 2.1 indicates that this is indeed the case. An attempt to fit the data to a Lorentzian (broken line in Figure 2-11) gave very poor correspondence. These spectra were again measured as a function of feedback power and the extracted 1/f linewidths are plotted against the square root of the feedback

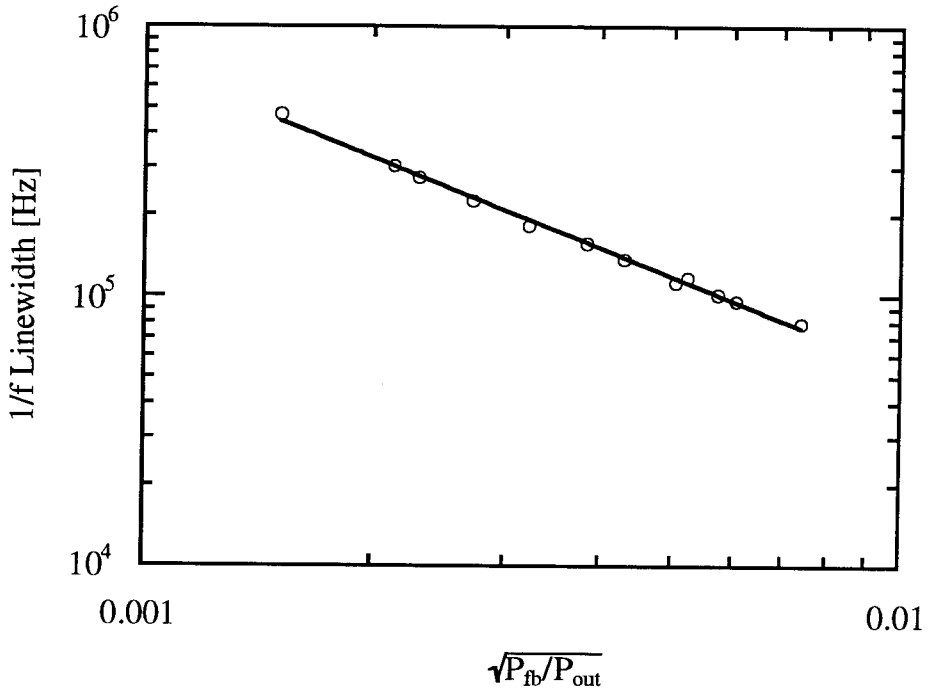

Figure 2-12: 1/f linewidth measurements, obtained from spectra as in Figure 2-11, as a function of feedback level. The fit indicates a 1/Q dependence.

power in Figure 2-12. Again it is found that $\Delta\omega_{1/f} \propto Q^{(-1.02\pm0.05)}$ in agreement with theory.

In order to measure the effect of feedback on the white noise linewidth as compared to the 1/f noise linewidth, the entire procedure above was repeated for the low Q line. Since $d\phi/d\omega$ was much smaller for this line, much lower values of Q could be obtained while still retaining enough feedback signal, κ, to be measured.

Figure 2-13 shows a typical self-heterodyne field spectrum for the laser when it was locked to the low-Q line. There appear to be two regions: one, near the center of the line, which falls off rapidly with $(\omega - \omega_m)$ and a second, in the wings, which falls off much more slowly. The solid line superimposed on the field spectrum is a twelve term approximation to the Voigt profile. As can be seen, the fit is close to the measured spectrum near the peak and also far from the peak but deviates the most in

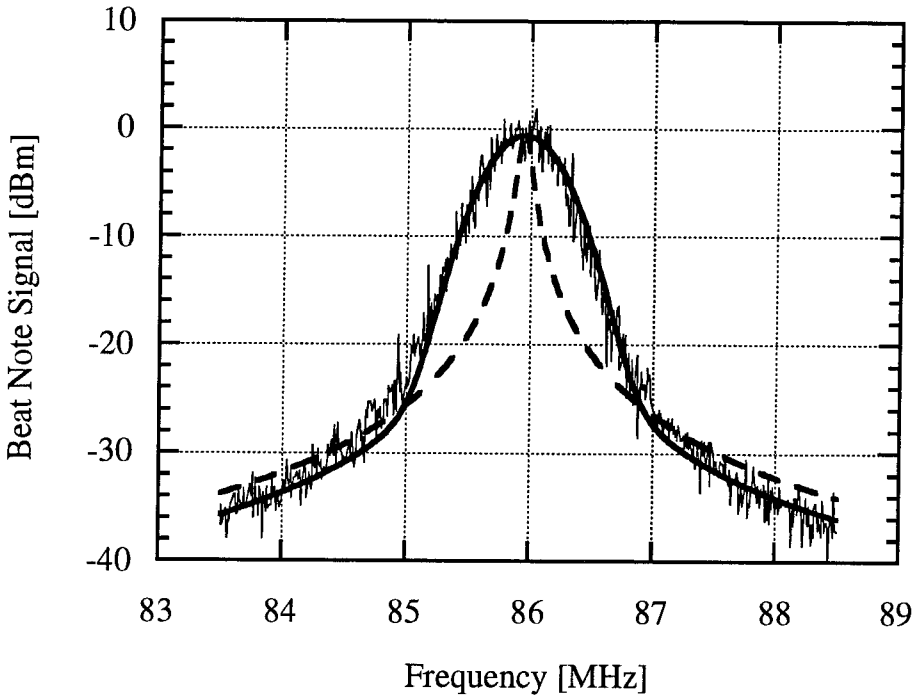

Figure 2-13: A typical self-heterodyne beatnote lineshape for the laser locked to the Doppler-broadened Cs line. The solid line is fit to a 12-term approximation to a Voigt profile. This provides a considerably better fit than either a pure Lorentzian (broken line) or a Lorentzian to the power 3/2. From the Voigt fitting parameters, both the 1/f linewidth and the white noise linewidth could be extracted.

the intermediate region. It is thought that in this region, the Gaussian approximation for the 1/f noise breaks down but the white noise component of the linewidth is still too small to dominate. Both a Lorentzian fit (broken line in Figure 2-13) and a Lorentzian to the power 3/2 failed to represent the data well.

Fitting the spectra to a Voigt Profile enabled the extraction of both a 1/f linewidth and a white noise linewidth from each measured spectrum. These are plotted in Figure 2-14 as a function of the square root of the feedback power. From the slopes of the two lines it is found that $\Delta\omega_{W.N.} \propto Q^{(-2.1\pm0.1)}$ and that $\Delta\omega_{1/f} \propto Q^{(-1.1\pm0.1)}$ again as predicted by the theory.

To confirm that the frequency noise spectrum was still behaving in the same way in these low-Q line measurements as it was for the high Q line, the dependence of the frequency noise spectrum on the feedback power was again measured and is shown in

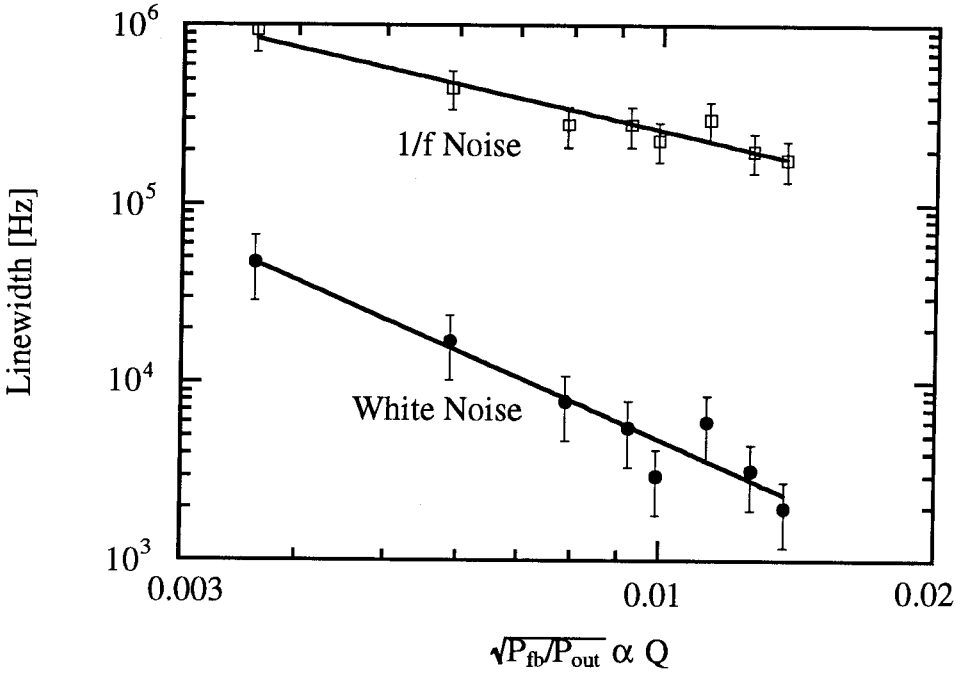

Figure 2-14: Linewidths extracted from the Voigt fit as in Figure 2-13 as a function of feedback level. The fits indicate that the 1/f noise linewidth drops by 1/Q while the white noise linewidth drops by $1/Q^2$, as expected.

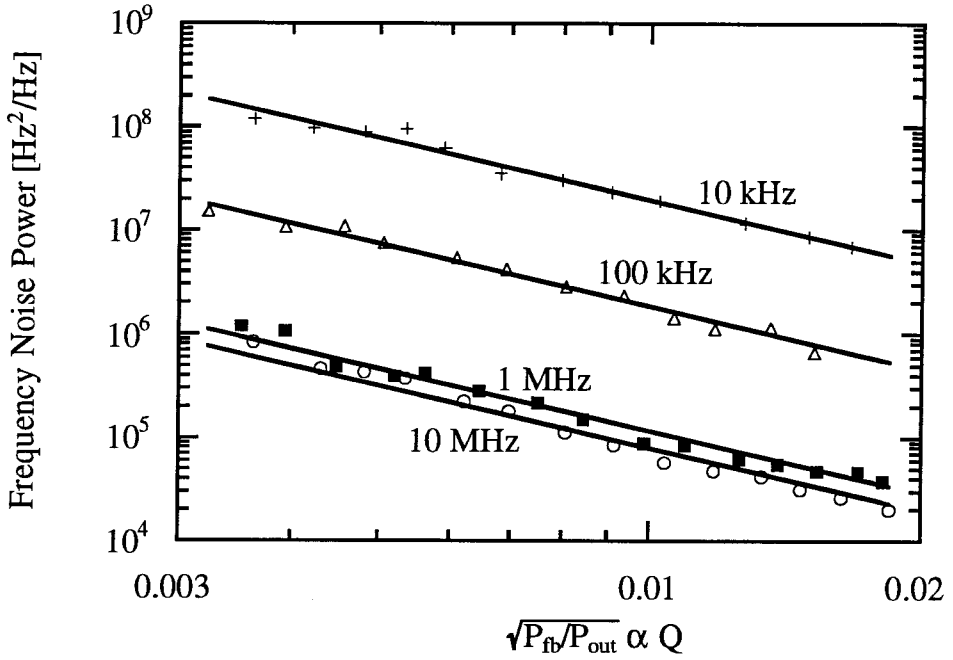

Figure 2-15: Frequency noise power spectrum as a function of the feedback level for the laser locked to the Doppler-broadened Cs line. The noise spectrum clearly drops by $1/Q^2$ agreeing with the measurement for the high-Q line.

Figure 2-15. Data were taken at ten different frequencies ranging from 1 kHz to 10 MHz, four of which are shown in the figure. As in the measurement with the high Q line, it is concluded that $S_{\dot{\phi}}(\Omega) \propto Q^{(-2.01\pm0.07)}$ for both the 1/f noise and the white noise.

From these results, it is confirmed that the entire low frequency ($\Omega < 10$ MHz) frequency noise spectrum is indeed reduced by a factor of $1/Q^2$ when feedback is applied from an external cavity. A reduction of up to 10^5 was measured in this quantity using feedback. When the self-heterodyne linewidth is measured, however, this dramatic reduction is somewhat masked by the fact that $\Delta\omega_{1/f} \propto \sqrt{S_{\dot{\phi}}^{1/f}}$ and so at high values of Q, when the noise reduction is the largest, the linewidth is only reduced by a factor of $1/Q$. But very low frequency fluctuations are readily reduced by other means such as electronic feedback. Such schemes can, of course, be applied to a system already operating with optical feedback and one such experiment is described

in the next chapter.

2.6 Conclusions

In this chapter, the effects of optical feedback on the frequency noise power spectrum and the spectral linewidth of a semiconductor laser have been examined both experimentally and theoretically. It is found that frequency noise power spectra containing a combination of 1/f noise and white noise are reduced uniformly within the bandwidth of the optical feedback by a factor of $1/Q^2$. When white noise component dominates the laser linewidth, the linewidth is reduced by this same factor of $1/Q^2$. However, when 1/f noise is the most important contribution, the linewidth reduction can be orders of magnitude smaller because the low-frequency portion of the noise spectrum, where the noise is higher, becomes increasingly more important as the linewidth is reduced. Thus, the existence of 1/f noise is a basic limitation to linewidth reduction using optical feedback techniques.

Chapter 3

Linewidth reduction with optical feedback and FM sideband locking

3.1 Introduction

In Chapter 2, it was found that under optimum optical feedback conditions, the laser linewidth reduction was limited by low-frequency 1/f noise. While the reduction of the white noise component of the frequency noise power spectrum led to a sub-kilohertz contribution to the linewidth, the reduced 1/f noise component generated a much larger (10 kHz) linewidth due to the square-root dependence of the linewidth on the level of the 1/f noise (and therefore on the feedback power). This suggests that if the 1/f frequency noise were to be substantially reduced by means other than optical feedback, the linewidth would approach the narrow white noise value.

Since 1/f noise occurs at low frequencies, it is a good candidate for reduction through electronic feedback. Electronic servo systems typically work best at lower frequencies, being limited by amplifier bandwidths and technical issues such as parasitic feedback phase shifts. As a result, a potential linewidth reduction system might be to use optical feedback to reduce the high-frequency white noise component of the noise and then use electronic feedback to further reduce the low-frequency noise. This chapter will focus on exactly this problem. Electronic feedback is added to the stabilization system alongside the optical feedback scheme using the FM sideband

locking technique [59,60]. Both feedback systems are implemented using the atomic transition in Cs as the reference frequency leading to excellent absolute low frequency stability. The addition of the electronic feedback requires few components in addition to those used in the optical feedback system and therefore is easy to add to the existing system.

3.2 Electronic feedback

The principle involved in electronic feedback schemes is simple and is shown in Fig. 3-1. The frequency of the laser is first compared to that of a fixed reference such as an external Fabry-Perot cavity or atomic transition. The difference between the two frequencies is then translated into an electrical signal and fed back into the laser injection current which in turn changes the laser frequency to bring it closer to the reference.

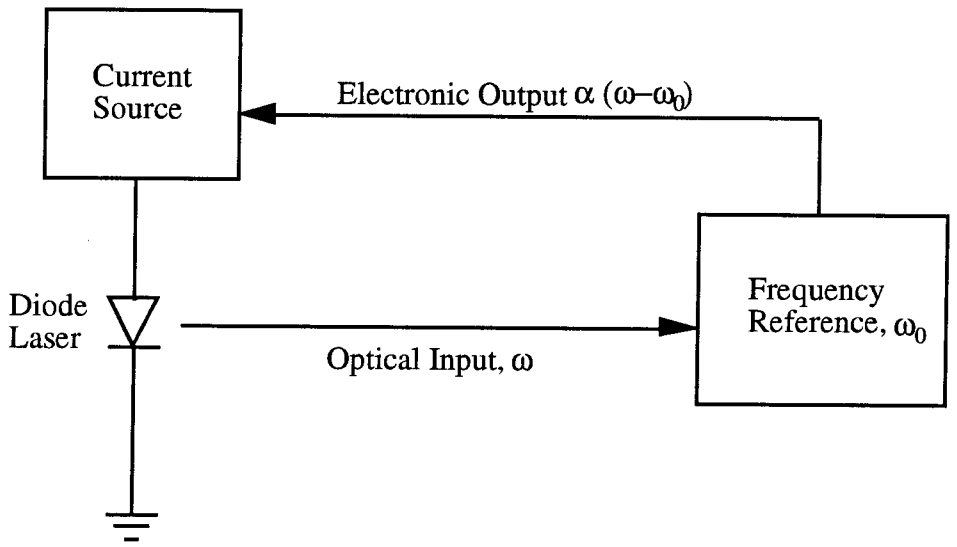

Figure 3-1: Schematic of electronic feedback experiments.

Several methods for translating the frequency difference into a voltage have been proposed, two of the more popular being the FM sideband locking technique [59,60]

and direct discrimination using the side of the resonance line. In the direct detection technique, the laser is tuned to the side of the resonance line and the reflected (or transmitted) power is measured with a photodetector. Frequency fluctuations are translated into intensity fluctuations by the local frequency dependence of the reflection (or transmission) coefficient which results in photocurrent fluctuations which can be amplified and sent directly back to the laser injection current driver. While this technique has the advantage of being simple to implement, it is unable to lock the laser to the peak of the resonance where the slope is zero. The low frequency amplitude noise of the laser is also a problem since this noise will be picked up by the detector and translated into frequency fluctuations by the feedback. FM sideband locking avoids both of the above problems and is discussed in the next section.

It should be noted that there is nothing which prevents electronic feedback schemes from being implemented simultaneously with optical feedback. In many ways they are complimentary techniques, the optical feedback being effective at reducing the higher frequency noise where electronic feedback is harder to use and the electronic feedback providing the additional noise control at lower frequencies where excess noise such as 1/f noise is often found.

3.2.1 FM sideband locking

FM sideband locking [59,60] can be used to electronically lock a laser to the top of a resonant transmission/reflection spectrum such as an optical cavity or atomic resonance. The principle of the technique is shown schematically in Figure 3-2. Frequency modulation is applied to the output optical field of the laser to be stabilized. This can be accomplished either electro-optically or by some other method. The small FM modulation creates frequency sidebands in the laser field spectrum which are spaced symmetrically about the carrier frequency. The beatnotes between each sideband and the carrier are initially equal in magnitude but out of phase by π resulting in no net signal at the modulation frequency when the light is photo-detected.

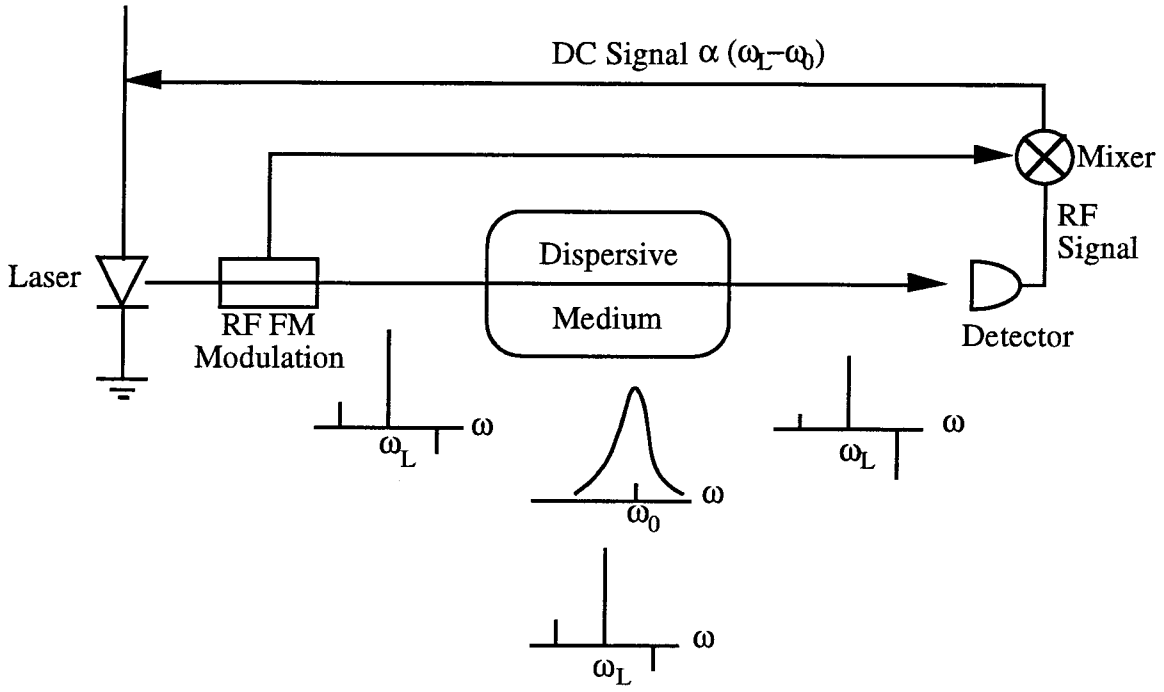

Figure 3-2: Schematic of the FM sideband locking technique.

The light is then passed through the resonant element and the laser roughly tuned to the peak of the transmission (or reflection) spectrum. If the spectrum is symmetrical and the laser carrier frequency is exactly equal to the peak frequency, each of the FM sidebands undergoes an identical attenuation and relative phase shift as it passes through the resonant element (see Figure 3-2). Thus, on photodetection, again no beatnote signal is observed. However, if the laser frequency drifts to one side of the transmission peak, one sideband will undergo a different attenuation/phase shift from the other and thus a signal at the modulation frequency is measured in the detector. This signal will be of one phase if the laser frequency moves to one side of the resonance peak and of a phase π different if it moves to the other side.

Next, the photodetector output is sent to a doubly balanced mixer which uses as a reference the original modulation signal. With the appropriate phase delay inserted into one of the input arms, the mixer output becomes a dispersive DC lineshape as

the laser frequency moves over the resonance, positive on one side of the peak and negative on the other. This error signal can then be electronically fed back into a frequency control element with the appropriate gain and filtering to reduce the laser noise.

The noise reduction here is limited at a fundamental level by shot noise in the photodetector [60] and therefore excellent signal-to-noise ratios in the feedback system can be obtained. In addition, large feedback bandwidths can be obtained if the reflection mode from an optical cavity is used due to the phase storage process which occurs in the cavity. As a result this method is currently an extremely useful operational technique for locking lasers to optical cavities.

3.3 Semiconductor laser locking to an atomic resonance

The extension of the FM sideband locking technique to semiconductor lasers is straightforward and has the advantage that the FM sidebands can be easily applied by modulating the laser's injection current. This eliminates the need for an expensive electro-optic modulator and simplifies the experimental setup somewhat. In addition, almost no optical extensions to the setup used for optical feedback alone are required and the sideband locking can operate concurrently with the optical feedback.

The experimental apparatus is shown in Figure 3-3. The optical feedback system is almost identical to that described in Section 2.2.3. The only change is the insertion of a polarizing beamsplitter (PBS in Figure 3-3) between the first polarizer, P_1, and the Cs cell. The purpose of this polarizing beam splitter (PBS) is to redirect part of the return optical feedback beam into a photodetector for use with the electronic feedback. By using a polarizing component, only the polarization perpendicular to P_1 is split off and since this component would otherwise be absorbed by P_1, no operational change to the optical feedback is needed.

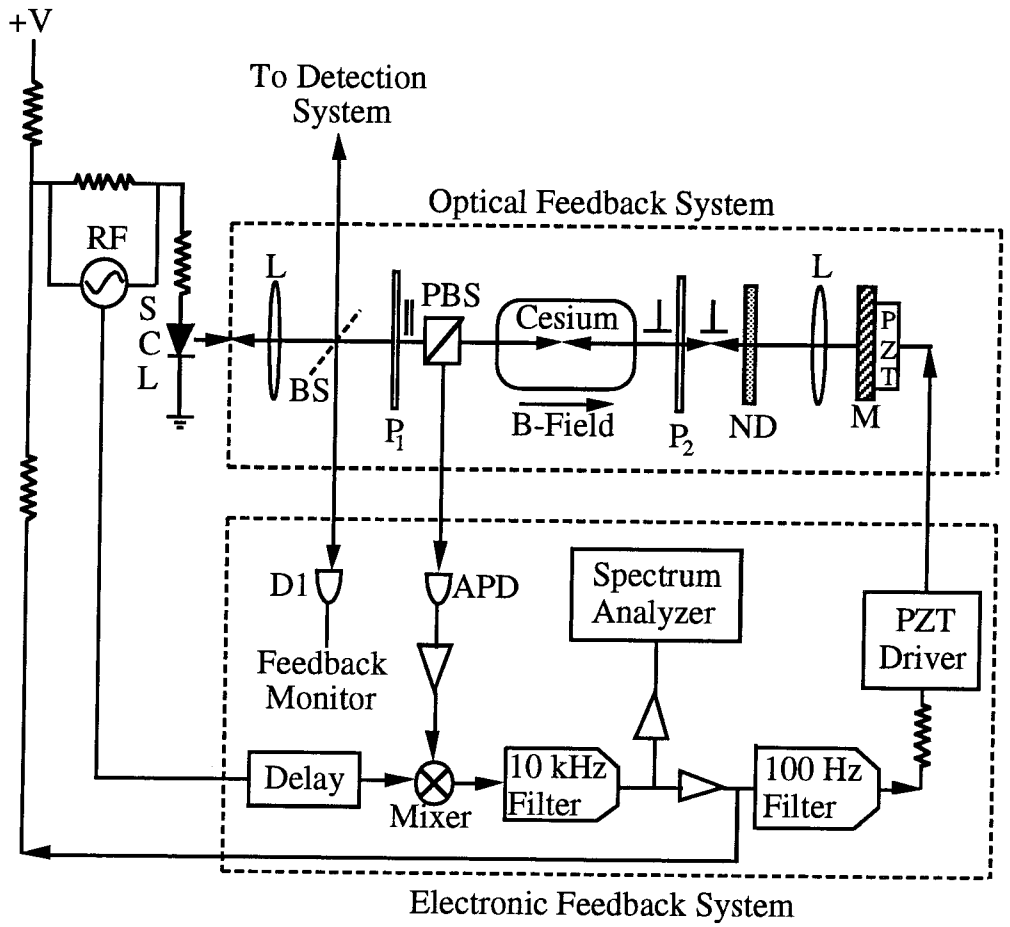

Figure 3-3: Experimental implementation of the FM sideband locking technique concurrently with optical feedback.

The laser (STC Model LT50A-03U) with a threshold current of 50 mA and operating at 120 mA (85 mW) was locked to the external cavity using optical feedback exactly as described in Section 2.2.3. The laser injection current was modulated at 28.7 MHz generating FM modulation at this frequency. As mentioned in Section 2.2.3 the frequency chirp is ordinarily substantially reduced by the application of optical feedback due to frequency-pulling effects. However, by modulating at a frequency corresponding to the external cavity FSR, the feedback fluctuations at this frequency are actually phase shifted by π with respect to the internal field fluctuations resulting in positive feedback and causing an enhancement of the modulation response [61]. Approximately 1% of the total laser power was measured to be in the sidebands.

The portion of the return beam reflected by the PBS was detected in an avalanche photodiode and the resulting photocurrent amplified before being sent to the doubly balanced mixer for demodulation. The driving RF signal, delayed appropriately, was used as the other input to the mixer and a dispersive lineshape was measured at the output. This error signal, shown in Figure 3-4, is obtained by scanning the end mirror PZT position. Trace A is the feedback power, measured at D_1, and trace B is the error signal after demodulation. Because of the strong frequency pulling at this feedback level, the laser frequency scans over the Doppler-free Cs line as the PZT position is changed. However, because of the changing feedback strength (which depends in turn on the lasing frequency), the abscissa in Figure 3-4 is not linear in frequency (although it *is* monotonically increasing). Nevertheless, it can be seen that a dispersive error signal is produced.

3.4 Results: noise reduction with electronic feedback

The error signal was amplified and then fed back into both the end mirror PZT and the laser injection current after some simple filtering. The intention was to reduce

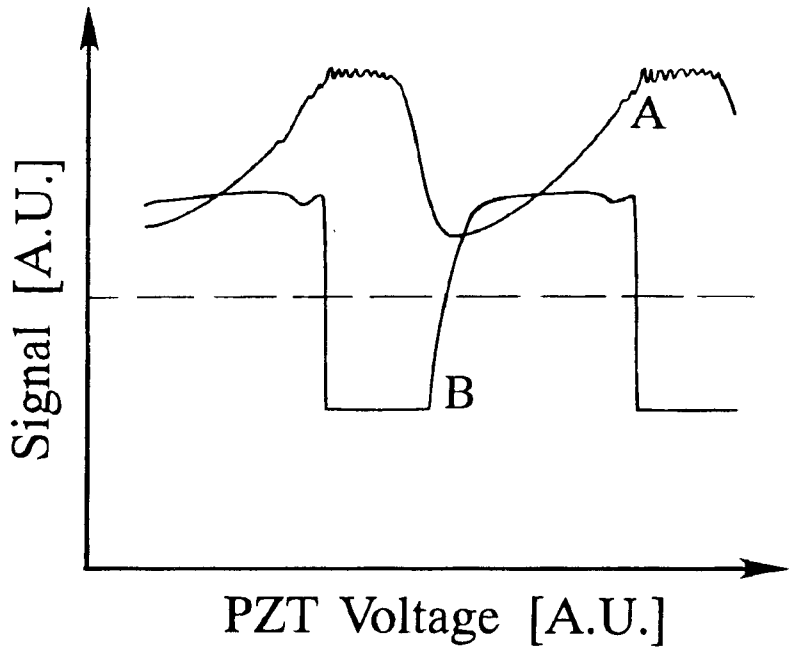

Figure 3-4: Optical feedback power (trace A) and electronic feedback error signal (trace B) as a function of the laser frequency. These curves were obtained by varying the end mirror PZT position (note that because of the chirp reduction, the horizontal axis is not linear with frequency).

the noise only at frequencies below a few tens of kHz since it is noise in the frequency regime which predominantly contributes to the linewidth under feedback conditions. Hence, a simple low pass RC filter with a cutoff frequency of 10 kHz was used for the injection current feedback. An additional, lower frequency, RC filter was used for the PZT feedback since the PZT was found to have a strong mechanical resonance at about 2 kHz. The frequency noise power at frequencies less than 100 kHz was measured within the servo loop using an electronic spectrum analyzer (see Figure 3-3). The noise level was calibrated by comparison at high frequencies ($>$ 100 kHz) with the noise level measured using an external optical cavity (as in Section 2.4). The laser was tuned to the side of the transmission fringe and a simple feedback loop was implemented at frequencies below 1 kHz to lock the cavity to the laser. The intensity fluctuations on the reflected beam were then measured using an electronic spectrum analyzer. Figure 3-5a shows the raw measured spectrum from the external cavity as a function of frequency. Trace A is the noise with optical feedback alone and trace B is with both optical and electronic feedback. Due to the cavity stabilization system which operated at low frequencies and vibrations of the cavity itself, this measurement could only be considered accurate at frequencies above a few tens of kHz.

The low frequency noise was measured inside the FM locking feedback loop itself using the atomic vapor as an absolute frequency reference. The noise measured this way was then calibrated by comparing it to the cavity measurements at higher frequencies. The noise power of the FM error signal is shown in Figure 3-5b as a function of frequency. The error signal (without electronic feedback but with optical feedback) was found to be at least 20 dB above the detector noise floor at low frequencies and 10 dB above at higher frequencies. Trace A in Figure 3-5b is the error signal noise without electronic feedback (but with optical feedback). The noise is found to be roughly 1/f at frequencies below 100 kHz. Trace B shows the noise when the electronic feedback is applied. It can be seen that at low frequencies, the frequency noise power is reduced by over two orders of magnitude from its value with optical

feedback alone. At higher frequencies, the reduction is smaller but still roughly an order of magnitude up to 100 kHz and the spectrum approaches that of white noise. The peaks in the spectra correspond to the 60 Hz line frequency (and harmonics) and to the end mirror PZT mechanical resonance of 2 kHz (for trace B).

The absolute measurement of the frequency noise power above suffers from the same difficulties described in Section 2.4. This measurement of the noise power was therefore double-checked by measuring the laser linewidth with a delayed self-heterodyne measurement system which incorporated a 5 km delay. The beatnote signal is shown in Figure 3-6, trace A being with optical feedback alone and trace B being with both optical and electronic feedback. The linewidth is clearly reduced from 20 kHz without electronic feedback to below the resolution of the measurement system. The delta-function peak in the center of trace B and the oscillation in the wings are characteristic of a coherence time longer than the optical delay between the two arms of the self-heterodyne measurement system [21].

From the experimental data in Figure 3-5, the actual laser linewidth could be calculated using the formula

$$S_E(\omega) = 4Re \int_{-\infty}^{\infty} \exp[2\pi i(\nu - \nu_0)\tau - 2(\pi\tau)^2\sigma^2(\tau)]d\tau \tag{3.1}$$

where

$$\sigma^2(\tau) = \int_0^{\infty} S_f(f)\frac{\sin^2(\pi f\tau)}{(\pi f\tau)^2}df. \tag{3.2}$$

This calculated field spectrum is shown in Figure 3-7 both without electronic feedback (trace A) and with (trace B). The calculated linewidth with electronic feedback is 1.4 kHz FWHM which represents over an order of magnitude improvement from with optical feedback alone (20 kHz FWHM). The comparison of this calculated value of the linewidth without electronic feedback with the self-heterodyne measurement serves as a good check of the calibration of the frequency noise power and is shown on a linear scale in Figure 3-8. Trace A is the measured self-heterodyne beatnote (for

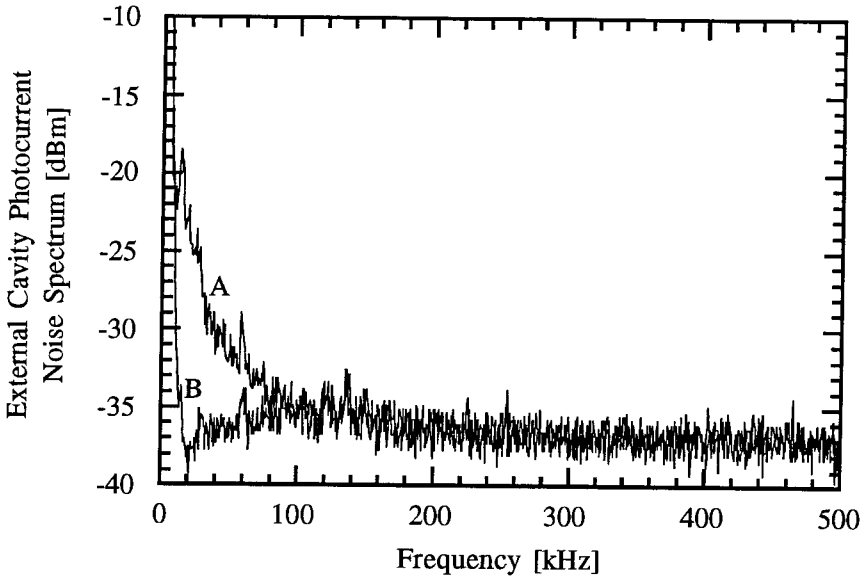

(a)

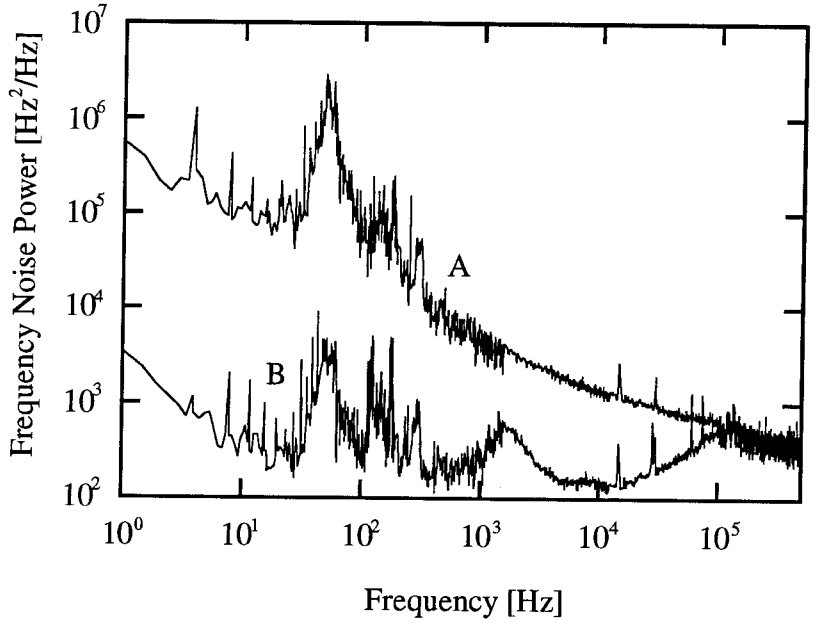

(b)

Figure 3-5: Frequency noise power spectral density. (a) Raw data measured with an external cavity. (b) Noise power measured inside the FM sideband locking feedback loop. In both figures trace A is obtained with optical feedback alone while trace B is with both optical and electronic feedback.

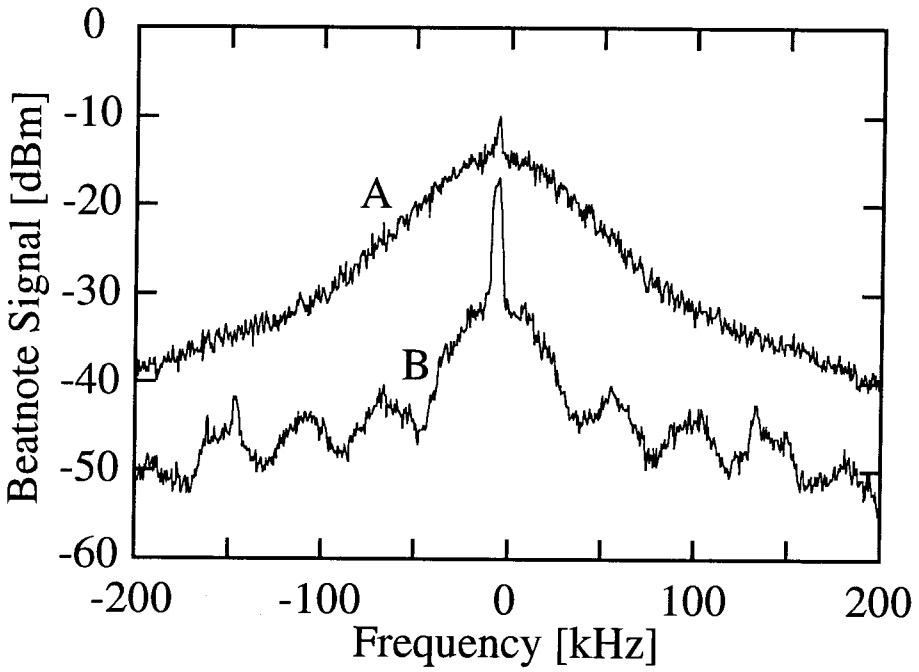

Figure 3-6: Self-heterodyne beat-note signal. Trace A is obtained with optical feedback alone while trace B is with both optical and electronic feedback. The ripples and central delta-function in trace B are an indication that the linewidth was below the resolution limit of the self-heterodyne measurement apparatus.

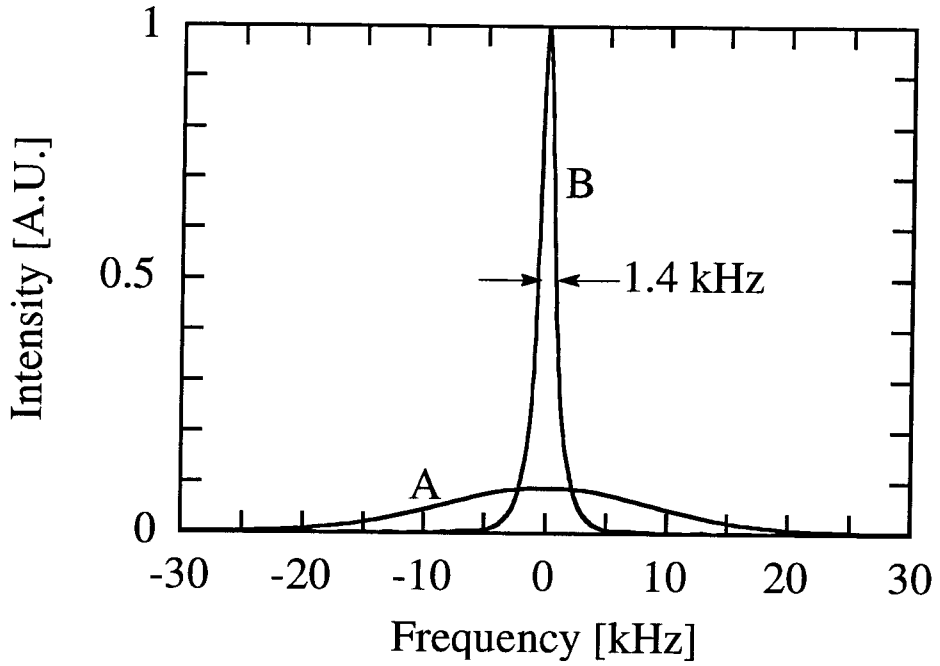

Figure 3-7: Field spectrum calculated with the data from Figure 3-5 with optical feedback alone (trace A) and with both optical and electronic feedback (trace B).

which the frequency axis has been expanded by a factor of two to account for the fact that self-heterodyne linewidths are double the real spectral linewidth) and trace B is the calculated spectrum. Reasonable agreement is found.

Another measure of the quality of the frequency stability is the Allen variance [62] which is defined by [62,63]

$$\sigma_y^2(\tau) = \frac{1}{4\pi\nu_0^2} \left\langle [\bar{\dot{\phi}}(t+\tau) - \bar{\dot{\phi}}(t)]^2 \right\rangle \tag{3.3}$$

where ν_0 is the nominal oscillation frequency, $\bar{\dot{\phi}}(t)$ is the average frequency deviation integrated over a time τ about t and $< ... >$ denotes an average over the statistical ensemble. This quantity represents the extent to which the oscillator could be used as a frequency reference if the output signal is measured for a time τ. It can be shown [63] that the Allen variance can be written in terms of the frequency noise power

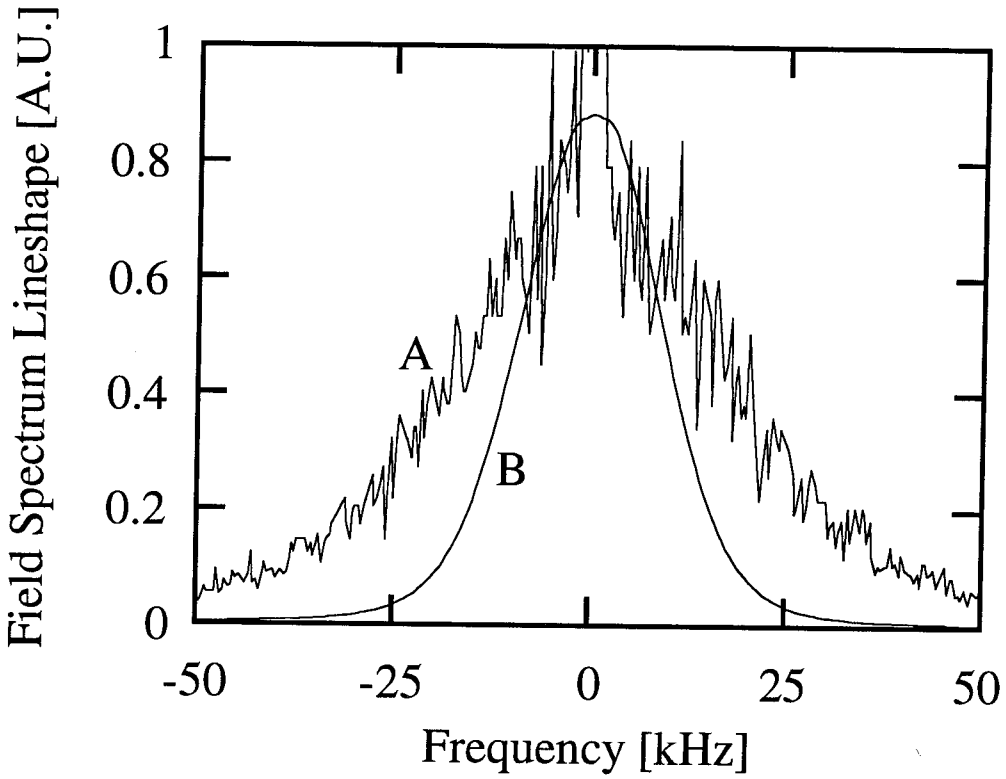

Figure 3-8: Comparison of measured self-heterodyne lineshape (trace A) with the field spectrum profile of Figure 3-5 (trace B). The self-heterodyne profile has been divided by $\sqrt{2}$ along the frequency axis to account for the difference between the measured linewidth and the self-heterodyne linewidth.

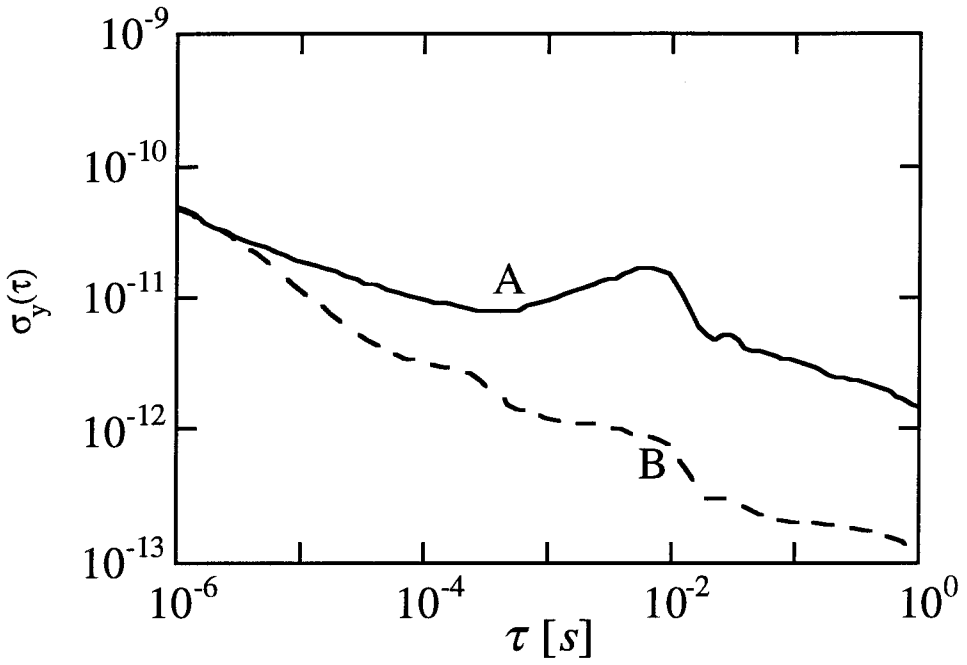

Figure 3-9: Square root of the Allen variance calculated from Figure 3-5 with optical feedback only (trace A) and with optical and electronic feedback (trace B).

spectrum as

$$\sigma_y^2(\tau) = \frac{2}{\nu_0^2}\int_0^\infty S_f(f)\frac{\sin^4(\pi f\tau)}{(\pi f\tau)^2}df. \tag{3.4}$$

The Allen variances calculated using (3.4) for the frequency noise power spectra in Figure 3-5 are shown in Figure 3-9. Trace A is with optical feedback alone and trace B is with both optical and electronic feedback. An improvement in the Allen variance by an order of magnitude is obtained at an integration time of 20 ms indicating a significant improvement in the absolute frequency stability of the laser.

There are several sources of noise which could have contaminated the electronic feedback system and which may have limited its effectiveness. Shot noise in the photodetector generates noise around the modulation frequency which will then be mixed down to near DC in the signal extraction process. In addition, avalanche photodiodes are known to have excess noise caused by the avalanche multiplication process [64]

which may have been substantially larger than the shot noise level. Amplitude noise in the laser itself near the modulation frequency would also have generated additional noise which would have been coupled into the laser frequency by the feedback. Finally, the interaction of the counter propagating beams in the atomic vapor could also have generated some excess noise on the probe beam, but since the details of the interaction are not fully known, it is difficult to ascertain how much this may have been.

Several other groups have recently reported an improvement in the linewidth of a semiconductor laser using electronic feedback [65,43,20,66,67,19,68]. The FM sideband locking technique has been employed for a semiconductor laser by Nakagawa et al. [65] using a multi-section DFB laser and an optical cavity as a frequency reference. A reduction in the frequency noise spectrum to less than 25 Hz^2/Hz was obtained leading to an estimated linewidth of 160 Hz FWHM. However, the free-running linewidth of this laser was already quite small at 680 kHz. Lee and Campbell [43] also demonstrated frequency stabilization using the FM sideband technique with velocity-selective Faraday transmission in Rubidium as the resonant locking element. They obtained a linewidth of 500 kHz under optimum conditions. Finally, a semiconductor laser linewidth of 7 Hz was reported by Shin and Ohtsu [20] using a commercially available Fabry-Perot laser with both optical feedback from a high-finesse cavity and electronic feedback.

3.5 Conclusion

It has been demonstrated that the frequency stability of a semiconductor laser operating initially with optical feedback can be significantly improved with the addition of electronic feedback to reduce the low-frequency fluctuations. A reduction of the frequency noise power spectrum by over two orders of magnitude was obtained leading to an improvement of the spectral linewidth by an order of magnitude. The mini-

mum linewidth calculated from the measured frequency noise power spectrum with both optical and electronic feedback operating simultaneously was 1.4 kHz, an improvement over the free-running linewidth by a factor of about 10^4. In addition, the low-frequency stability with electronic feedback, as measured by the Allen variance, is improved by an order of magnitude from the stability with optical feedback alone. An Allen variance of $\approx 2 \times 10^{-13}$ is measured at an integration time of 20 ms.

Chapter 4

Effects of optical feedback on the quantum noise properties of semiconductor lasers

4.1 Introduction

The generation of squeezed states of the electromagnetic field [69] has received considerable interest in recent years. Such states feature a redistribution of the fundamental quantum mechanical fluctuations which occur in the optical field due to the Heisenberg Uncertainty Principle. Quadrature squeezed states, the first squeezed states to be produced in the lab [70,71,72], feature reduced noise in one quadrature of the electric field operator and increased noise in the other. Amplitude squeezed states exhibit a reduction in the fluctuations in the photon number operator at the expense of the field phase, a perfectly amplitude squeezed state being the familiar number state or Fock state.

In addition to the fundamental scientific interest in the generation of non-classical states of the electromagnetic field, squeezed states have a number of potential applications to situations where precision, low-noise measurements must be made. These applications include optical communication [16], quantum cryptography [17], gravitational wave detection [15] and sensitive spectroscopy [73,74] and interferometry [75]. It should be noted that while the application of amplitude-squeezed states to the above problems certainly seems possible, it is not clear that the advantages out-

weigh the difficulties. With the exception, perhaps, of quantum cryptography, one can achieve similar improvements in performance by just increasing the output power of the laser. In addition, the sensitivity of the degree of squeezing to optical losses would make the application of squeezed light in a commercial setting somewhat difficult, especially for long-distance communications systems. Thus, although there would appear to be the *potential* for using amplitude-squeezed states in a variety of applications, the actual demonstration of a definite advantage in a specific situation remains to be performed.

Of the methods proposed for the generation of amplitude squeezed light, one of the most successful to date has been the use of a pump-suppressed semiconductor laser [10]. If the laser is pumped far above threshold, the amplitude noise on the output field is determined almost entirely by fluctuations in the pumping rate. If, in addition, the laser is driven with a constant-current source, then the statistical pump fluctuations in the injection current (which result in shot noise) can be suppressed [76] and are replaced instead by thermal noise generated by the series resistance of the current source. This thermal noise can be made arbitrarily small by making the series resistance large enough. The result is that the light at the laser output is amplitude squeezed, the degree of squeezing under strong pumping being limited on a fundamental level only by the efficiency of the device.

4.2 Amplitude noise in semiconductor lasers

4.2.1 The quantum theory of amplitude noise in semiconductor lasers

While the phase noise and linewidth of a semiconductor laser can be treated adequately within the semiclassical theory of the laser, a proper analysis of the low frequency amplitude noise requires the use of a fully quantum mechanical optical field. The reason for this is that because of the strong gain clamping mechanism above

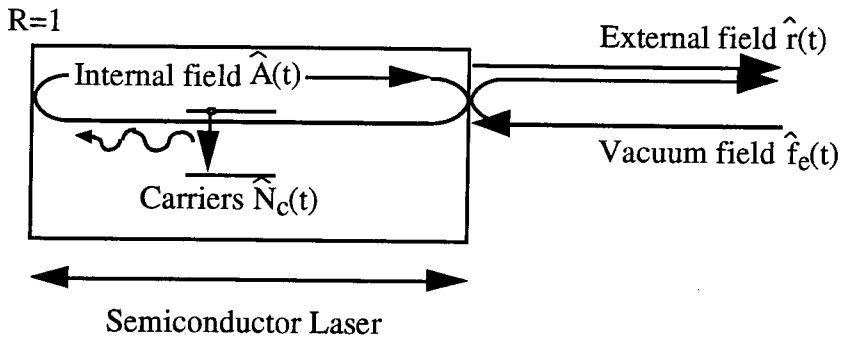

Figure 4-1: The basic model of a semiconductor laser used in the analysis of the quantum mechanical amplitude noise. The internal field, $\hat{A}(t)$, is coupled to both the electron system, $\hat{N}_c(t)$, and external field $\hat{r}(t)$.

threshold, the low frequency amplitude noise of a semiconductor laser approaches the SQL even at moderate pump rates. Since it is precisely the quantum nature of the field which gives rise to the SQL, the fully quantum mechanical theory of the laser must be used. While the low frequency part of the spectrum is intrinsically non-classical at moderate or high pump rates, it should be noted that some amplitude noise phenomena such as the noise around the relaxation resonance peak or the noise very close to threshold can be calculated correctly within the semiclassical theory [77].

The quantum theory of intensity noise in semiconductor lasers used here is based on the basic Langevin equation model [78] with modifications and extensions due to McCumber [79], Lax [80], Haug [9] and Yamamoto [10,76]. The model is shown in Figure 4-1. The laser can be described, after the adiabatic elimination of the dipole-moment operator, using two quantum Langevin equations for the inversion operator $\hat{N}_c(t)$ and the slowly-varying internal optical field annihilation operator $\hat{A}(t)$ in addition to the input/output relation connecting the slowly-varying external field

$\hat{r}(t)$ with the internal field. These can be written [10]

$$\frac{d}{dt}\hat{N}_c(t) = P - (1-\beta)\frac{\hat{N}_c(t)}{\tau_{sp}} - \frac{\omega}{\mu^2}\hat{\chi}_i\hat{A}^\dagger\hat{A} - \left\langle \frac{\omega}{\mu^2}\chi_i \right\rangle + \hat{\Gamma}_p(t) + \hat{\Gamma}_{sp}(t) + \hat{\Gamma}(t) \tag{4.1}$$

$$\frac{d}{dt}\hat{A}(t) = -\frac{1}{2}\left[\frac{1}{\tau_{p0}} + \frac{1}{\tau_{pe}} + 2i(\omega_L - \omega_0) - \frac{\omega}{\mu^2}(\hat{\chi}_i - i\hat{\chi}_r)\right]\hat{A}(t) + \hat{G}(t) + \hat{g}(t) + \sqrt{\frac{1}{\tau_{pe}}}\hat{f}_e(t) \tag{4.2}$$

$$\hat{r}(t) = -\hat{f}_e(t) + \frac{\hat{A}(t)}{\sqrt{\tau_{pe}}} \tag{4.3}$$

where P is the pump rate, β is the fraction of the spontaneous emission which is emitted into the lasing mode, τ_{sp} is the spontaneous emission lifetime, μ is the non-resonant refractive index, $\hat{\chi}(N_c)$ is the resonant optical susceptibility, τ_{p0} and τ_{pe} are the cavity photon lifetimes due to internal absorption and mirror losses respectively, ω_L is the lasing frequency and ω_0 is the cold cavity resonant frequency. The inclusion of β (which is typically $\ll 1$ for large cavity lasers) allows the treatment of micro-cavity lasers. Note that the second term in (4.1) represents the spontaneous emission into non-lasing modes while the fourth term represents spontaneous emission into the lasing mode itself. The Langevin noise terms $\hat{\Gamma}_p(t)$, $\hat{\Gamma}_{sp}(t)$ and $\hat{\Gamma}(t)$ drive the carrier variable and represent noise due to the pumping process, spontaneous emission into non-lasing modes and dipole moment fluctuations respectively. Noise terms $\hat{G}(t)$ and $\hat{g}(t)$ generate fluctuations in optical field variable and are due to dipole moment fluctuations and noise from internal optical losses. Finally, $\hat{f}_e(t)$ is the vacuum field incident on the front facet of the laser and accounts explicitly for noise due to spontaneous emission into the lasing mode. The vacuum field $\hat{f}_e(t)$ is also partially reflected off the front facet of the laser and therefore appears in the output coupling relation, (4.3). Note that in this model, it is assumed that the front facet reflectivity is close to unity and that the rear facet reflectivity is unity. This assumption is not justified for semiconductor lasers which have uncoated or anti-reflection coated facets. A more

general and considerably more complicated model has recently been developed by Tromborg [81] and others which addresses this issue. In this treatment, it was found that when the rear facet is high-reflection coated, the noise on the output from the front facet does not depend strongly on the front facet reflectivity, justifying, to some extent, the model used here.

The Langevin noise terms in (4.1)-(4.3) have correlation functions [10,82]

$$\left\langle \hat{f}_{er}(t)\hat{f}_{er}(u)\right\rangle = \left\langle \hat{f}_{ei}(t)\hat{f}_{ei}(u)\right\rangle = \frac{1}{4}\,\delta(t-u) \tag{4.4}$$

$$\langle \hat{g}_r(t)\hat{g}_r(u)\rangle = \langle \hat{g}_i(t)\hat{g}_i(u)\rangle = \frac{1}{4}\frac{1}{\tau_{p0}}\,\delta(t-u) \tag{4.5}$$

$$\left\langle \hat{G}_r(t)\hat{G}_r(u)\right\rangle = \left\langle \hat{G}_i(t)\hat{G}_i(u)\right\rangle = \frac{1}{4}\left(E_{cv}+E_{vc}+\frac{\beta N_{c0}}{A_0^2\tau_{sp}}\right)\,\delta(t-u) \tag{4.6}$$

$$\left\langle \hat{\Gamma}(t)\hat{\Gamma}(u)\right\rangle = \left[(E_{cv}+E_{vc})A_0^2+\frac{\beta N_{c0}}{\tau_{sp}}\right]\,\delta(t-u) \tag{4.7}$$

$$\left\langle \hat{\Gamma}(t)\hat{G}_r(u)\right\rangle = -\frac{1}{2}\left[A_0(E_{cv}+E_{vc})+\frac{\beta N_{c0}}{A_0\tau_{sp}}\right]\,\delta(t-u) \tag{4.8}$$

$$\left\langle \hat{\Gamma}(t)\hat{G}_i(u)\right\rangle = 0 \tag{4.9}$$

$$\left\langle \hat{\Gamma}_{sp}(t)\hat{\Gamma}_{sp}(u)\right\rangle = (1-\beta)\frac{N_{c0}}{\tau_{sp}}\,\delta(t-u) \tag{4.10}$$

$$\left\langle \hat{\Gamma}_p(t)\hat{\Gamma}_p(u)\right\rangle = \begin{cases} \frac{4k_BT}{q^2R_s}\,\delta(t-u) & (\textit{pump suppressed}) \\ P\,\delta(t-u) & (\textit{constant voltage}) \end{cases} \tag{4.11}$$

where $\hat{f}_{er} = (\hat{f}_e + \hat{f}_e^\dagger)/2$ and $\hat{f}_{ei} = (\hat{f}_e - \hat{f}_e^\dagger)/2i$ are the real and imaginary parts of the noise operator $\hat{f}_e$, $E_{cv} - E_{vc} = \langle(\omega/\mu^2)\hat{\chi}_i\rangle = E_{cv}/n_{sp}$ is the net stimulated emission rate, A_0^2 is the mean photon number, q is the charge on an electron, and R_s is the value of the resistance in series with the laser in the case of pump-suppression. The terms in (4.4)-(4.11) can be derived using the quantum regression theorem (generalized Einstein relations) or understood by considering each noise source as being composed of a large number of independent events, each producing an impulse change in the variables $\hat{a}(t)$ and $\hat{N}_c(t)$. In this case, the mean-square fluctuation of the variable is just equal to the mean rate of occurrence of the events multiplied by the mean-

square change in the variable from each event. For the carrier noise, for example, the three ways in which the carrier density can change are through pumping, spontaneous emission or stimulated emission/absorption. Thus the total correlation function

$$\langle \hat{\Gamma}_p(t)\hat{\Gamma}_p(u)\rangle + \langle \hat{\Gamma}_{sp}(t)\hat{\Gamma}_{sp}(u)\rangle + \langle \hat{\Gamma}(t)\hat{\Gamma}(u)\rangle \tag{4.12}$$

is equal to a delta function (Markoffian processes are assumed) multiplied by the rates of occurrence for each process, P (for pump noise), N_{c0}/τ_{sp} (for spontaneous emission) and $E_{CV}\langle \hat{a}^\dagger \hat{a} + 1\rangle + E_{VC}\langle \hat{a}^\dagger \hat{a}\rangle$ (for stimulated emission/absorption) multiplied again by the effect of each event, which is to change the carrier density by unity. The cross-correlation functions include only those events which change both quantities simultaneously. Poissonian pumping statistics have been assumed here and will be discussed further below.

Equations (4.1) and (4.2) can be solved by writing the carrier density and fields in terms of small signal quantities which fluctuate about mean values: $\hat{N}_c(t) = N_{c0} + \Delta\hat{N}_c(t)$, $\hat{a}(t) = [A_0 + \Delta\hat{A}(t)]e^{i\Delta\hat{\phi}(t)}$ and $\hat{r}(t) = [r_0 + \Delta\hat{r}(t)]e^{i\Delta\hat{\psi}(t)}$. It has been pointed out [83,84] that there is some difficulty in defining a quantum mechanical operator which corresponds to the classical notion of the phase of an oscillator such as the optical field. As a result, the small-signal decomposition of the field operators is not, strictly speaking, valid in a quantum mechanical sense. However, this approach is approximately valid in the limit of small fluctuations about a large mean photon number. In this case the noise on the field can be described by small fluctuations in the quadrature phase amplitudes about a large mean value as in Figure 4-2. The amplitude fluctuations are then approximately equal to the fluctuations in the quadrature amplitude in phase with the optical field while the phase fluctuations are proportional to the quadrature amplitude out of phase with the optical field. Thus, the amplitude and phase fluctuations may be defined by

$$\Delta\hat{A}(t) = \frac{1}{2}\left(\hat{a}(t) + \hat{a}^\dagger(t)\right) \tag{4.13}$$

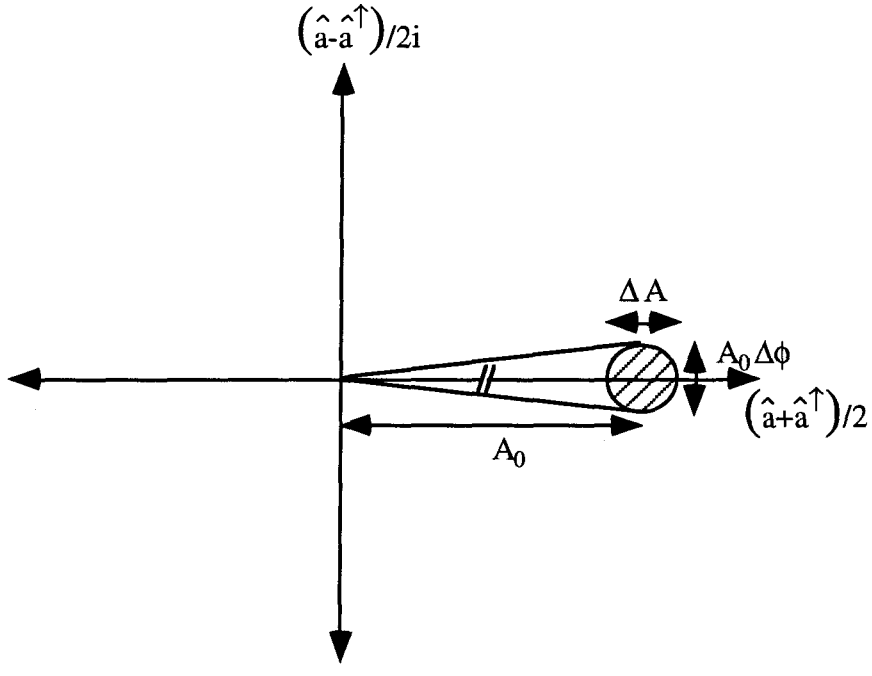

Figure 4-2: The quantum mechanical amplitude and phase flucutations are defined in terms of the in-phase and out-of-phase quadratre amplitude fluctuations of the field. Here $A_0 = \sqrt{<\hat{a}^{\dagger}\hat{a}>}$.

$$\Delta\hat{\phi}(t) = \frac{1}{2i\sqrt{<\hat{a}^{\dagger}\hat{a}>}}\left(\hat{a}(t) - \hat{a}^{\dagger}(t)\right) \tag{4.14}$$

and a correspondence to the classical definition of the optical phase may be expected as long as the photon number is much greater than unity.

The small-signal expressions are substituted into equations (4.1)-(4.3) and Fourier transforms taken to solve them. The Fourier transformed algebraic equations are then solved for each fluctuation variable $\tilde{\Delta N_c}(\Omega)$, $\tilde{\Delta A}(\Omega)$ and $\tilde{\Delta\phi}(\Omega)$, the fluctuation of the external field $\tilde{\Delta r}(\Omega)$ is calculated using (4.3) and the single-sided power spectral density of this quantity $P_{\Delta\hat{r}}(\Omega)$ is found. In general, $P_{\Delta\hat{r}}(\Omega)$ is a fairly complicated expression, but it can be simplified when the noise frequency is much lower than the inverse of the stimulated emission lifetime of the carriers. In this case, the amplitude noise power spectral density of the external field, normalized to the shot noise limit,

is given by

$$\frac{P_{\Delta\hat{r}}(0)}{SQL} = (1-\eta) + \eta\left[1 + \frac{1}{R} + \frac{1}{R} + \frac{2}{n_{sp}R^2}\right] \tag{4.15}$$

where η is the external differential quantum efficiency. The contributions from the different noise sources in this expression can be easily identified. Optical losses inside the laser are accounted for by η, pump noise by the unity term inside the brackets and one of the $1/R$ terms, spontaneous emission into non-lasing modes by the other of the $1/R$ terms, dipole moment vacuum fluctuations (spontaneous emission into the lasing mode) by the last. It can be seen that far above threshold, if the internal losses are small compared to the facet losses ($\eta \approx 1$), the noise is at the SQL and is determined by the pump noise only.

4.2.2 Vacuum cancellation, pump suppression and amplitude squeezing

Two aspects of the theory outlined in the previous section are now discussed: the reason for which the vacuum field does not generate the SQL and methods for suppressing the pump noise. These two elements are keys to understanding how amplitude squeezed light is generated from a semiconductor laser. The absence of the vacuum field fluctuations at high pump rates is due to interference between the component of the vacuum field reflected from the front facet of the laser and the transmitted internal laser field itself, which of course contains information about the vacuum component transmitted through the facet. The pump noise is eliminated by driving the laser with a constant-current source.

As has been described by Yamamoto [10], it is the interference between the transmitted internal field and the reflected vacuum field which results in a complete cancellation of the noise due to $\hat{f}_e(t)$ at high pump rates. This cancellation can be thought of in the following way. Imagine $\hat{f}_e(t)$ to be not a vacuum field but an arbitrary classical optical field. This field incident on the laser facet causes the internal field of

the laser to see an altered facet loss which is either smaller or larger than the original depending on the relative phase of the two fields. As a result, the gain (inversion) must also change to satisfy the gain=loss condition. But if the pump rate remains the same, this translates into an increased or decreased rate of stimulated emission into the mode. The amplitude of the internal field is therefore altered in a fashion which is correlated with the injected signal. In fact, when the simple calculation outlined above is carried out (see Appendix A), one finds that the change in the portion of the internal field transmitted through the facet exactly cancels the portion of the injected field reflected from the facet. Since this argument holds for an arbitrary weak optical field, it is certainly true for the vacuum field $\hat{f}_e(t)$ as long as we consider only fluctuations which occur at frequencies well below the inverse of the carrier stimulated emission lifetime.

The noise due to pump fluctuations is now considered in more detail using arguments proposed for semiconductor lasers by Yamamoto [76]. There are three obvious ways to pump a semiconductor laser, each interacting with the carrier density in the active region in a different way. The first is to pump the laser optically with classical light. In this case carriers are generated in a random fashion and therefore the pump current is indeed Poissonian and results in shot noise limited pump noise as is found in the second expression in (4.11). This is the type of pumping usually considered in laser models [9,85]. A second way of pumping a semiconductor laser is with a voltage source. Since the junction voltage is proportional to the carrier density, this fixes the carrier density at a constant value. Fluctuations in the rate of stimulated emission, which are caused by the random nature of the emission process, cause corresponding fluctuations in the pump rate since, in order to keep the junction voltage constant, the carriers in the active region must be replaced as soon as they recombine to create a stimulated photon. Thus, in this case also, the pump current is Poissonian, the noise being caused by the random nature of the emission process rather than by fluctuations in the generation rate.

Finally, one can consider driving the laser with a constant current source or voltage source in series with a large resistor. In this case, fluctuations in the rate of stimulated emission cause the carrier density (junction voltage) to fluctuate and therefore change the gain in exactly the direction to compensate for the original fluctuation. If the rate of stimulated emission increases, the junction voltage decreases reducing the gain and therefore reducing the stimulated emission rate back towards its steady-state value. This "self-correcting" mechanism reduces the pump fluctuations to zero in the limit of the current source series resistor being much larger than the diode differential resistance [76]. The only pump noise that remains is the thermal noise in the source resistor which may be reduced to an arbitrarily small value by using a large enough resistance. In this case the pump noise correlation function becomes the first expression given in (4.11).

The frequency-dependence of the amplitude noise on the external field is now described when the laser is pumped far above threshold [10]. At frequencies above the cavity bandwidth, the contribution from the incident vacuum field is equal to the SQL since the internal field of the laser cannot respond quickly enough to provide the canceling effect discussed above. At low frequencies, however, the vacuum fluctuations do cancel out, and, under Poissonian pumping, the low frequency noise is dominated by the pump noise which generates the shot noise limit. But above the cavity bandwidth, the pump noise falls off due, again, to the inability of the internal field to communicate with the external field on short time scales. Thus, for Poissonian pumping, the total amplitude noise is a constant, at the SQL at all frequencies. When the laser is pump-suppressed by driving it with a constant current source, however, the pump noise is drastically reduced, generating large amplitude squeezing at frequencies well below the cavity bandwidth.

The generation of squeezed light from a semiconductor laser has several significant advantages over other methods of producing squeezed light such as parametric down conversion [72] and four-wave mixing [70]. One is the relative ease with which the

squeezing can be produced. Typical quadrature squeezing experiments require a table full of optics and complicated servo locking systems [72]. The generation of amplitude squeezed light from a semiconductor laser in principle requires only a resistor! It thus seems even feasible to produce amplitude squeezed light sources in a commercial setting. In addition, the squeezing bandwidth for a semiconductor laser is essentially the cold cavity bandwidth if high enough pump rates can be achieved [86], which can be many GHz. In experiments using optical parametric oscillators, one of the most successful devices for generating quadrature-squeezed light, high finesse cavities have been used thereby limiting the bandwidth significantly. Finally, semiconductor lasers generate "bright" squeezed light rather than squeezed vacuum: the squeezing sits on a large steady-state optical field, which is a useful property for many applications. However, the characteristics of the amplitude squeezing generated from semiconductor lasers are probably less well understood than other methods due to the many competing physical processes which can generate noise in these devices. As a result, the agreement of experimental results with theory has not been particularly good, making the experiments somewhat more difficult to interpret.

4.2.3 Experimental issues in the generation of amplitude squeezed light

Several experimental groups have reported measuring amplitude squeezed light from a pump-suppressed semiconductor laser [86,87,88,89,90,91,92,93,94,12,95] or light emitting diode (LED) [96,97]. The amplitude noise is usually measured in one of two ways. The first is by directly detecting the light in a photodetector, measuring the photocurrent noise and comparing the measured noise level to that from a source thought to be shot noise limited, usually an LED. The second method is through the use of a balanced detector [88,98]. This method of detection has the advantage that the shot noise level can be internally calibrated by measuring the noise when the detector photocurrents are subtracted rather than added. The shot noise level can

then be rechecked using LED's. Pump-suppression can be achieved either by placing a large resistor in series with a high voltage source or by replacing the resistor with an inductor which allows the DC current to pass unimpeded while suppressing the current noise at higher frequencies. Also, most experiments are carried out with the laser (and often the detectors) cooled to cryogenic temperatures in order to increase differential quantum efficiencies and to enable the pumping of the laser far above threshold. However, several groups [87,94,95,12] have now obtained squeezing from room temperature lasers and there are no fundamental reasons why such generation should be significantly less effective.

The largest degree of squeezing (of any kind) produced to date, 8.3 dB below the shot noise level, was reported by Yamamoto's group at NTT [90]. They used cryogenically cooled lasers with LED calibration of the shot noise level. Their measurements were performed in the frequency range of 50-150 MHz, and squeezing was obtained at pump rates above $R = 10$. Interestingly, their minimum noise level is actually below what would be expected from an efficiency argument alone without any added noise from the laser itself. They explain this by assuming the existence of a non-lasing junction in parallel with the lasing junction and analyzing the current branching noise in the electronic circuit [99]. They find that in this situation, current branching can reduce the external efficiency of the laser without affecting the noise adversely.

With the exception of the one result described above, all other measurements of amplitude squeezing in semiconductor lasers have turned up less than 4 dB of squeezing. Although poor current-to-current efficiencies are certainly one reason, the agreement between experiment and theory has not been particularly good either, indicating that additional mechanisms not described by the basic theory may be generating excess noise in the laser. Foremost among these is possible excess noise caused by the existence of weak side modes [90,93]. In an inhomogeneously broadened medium, such modes would have a noise level far in excess of their SQL (due to their

being close to threshold), and thus, although they would not contribute much of the total power, their noise contribution could be significant. Another mechanism, asymmetrical cross-mode non-linear gain in an otherwise homogeneously broadened medium [100], can generate substantial excess noise at low frequencies through a renormalization of the weak mode relaxation resonance as a result of the inter-mode coupling [101]. A number of other possible noise sources are outlined in Section 6.3.

Another candidate to explain the excess noise measured in some experiments has been optical feedback [89]. While it is believed that optical feedback can lead to mode instabilities and therefore indirectly affect the amplitude noise, it is demonstrated in Chapter 6 that optical feedback can be used to actually enhance the squeezing and therefore may not be an important source of excess noise.

4.2.4 Correlation schemes and squeezing enhancement

Several schemes have been proposed to enhance the squeezing in pump-suppressed semiconductor lasers. These include amplitude-phase decorrelation [102,11], junction voltage feedforward [11], injection locking [93] and optical feedback [103,104,94,12]. The method of injection locking seeks to eliminate the excess noise caused by multi-mode operation by selectively reducing the loss seen by one particular mode. In one experiment [93], a dye laser was used to injection lock a commercial quantum-well laser at 10 K, suppressing the side mode power by more than 10 dB and reducing the amplitude noise from 1 dB below the SQL to more than 3 dB below it. Similar results were recently obtained with a room-temperature injection-locked laser [95].

The three other schemes take advantage of the residual correlations which occur between the field amplitude, phase and the carrier density at moderate injection currents. Using optical feedback (see Section 4.4), the phase-amplitude correlation [see (2.6)] can be used to reduce the amplitude noise at injection currents near the onset of squeezing around $R = i/i_{th} - 1 = 2$. In this regime, the amplitude noise is close to the shot noise limit and the phase-amplitude correlation [calculated using

(2.6)] is about 0.5, and hence a reduction in the noise by a factor of two is expected. This range of injection currents is potentially important for the generation of squeezed light from room-temperature semiconductor lasers. Due to the danger of thermal damage to the laser facet, most room temperature semiconductor lasers cannot be pumped by more than a few times the threshold current which necessarily limits the squeezing due to the incomplete suppression of the dipole moment and vacuum fluctuations and also due to noise from spontaneous emission into non-lasing modes. Optical feedback could play a role in enhancing the squeezing from such lasers. Recent experimental results [94,12] (see Chapter 6) have demonstrated the utility of optical feedback in the generation of amplitude squeezed light from a room temperature semiconductor laser. Optical feedback can also be used to substantially reduce the classical noise in a laser close to threshold [5,8] (see Chapter 5) where the amplitude-phase correlation is high.

Amplitude-phase decorrelation is a noise reduction technique in which the output field of the laser is sent through an interferometer which translates phase noise into amplitude noise. This results in a simultaneous decorrelation of the field amplitude and phase and reduction of the amplitude noise. Reduction of the classical noise in lasers close to threshold by more than 10 dB has been demonstrated experimentally by Newkirk and Vahala [105]. This method can also be used to enhance the squeezing of semiconductor lasers [11]. The final method of amplitude noise reduction mentioned here is feedforward of the junction voltage fluctuations. The correlation between junction voltage and field amplitude is exactly equal in magnitude to the amplitude-phase correlation, (2.6), in the limit $\alpha \rightarrow \infty$. By feeding the junction voltage signal forward to an intensity modulator, the amplitude noise can be reduced by a factor of 2 when $R = 2$.

4.3 Amplitude noise reduction using optical feedback

As discussed in the previous chapters, weak optical feedback from a dispersive element can reduce both the linewidth and the amplitude noise of semiconductor lasers. This type of noise reduction relies on the phase-amplitude coupling [3,4] which takes place in a semiconductor laser as a result of the asymmetrical gain profile and detuned oscillation of the laser. Because of this phenomenon, part of the amplitude noise is coupled into the field phase generating both a linewidth in excess of the Schawlow-Townes linewidth and also a correlation between amplitude and phase noise. Semiclassical analyses [35,7] have predicted a reduction in the amplitude noise by a factor of $(1+\alpha^2)$, the reduction being limited by the extent to which the amplitude and phase are correlated. Such approaches can only be used when the laser is close to threshold, however, since only then is the amplitude noise far enough above the SQL that a semiclassical treatment is valid. At moderate pump rates, the laser noise approaches the SQL and a fully quantum mechanical analysis must be performed in order to correctly predict the effects of optical feedback on the amplitude noise of the laser. A recent analysis by Nabiev et al. [103] using the dispersive loss model outlined in Section 2.2.2 based on (2.7) has shown that the addition of a frequency dependent loss to the laser cavity could in fact enhance the squeezing. The theory in this chapter extends the analysis of Ref. [103] to the experimentally accessible configuration of optical feedback.

As discussed in Section 4.2.1, there are five fundamental noise sources in semiconductor lasers: vacuum noise, dipole moment noise, noise due to optical losses, noise due to spontaneous emission into non-lasing modes and pump noise. Each of these noise sources is affected differently by the application of optical feedback to a semiconductor laser. Noise reduction with optical feedback works by taking advantage of correlations which exist between the amplitude and phase of the external field. A preexisting correlation between the field amplitude and phase is therefore necessary

if a reduction in the laser amplitude noise is to be obtained through optical feedback; the size of the reduction will depend on the strength of the correlation.

It is therefore pertinent to ask which of the noise sources mentioned above produce correlated noise in both the amplitude and the phase. Dipole moment and vacuum fluctuations involve transitions between conduction and valence bands which also add photons to the lasing mode. As a result, a given fluctuation event causes a direct change in both the internal field photon number and the gain/refractive index of the laser medium so the amplitude and phase are indeed correlated for these noise sources. For spontaneous emission noise, however, the situation is different. Under constant current operation, the rate of injection of carriers into the active region is fixed. Any fluctuation in the rate of spontaneous emission into non-lasing modes is compensated by a change in the rate of stimulated emission into the lasing mode of the opposite sign. However, the carrier density in this case remains the same since the gain is clamped by the threshold condition. Thus, the field amplitude changes but no correlated noise is added to the phase since the carrier density, and therefore the refractive index, is fixed. The same argument also applies to pump fluctuations. Thus, it might be expected that dipole moment and vacuum noise (which dominate at low pump rates near threshold) can be reduced by optical feedback and that spontaneous emission noise will be unaffected. The various noise sources, their dependence on pump rate and phase-amplitude correlation are summarized in Table 4.1.

The analysis of a semiconductor laser with optical feedback is performed here using the quantum Langevin equation approach. This method offers the advantage over other methods (such as Fokker-Planck equations) that the feedback can be included in a straightforward way in analogy with the semi-classical analysis. Section 4.4 starts with feedback-modified equations of motion for the internal field, carrier density and external field and expressions are derived for the external field amplitude and phase spectral density functions as well as for the amplitude-phase cross correlation. Section 4.5 presents some numerical plots illustrating the effects of optical feedback on

Noise Source	Noise Dependence on $R = i/i_{th} - 1$	Contribution to P-A Correlation
Pump	1	≈ 0
Spontaneous emission into non-lasing modes	1/R	≈ 0
Vacuum	$1/R^2$	$\alpha/\sqrt{1+\alpha^2}$
Dipole moment	$1/R^2$	
Internal losses	$1-\eta$	≈ 0

Table 4.1: Summary of the fundamental noise sources in a semiconductor laser, with their dependence on pump rate, R, and phase-amplitude correlation. Optical feedback is expected to reduce the noise from only those sources which exhibit a significant phase-amplitude correlation.

the amplitude and phase noise spectra of the laser. Section 4.6 discusses the noise spectra in the low-frequency limit where simple analytical results can be obtained. The spectral uncertainty product and quantum mechanical consistency are examined in Section 4.7. Finally, Section 4.8 provides a discussion of the results and conclusions.

4.4 Quantum Langevin analysis of a semiconductor laser with optical feedback

The configuration to be considered is shown in Figure 4-3. The internal optical field of a semiconductor laser is weakly coupled to an external cavity through the front laser facet. The output beam, reflected by a beamsplitter ($R \approx 1$) out of the external cavity, constitutes the external optical field, its quantum mechanical operator denoted by $\hat{r}(t)$, and it will be our goal to calculate the amplitude and phase fluctuations of this field. The transmitted beam passes into the external cavity and through a dispersive element before being reflected back into the semiconductor laser by an end mirror. The dispersive element could be an atomic vapor or Fabry-Perot cavity. In order to

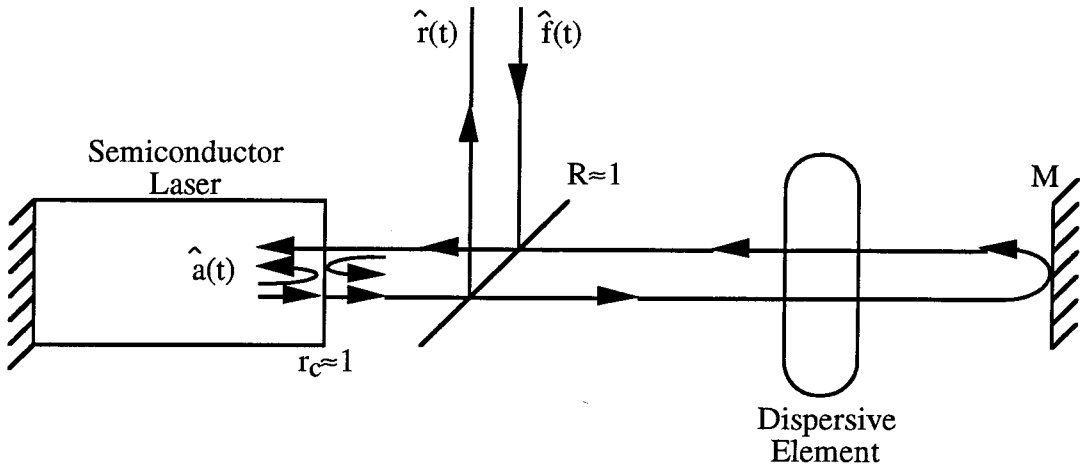

Figure 4-3: Optical feedback configuration to be considered.

simplify the analysis, it will be assumed that the laser is tuned to the transmission peak of whatever dispersive element is used. In this case, the optical losses through the element will not be locally frequency dependent. The frequency dependent phase shift, manifested as an increase in the cavity round-trip delay time, is therefore the only effect of the dispersive element. It is also assumed that the bandwidth of the dispersive element is much larger than the noise frequencies of interest so that group velocity dispersion can be neglected.

The fully quantum mechanical equation of motion for the optical field inside a semiconductor laser has been extensively studied by Haug [9] and Yamamoto [10]. In the weak feedback limit, the modification to this equation of motion given by (4.2) is simple [32]. The resulting equation for the slowly varying Heisenberg internal field operator $\hat{A}(t)$ is

$$\frac{d\hat{A}(t)}{dt} = -\frac{1}{2}\left[\frac{1}{\tau_{pe}} + \frac{1}{\tau_{p0}} + 2i(\omega_L - \omega_0) - \frac{\omega}{\mu^2}(\hat{\chi}_i - i\hat{\chi}_r)\right]\hat{A}(t) + \hat{G}(t) + \hat{g}(t) + \sqrt{\frac{1}{\tau_{pe}}}\hat{f}_e(t) + \kappa e^{i\phi_0}\sqrt{\tau_{pe}}\,\hat{r}(t-\tau) \tag{4.16}$$

where ω_L the laser frequency. The last term in (4.16) is the modification due to the feedback. Here κ is the (locally frequency independent) feedback coupling rate defined by (2.11) and $\hat{r}(t)$ is the operator for the external optical field defined by (4.3). Since the reflection coefficient of the beamsplitter is close to unity, the quantum mechanical noise added by any absorption (losses) in the dispersive element and by the vacuum entering the rear open port of the beamsplitter (opposite the output port) can be ignored. The equations of motion for the carrier density operator $\hat{N}_c(t)$ and external field $\hat{r}(t)$ are unmodified by the optical feedback and are given by (4.1) and (4.3).

As in Section 4.2, the operators for the carrier density, internal and external fields are now written as a combination of average values and fluctuation operators. Thus

$$\hat{A}(t) = \left[A_0 + \Delta\hat{A}(t)\right] e^{i\Delta\hat{\phi}(t)} \tag{4.17}$$

$$\hat{r}(t) = \left[r_0 + \Delta\hat{r}(t)\right] e^{i\Delta\hat{\psi}(t)} \tag{4.18}$$

$$\hat{N}_c(t) = N_{c0} + \Delta\hat{N}_c(t) \tag{4.19}$$

$$\hat{\chi}(N_c) = \hat{\chi}_r + i\hat{\chi}_i = \langle\hat{\chi}_r\rangle + i\langle\hat{\chi}_i\rangle + \xi_i(\alpha + i)\Delta\hat{N}_c \tag{4.20}$$

$$\Delta\hat{\phi}(t+\tau) - \Delta\hat{\phi}(t) \ll 1 \tag{4.21}$$

where it has also been assumed in (4.21) that the phase change of the field during a round-trip time of the external cavity is small, i.e., $\Delta\nu \ll 1/\tau$ where $\Delta\nu$ is the laser linewidth. For cavity lengths of up to meters and linewidths of megahertz, this condition is certainly satisfied.

When (4.17)-(4.21) are substituted into (4.16) and (4.1), both the steady-state values for the field and carriers as well as the equations for fluctuations about this steady state can be obtained. The steady state equations are

$$-\frac{1}{2}\left[\frac{1}{\tau_p} + 2i(\omega_L - \omega_0) - \frac{\omega}{\mu^2}\left(<\hat{\chi}_i> - i<\hat{\chi}_r>\right)\right] A_0 + \kappa_0 e^{-i\phi_0} e^{-i\omega_L\tau} A_0 = 0 \tag{4.22}$$

$$P - \frac{N_{c0}}{\tau_{sp}} - \frac{E_{cv}}{n_{sp}} A_0^2 - E_{cv} = 0. \tag{4.23}$$

From (4.22) the gain and lasing frequency are determined to be

$$\frac{E_{cv}}{n_{sp}} = \frac{1}{\tau_p} - 2\kappa_0 \cos\phi_0 \tag{4.24}$$

$$\omega_L = \omega_0 - \frac{\alpha}{2\tau_p} - \kappa_0\sqrt{1+\alpha^2}\sin\left(\phi_0 + \omega_L\tau + \arctan\alpha\right). \tag{4.25}$$

where $\omega_0 - \alpha/2\tau_p$ is the lasing frequency without feedback. The field amplitude A_0 is determined by (4.23) along with the Einstein relation $\beta N_{c0}/\tau_{sp} = E_{cv}$ and the threshold condition $P_{th} = E_{cv}/\beta$ which defines threshold as being the point at which the spontaneous emission rate into the lasing mode equals the stimulated emission rate [106]. The field amplitude is thus given by

$$A_0^2 = n_{sp}\left(\frac{R}{\beta} - 1\right) \approx \frac{n_{sp}R}{\beta}. \tag{4.26}$$

where the approximation is valid as long as $A_0^2 \gg 1$ which has been assumed above. Finally, the mean carrier density above threshold, N_{c0}, is determined by (4.24) along with the Einstein relation.

The equations for the Fourier transformed fluctuation operators are given by

$$(i\Omega - A_1)\Delta\tilde{N}_c(\Omega) = A_2\Delta\tilde{A}(\Omega) + \tilde{\Gamma}(\Omega) + \tilde{\Gamma}_{sp}(\Omega) + \tilde{\Gamma}_p(\Omega) \tag{4.27}$$

$$i\Omega(1+C_i)\Delta\tilde{A}(\Omega) + i\Omega C_r A_0\Delta\tilde{\phi}(\Omega) = A_3\Delta\tilde{N}_c(\Omega) + \tilde{G}_r(\Omega) + \tilde{g}_r(\Omega) + \sqrt{\frac{1}{\tau_{pe}}}\tilde{f}_{er}(\Omega) \tag{4.28}$$

$$-i\Omega C_r\Delta\tilde{A}(\Omega) + i\Omega(1+C_i)A_0\Delta\tilde{\phi}(\Omega) = -\alpha A_3\Delta\tilde{N}_c(\Omega) + \tilde{G}_i(\Omega) + \tilde{g}_i(\Omega) + \sqrt{\frac{1}{\tau_{pe}}}\tilde{f}_{ei}(\Omega) \tag{4.29}$$

where

$$A_1 = -\left(\frac{1}{\tau_{sp}} + \frac{1}{\tau_{st}}\right) = -\frac{(1+\beta A_0^2)}{\tau_{sp}} \tag{4.30}$$

$$A_2 = -\frac{2A_0}{\tau_p} \tag{4.31}$$

$$A_3 = \frac{\omega}{2\mu^2}\xi_i A_0 = \frac{\beta(1+A_0^2)}{2A_0\tau_{sp}} \tag{4.32}$$

$$C_i(\Omega) = \kappa_0\tau\cos\phi_0\left(\frac{1-e^{-i\Omega\tau}}{i\Omega\tau}\right) \tag{4.33}$$

$$C_r(\Omega) = -\kappa_0\tau\sin\phi_0\left(\frac{1-e^{-i\Omega\tau}}{i\Omega\tau}\right). \tag{4.34}$$

Equations (4.27)-(4.29) along with (4.3) can be solved for the external field fluctuation operators $\Delta\tilde{r}(\Omega)$ and $\Delta\tilde{\psi}(\Omega)$ giving

$$\begin{aligned}\Delta\tilde{r}(\Omega) &= R_1(\Omega)\left[\tilde{\Gamma}+\tilde{\Gamma}_{sp}+\tilde{\Gamma}_p\right] + R_2(\Omega)(1+C_i(\Omega))\left[\tilde{G}_r+\tilde{g}_r+\sqrt{\frac{1}{\tau_{pe}}}\tilde{f}_{er}\right] + \\ &\quad R_2(\Omega)C_r(\Omega)\left[\tilde{G}_i+\tilde{g}_i+\sqrt{\frac{1}{\tau_{pe}}}\tilde{f}_{ei}\right] - \tilde{f}_{er} \qquad (4.35)\\ \Delta\tilde{\psi}(\Omega) &= R_3(\Omega)\left[\tilde{\Gamma}+\tilde{\Gamma}_{sp}+\tilde{\Gamma}_p\right] + R_4(\Omega)\left[\tilde{G}_r+\tilde{g}_r+\sqrt{\frac{1}{\tau_{pe}}}\tilde{f}_{er}\right] + \\ &\quad R_5(\Omega)\left[\tilde{G}_i+\tilde{g}_i+\sqrt{\frac{1}{\tau_{pe}}}\tilde{f}_{ei}\right] - \frac{\sqrt{\tau_{pe}}}{A_0}\tilde{f}_{ei} \qquad (4.36)\end{aligned}$$

where

$$R_1(\Omega) = \sqrt{\frac{1}{\tau_{pe}}}\frac{A_3}{D(\Omega)}\left[1+C_i+\alpha C_r\right] \tag{4.37}$$

$$R_2(\Omega) = \sqrt{\frac{1}{\tau_{pe}}}\frac{(i\Omega-A_1)}{D(\Omega)} \tag{4.38}$$

$$R_3(\Omega) = \frac{1}{A_0}\frac{A_3}{D(\Omega)}\left[\alpha(1+C_i)-C_r\right] \tag{4.39}$$

$$R_4(\Omega) = \frac{1}{A_0}\frac{1}{1+C_i+\alpha C_r}\left[\frac{\alpha}{i\Omega} - \frac{[\alpha(1+C_i)-C_r](i\Omega-A_1)}{D(\Omega)}(1+C_i)\right] \tag{4.40}$$

$$R_5(\Omega) = \frac{1}{A_0}\frac{1}{1+C_i+\alpha C_r}\left[\frac{1}{i\Omega} + \frac{[\alpha(1+C_i)-C_r](i\Omega-A_1)}{D(\Omega)}C_r\right] \tag{4.41}$$

$$D(\Omega) = i\Omega(i\Omega-A_1)[(1+C_i)^2+C_r^2] - A_2A_3(1+C_i+\alpha C_r). \tag{4.42}$$

Equations (4.35) and (4.36), along with the correlation functions (4.4)-(4.11), enable the calculatation of the external field amplitude and phase noise power spectra as a function of the feedback strength and phase. It can be seen from (4.28) and

(4.29) that the feedback, which causes a non-zero C_r coefficient, adds a coupling between the amplitude and phase. Since the amplitude and phase were originally correlated through the α-parameter, this additional coupling can serve to decorrelate the two quantities and, at the same time, reduce the noise in one or both. The feedback parameters $C_i(\Omega)$ and $C_r(\Omega)$ are actually frequency dependent extensions of the parameters C_r and C_i defined in Section 2.2.2 [7,6,41] to the case where a feedback delay is included. At low frequencies, when the feedback delay is unimportant, the terms in parentheses in (4.33) and (4.34) reduce to unity and the coefficients become those given in Section 2.2.2 [41]. In particular, if $\phi_0 = -\pi/2$ then $C_i(0) = 0$ and $C_r(0) = \kappa_0\tau$ becomes equivalent to the parameter C introduced in Refs. [7,103] and given in Section 2.2.2 to describe a frequency dependent loss in a carrier-independent model of the laser.

The physical role of C_r and C_i is illustrated in Figure 4-4. Independent noise sources create fluctuations in both the amplitude and the phase of the internal optical field. Through the α parameter, the portion of the amplitude noise with a correlated component in the carrier density fluctuations (dipole moment and vacuum fluctuations) is translated into phase noise (and therefore frequency noise) producing a correlation between the amplitude and instantaneous oscillation frequency of the laser. The optical feedback creates corrections to the field amplitude and phase which depend on the frequency of the output field. The parameter C_r describes the correction to the field amplitude while the parameter C_i describes the direct correction to the field phase.

From equations (4.35) and (4.36), the power spectra of the amplitude noise, $P_{\Delta\hat{r}}(\Omega)$, and phase noise, $P_{\Delta\hat{\psi}}(\Omega)$, as well as the amplitude-phase cross correlation function, $P_{\Delta\hat{r}\Delta\hat{\psi}}(\Omega)$, can be calculated. These are given by

$$P_{\Delta\hat{r}}(\Omega) = 2|R_1|^2\left[\frac{4kT}{q^2R_s} + (1-\beta)\frac{N_{c0}}{\tau_{sp}}\right] + \frac{1}{2}\left|1 - \frac{R_2(1+C_i)}{\sqrt{\tau_{pe}}}\right|^2$$

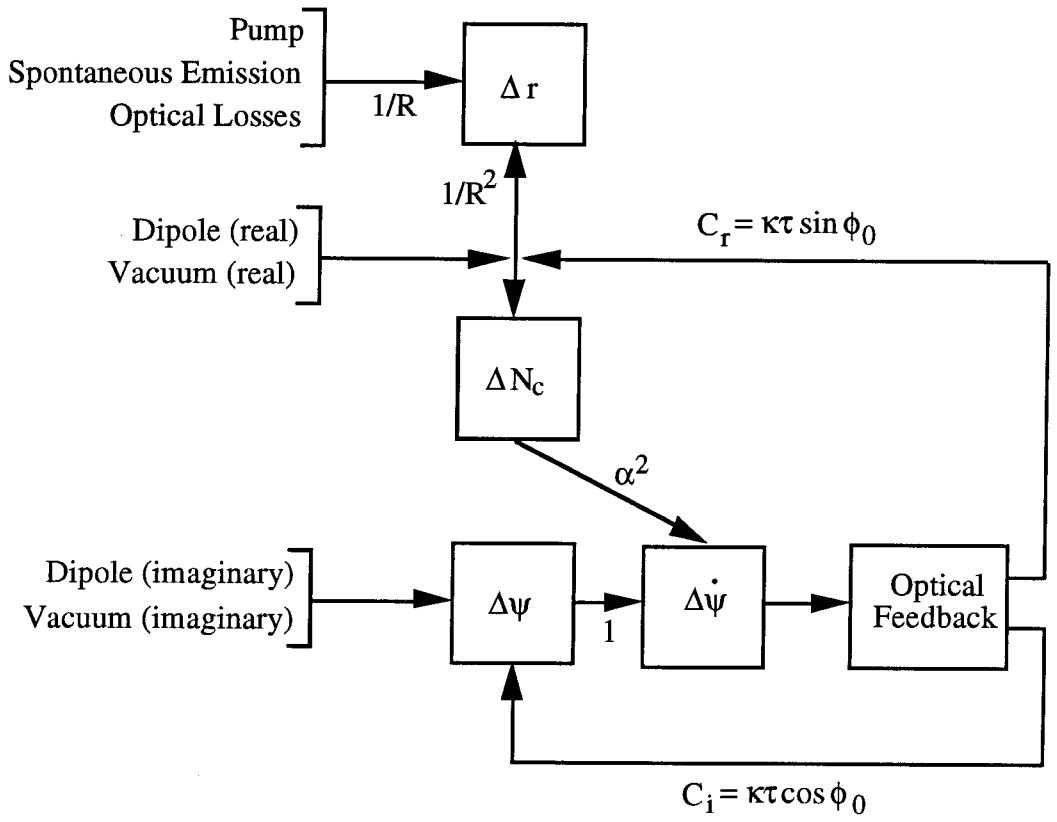

Figure 4-4: Correlations between the field amplitude and phase are produced through phase-to-amplitude coupling. Optical feedback introduces changes in both the facet loss rate and phase shift proportional to the phase of the output optical field. These changes can correct for the original fluctuations.

$$+\frac{2n_{sp}-1}{2\tau_p}|R_2(1+C_i)-2R_1A_0|^2$$
$$+\frac{1}{2\tau_{p0}}|R_2|^2|1+C_i|^2+\frac{n_{sp}}{\tau_p}|R_2|^2|C_r|^2 \tag{4.43}$$

$$P_{\Delta\hat{\psi}}(\Omega)=2|R_3|^2\left[\frac{4kT}{q^2R_s}+(1-\beta)\frac{N_{c0}}{\tau_{sp}}\right]+\frac{1}{2}\left|\frac{\sqrt{\tau_{pe}}}{A_0}-R_5\sqrt{\frac{1}{\tau_{pe}}}\right|^2+$$
$$\frac{2n_{sp}-1}{2\tau_p}|2R_3A_0+R_4|^2+\frac{2n_{sp}-1}{2\tau_p}|R_5|^2+\frac{|R_4|^2}{2\tau_p}+\frac{|R_5|^2}{2\tau_{p0}} \tag{4.44}$$

$$P_{\Delta\hat{r}\Delta\hat{\psi}}(\Omega)=\left[2R_1^*R_3\left(\frac{4kT}{q^2R_s}+(1-\beta)\frac{N_{c0}}{\tau_{sp}}\right)+\right.$$
$$\frac{2n_{sp}-1}{2\tau_p}\left(4R_1^*R_3A_0^2-2(R_1^*R_4+R_2^*(1+C_i^*)R_3)A_0\right.$$
$$\left.+(R_2^*(1+C_i^*)R_4-R_2^*C_r^*R_5)\right)+\frac{1}{2\tau_p}\left(R_2^*(1+C_i^*)R_4-R_2^*C_r^*R_5\right)$$
$$\left.-\frac{1}{2\sqrt{\tau_{pe}}}\left(R_4-\frac{R_2C_r\sqrt{\tau_{pe}}}{A_0}\right)\right]\frac{1}{\sqrt{P_{\Delta\hat{r}}(\Omega)P_{\Delta\hat{\psi}}(\Omega)}} \tag{4.45}$$

These expressions (4.43)-(4.45) are the main result of this chapter. The first term in each expression corresponds to pump noise (assuming the pump-suppressed case) and spontaneous emission noise. The second term is the noise due to vacuum fluctuations (or spontaneous emission into the lasing mode). The third term is due to fluctuations in dipole moment, and the fourth term is due to internal optical losses. The last term in (4.43) is uncorrelated phase noise which has been coupled into the field amplitude through the feedback.

4.5 Numerical results

To get a feeling for how the noise spectra are affected by optical feedback, the expressions (4.43)-(4.45) can be plotted as a function of frequency for various parameter values. The values chosen here are $n_{sp}=2$, $\beta=10^{-5}$, $\tau_p=2\times10^{-12}s$, $\tau_{sp}=2\times10^{-9}s$, $\tau_{p0}=10^{-11}s$, $\alpha=5$ and $R_s=1M\Omega$ (complete pump suppression). In the first set of plots (Figures 4-5 through 4-8), the limiting case of a short cavity length is as-

sumed ($\tau = 10^{-14}s$) to avoid the complication due to the frequency dependence of the feedback parameters (which will be discussed later). The phase is set to $\phi_0 = -\pi/2$ thereby making $C_i = 0$ and $C_r = \kappa_0\tau$. Figure 4-5(a) shows the amplitude noise power spectrum, $P_{\Delta r}$, as a function of frequency at $R = i/i_{th} - 1 = 0.1$ for feedback levels $C_r = 0, 0.1, 0.3, 1$. The low-frequency noise is seen to be reduced as the feedback is increased. In addition, the relaxation resonance moves to somewhat higher frequencies. The phase noise power is also observed to decrease (Figure 4-5b) indicating a reduction in the laser linewidth. Finally, the low frequency phase-amplitude correlation (Figure 4-6) is reduced from its free-running value of $\alpha/\sqrt{1+\alpha^2}$ with increasing feedback. Thus, at injection currents close to threshold, both the phase noise and the amplitude noise can be significantly reduced along with an accompanying reduction in the phase-to-amplitude correlation. All of these results have been obtained in the past through semi-classical analyses [34,7].

As the pump rate is increased, however, (Figure 4-7, $R = 1$) and the amplitude noise approaches the SQL at low frequencies, the low frequency reduction in the amplitude noise is smaller. If the feedback is made too large, the low frequency noise actually starts to increase. In fact, at very high pump rates (e.g., Figure 4-8, $R = 10$) no reduction is possible at all and the low frequency amplitude noise increases uniformly with increasing feedback power. The relaxation resonance frequency still increases, however, as does the bandwidth of the low-noise part of the spectrum. At these high pump rates, there would appear to be a tradeoff between noise reduction and bandwidth: very low noise operation is sacrificed to achieve an increased bandwidth.

The behavior of the low-frequency noise can be understood in the following way. When no feedback is applied, the phase and amplitude noise of the laser are correlated through the α-parameter. As the feedback is increased, some fraction of the phase noise is added to the amplitude noise in such a way as to correct for the correlated fluctuations and reduce the noise. In the process, however, the part of the phase noise

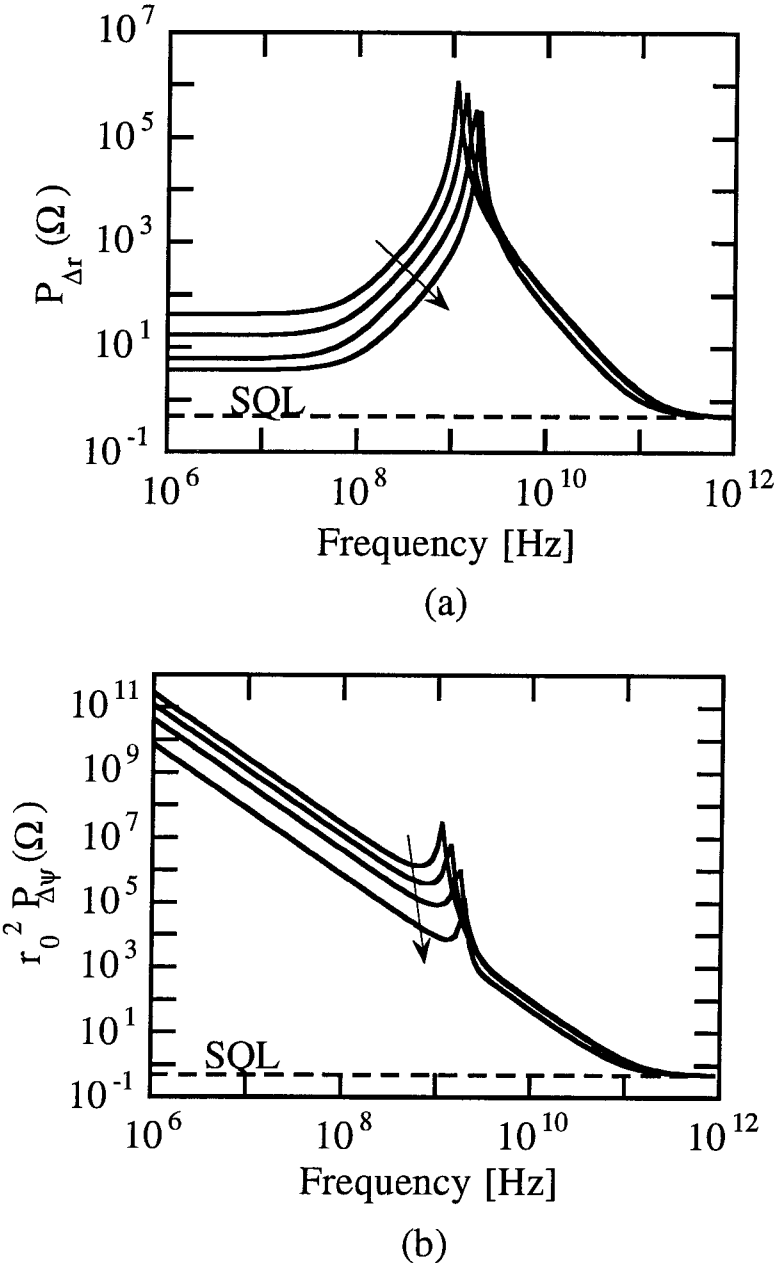

Figure 4-5: External field noise spectra at $R = i/i_{th} - 1 = 0.1$ and $C = 0, 0.1, 0.3, 1$ in order along the arrow path. (a) Amplitude noise and (b) phase noise. Amplitude noise reduction by over an order of magnitude is possible at this pump rate. The dashed line indicates the SQL.

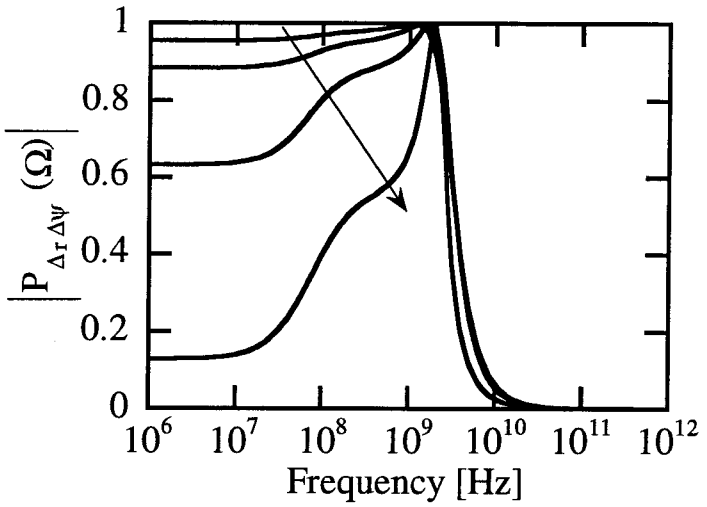

Figure 4-6: External field amplitude-phase cross-spectral density at $R = i/i_{th} - 1 = 0.1$.

not initially correlated with the amplitude is also coupled into the amplitude noise producing excess noise which increases with feedback strength. The amplitude noise minimum thus occurs when there is enough feedback to reduce the phase-amplitude correlation to zero. Any additional feedback causes too much of the uncorrelated phase noise to be coupled into the amplitude leading to an increase in the amplitude noise.

A more realistic situation occurs when the short cavity length assumption is relaxed and the frequency dependence of the feedback parameters $C_i(\Omega)$ and $C_r(\Omega)$ becomes important in determining the structure of the noise spectrum. Plots of the three spectra are shown in Figures 4-9 and 4-10 with the same parameter values as above but with $\tau = 6.6 \times 10^{-9} s$ (corresponding to an external cavity length of 1m), $R = 0.1$, $C_i = 0$ and $C_r = 0, 0.1, 0.3, 1$. As the frequency changes, C_r oscillates in magnitude between the limits $\pm\kappa_0/\Omega$, its phase also changing. At frequencies where C_r is real, the noise behaves like the short cavity limiting case but with reduced effect at higher frequencies due to the decay of C_r with Ω. At these frequencies, the

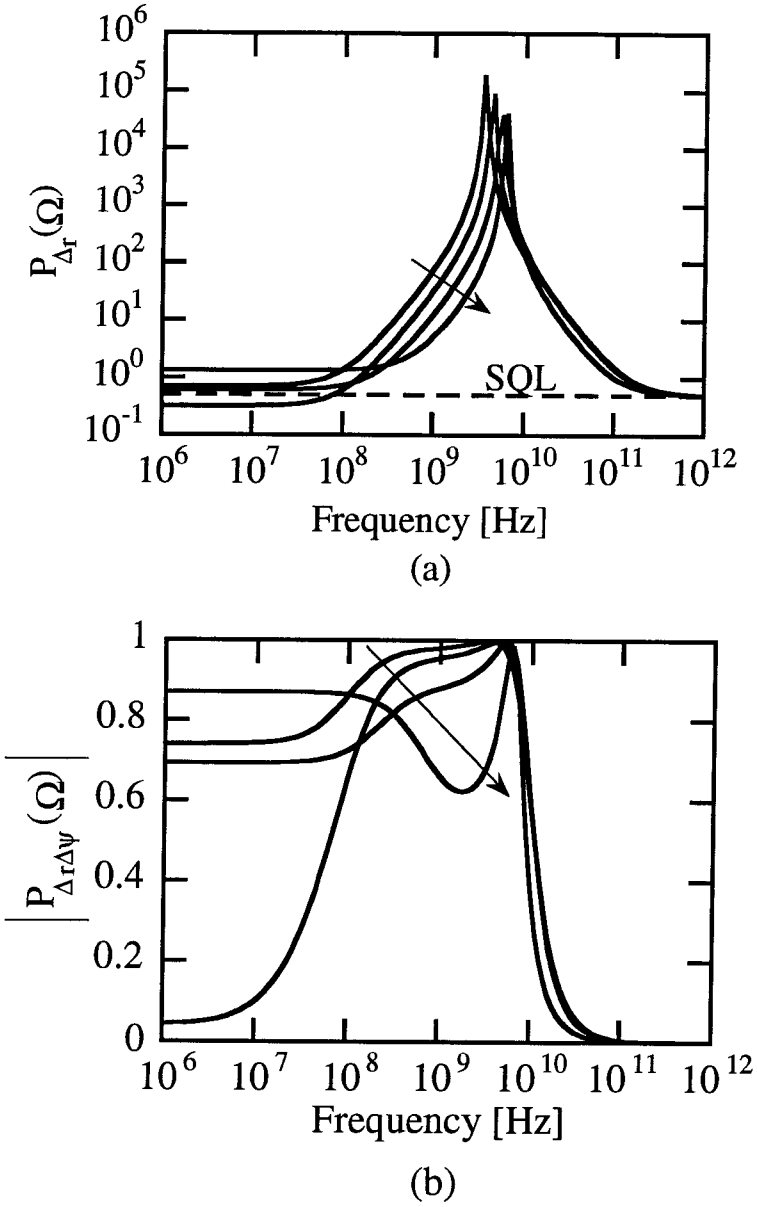

Figure 4-7: Spectra as in Figure 4-5 but with $R = 1$. The low frequency amplitude noise initially decreases to below the SQL and then increases as further feedback is applied.

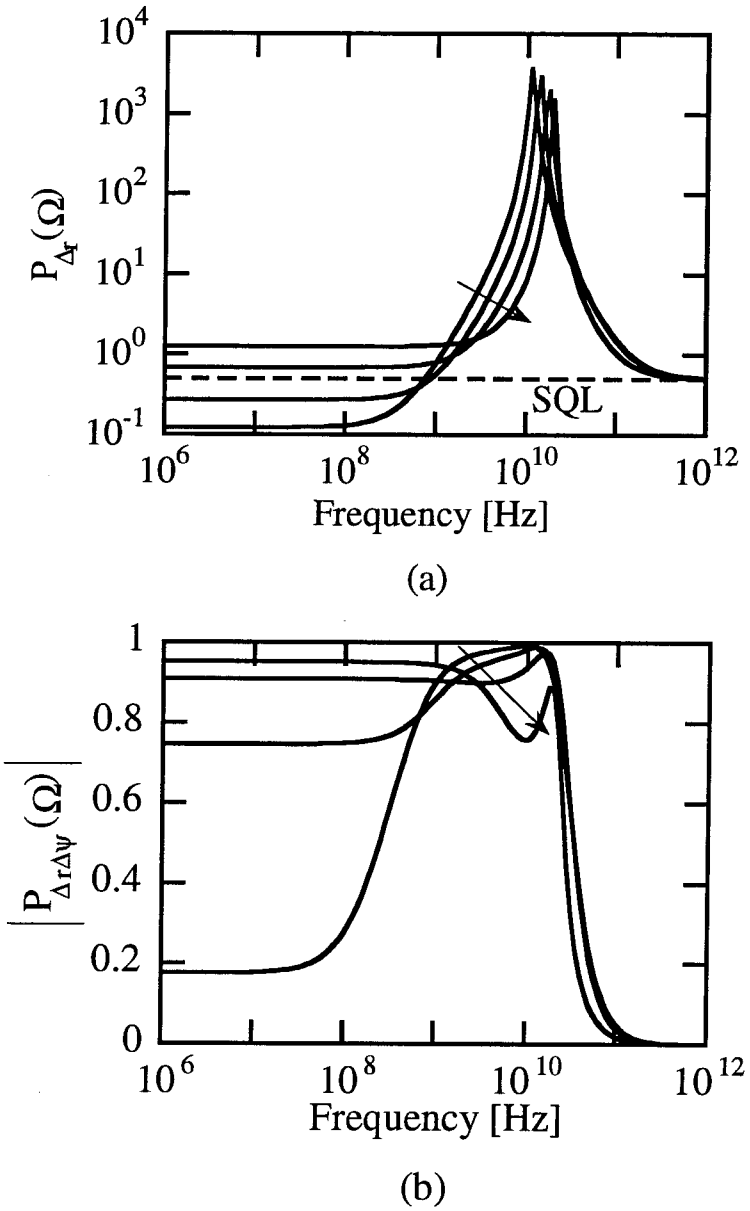

Figure 4-8: Spectra as in Figure 4-5 but with R=10. The low frequency noise increases with increasing feedback but the bandwidth widens. The low-frequency correlation between amplitude and phase also increases.

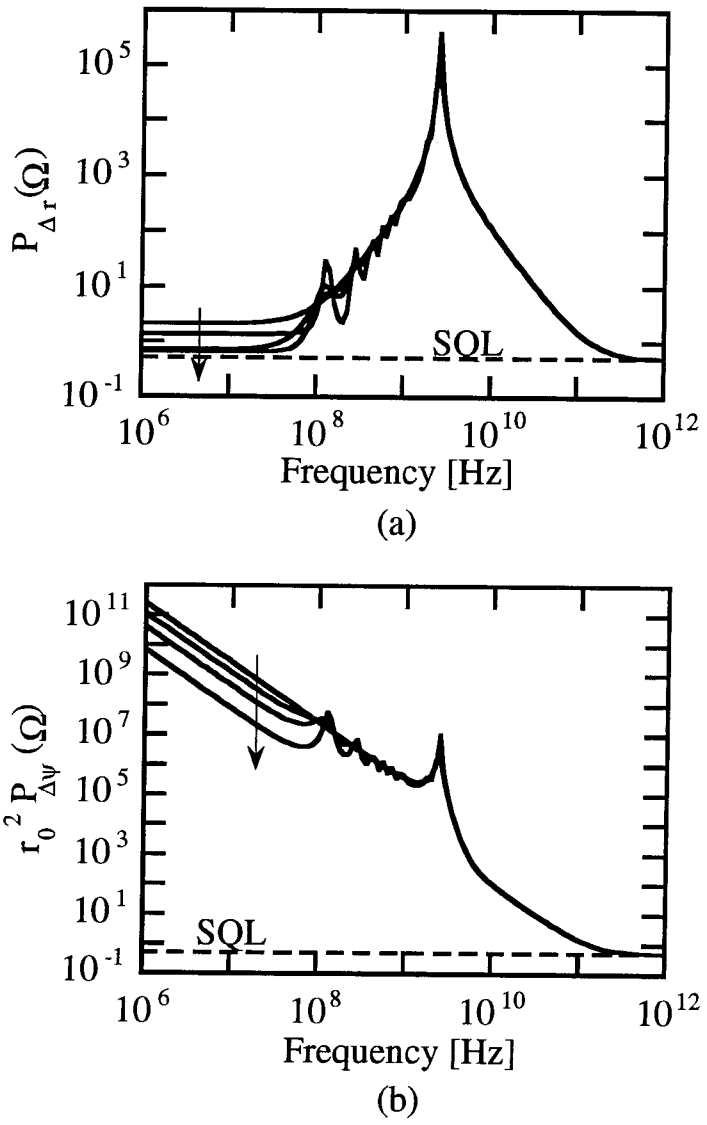

Figure 4-9: Noise spectra at $R = 0.5$ when a delay ($\tau = 6.6 \times 10^{-9} s$) in the feedback is included. Peaks in the spectra occur when the delay introduces a net round-trip phase shift in the feedback noise of π. Here $C = 0, 0.1, 0.3, 1$ increasing along the arrow path.

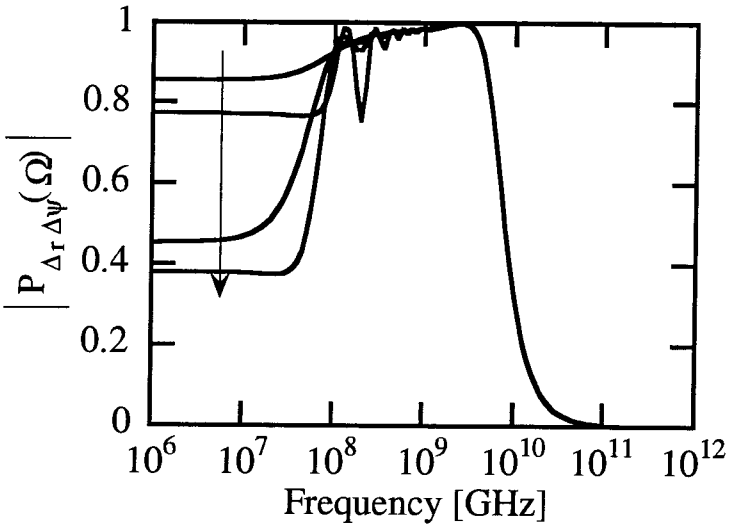

Figure 4-10: Amplitude-phase correlation at $R = 0.5$ when a delay ($\tau = 6.6 \times 10^{-9} s$) in the feedback is included. Here $C = 0, 0.1, 0.3, 1$ increasing along the arrow path.

delay due to the external cavity causes a phase shift in the fluctuation signal equal to a multiple of 2π resulting in negative feedback. At other frequencies, however, the phase shift of the noise signal as the light passes through the external cavity is different from 2π and positive feedback can result leading to peaks in the amplitude and phase noise spectra.

4.6 Low frequency noise

Noise in the frequency region between about 10 MHz and 1 GHz is of particular interest in semiconductor lasers due to the utility of RF modulation techniques at these frequencies; it is in this region that noise reduction will likely play its most important role. It is assumed throughout this section that the noise frequency Ω is well below both the inverse of the stimulated emission lifetime and the external cavity free-spectral range. The expressions for the amplitude and phase noise then become

very simple:

$$P_{\Delta r}(\Omega) = \frac{1}{2}(1-\eta) + \frac{\eta}{2}\left[\frac{1}{R} + 2n_{sp}\left|\frac{\alpha C(\Omega) - 1/(n_{sp}R)}{1+\alpha C(\Omega)}\right|^2 + 2n_{sp}\left(1+\frac{1}{n_{sp}R}\right)^2 \frac{|C(\Omega)|^2}{|1+\alpha C(\Omega)|^2}\right] \tag{4.46}$$

$$P_{\Delta\hat{\psi}}(0) = \frac{n_{sp}}{A_0^2\tau_p}\frac{1}{\Omega^2}\frac{1+\alpha^2}{(1+C_i+\alpha C_r)^2} \tag{4.47}$$

where $C(\Omega) = C_r(\Omega)/(1+C_i(\Omega))$ and η is the external efficiency of the laser. It has also been assumed that the feedback is not strong enough to bring the phase noise down to near the SQL so that only the phase diffusion noise from dipole moment and vacuum fluctuations need be considered.

From these expressions a number of observations can be made. Firstly, the pump noise and spontaneous emission noise are unaffected by the optical feedback as can be seen from the first term inside the brackets in (4.46). This just reflects the fact that these sources produce fluctuations in the amplitude without corresponding fluctuations in the phase. The second term inside the brackets in (4.46) comes from the combined contribution of the dipole and vacuum fluctuations. It clearly does depend on the feedback parameters and can, in fact, be reduced. The final term in (4.46) is the uncorrelated component of the phase noise which has been coupled into the amplitude noise by the feedback. In addition, the amplitude noise power spectrum depends not on the independent contributions of the two feedback quadratures but only on the combined quantity $C = C_r/(1+C_i)$. This is not surprising since C_r represents the part of the feedback responsible for altering the photon lifetime (rather than the phase shift) inside the semiconductor laser cavity (see Figure 4-5) and in order to change the amplitude noise, the photon lifetime must be altered. On the other hand the reduction in the laser phase noise (and hence the linewidth) does depend independently on C_i which just indicates that since the feedback phase changes with laser frequency (or phase), the phase noise can be corrected directly without relying

on phase-to-amplitude coupling. Thus, by making C_i large and then tailoring C_r to reduce the amplitude noise, the noise in both field variables can be reduced simultaneously. The limit to the amount of phase noise reduction possible with optical feedback is set by the Heisenberg Uncertainty Principle: (4.47) is only valid as long as $P_{\Delta\psi}(0) \gg 1/2$.

From (4.46) it is possible to deduce the maximum reduction of the dipole and vacuum terms under feedback conditions. This occurs when $C = \alpha/[1+(1+\alpha^2)n_{sp}R]$ resulting in a reduction of the dipole and vacuum noise by a factor of $1+\alpha^2$. The low frequency amplitude noise then becomes

$$P_{\Delta r}(\Omega \approx 0) = \frac{1}{2}(1-\eta) + \frac{\eta}{2}\left(\frac{1}{R} + \frac{1}{1+\alpha^2}\frac{2}{n_{sp}R^2}\right). \tag{4.48}$$

Thus, close to threshold, where the dipole and vacuum noise dominate, the amplitude noise can be reduced by as much as 14 dB using optical feedback in addition to large reductions in the laser linewidth. At higher pump rates, however, the spontaneous emission noise dominates the other noise sources and the maximum amplitude noise reduction decreases.

The expressions (4.43) and (4.45) are plotted against pump rate R in the low frequency limit in Figure 4-11. The parameter values are taken to be $\Omega = 10^6 rad/s$, $n_{sp} = 2$, $\beta = 10^{-5}$, $\tau_p = 2\times10^{-12}s$, $\tau_{sp} = 2\times10^{-9}s$, $\tau_{p0} = 10^{-11}s$, $\alpha = 5$, $R_s = 1M\Omega$ and $\phi_0 = -\pi/2$ ($C_i = 0$ and $C_r > 0$). Features to note are that the amplitude noise close to threshold can be reduced significantly, whereas at pump rates far above threshold, the noise is always increased due to the added uncorrelated phase noise. Figure 4-12 shows the maximum noise reduction under optical feedback conditions as well as the value of C required to produce this reduction. At moderate pump rates ($R \approx 1$) it can be seen that optical feedback can enhance the squeezing in a semiconductor laser by as much as 3 dB. In addition, the injection current at which the onset of squeezing occurs is reduced by up to a factor of 2 (see Figure 4-13, an expanded version of Figure 4-12).

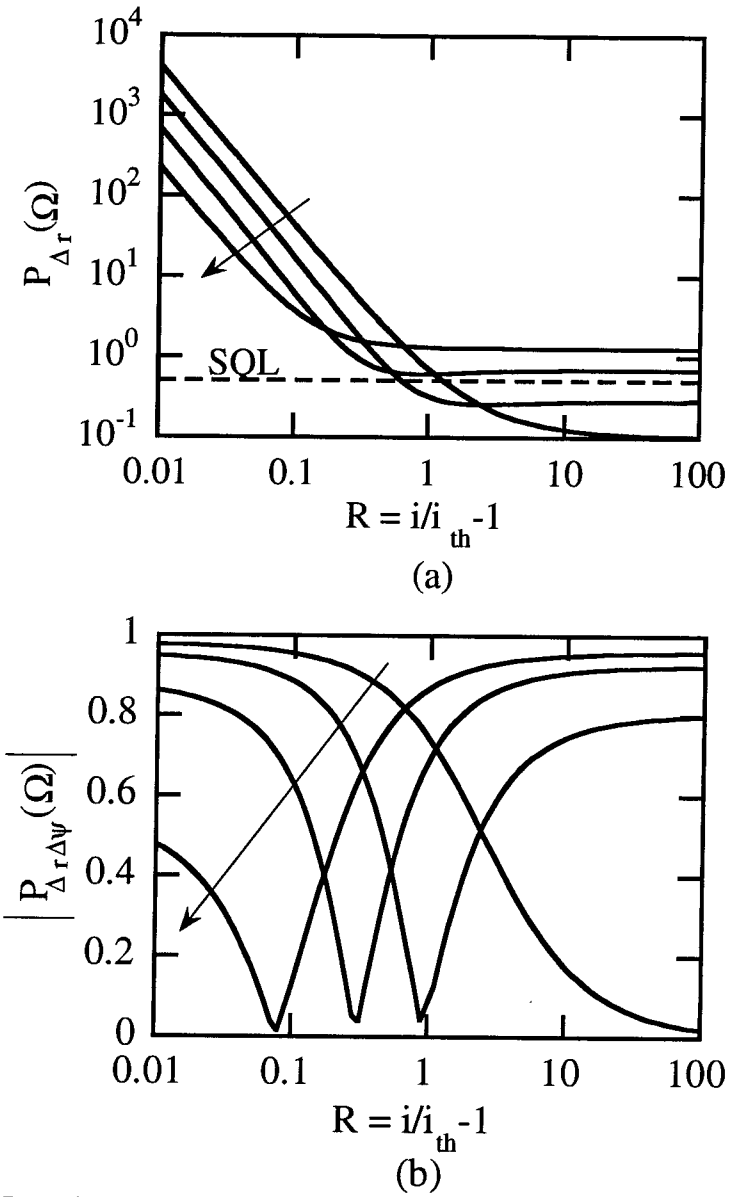

Figure 4-11: Low frequency amplitude noise power and phase-amplitude correlation. Here $C = 0, 0.1, 0.3, 1$ increasing along the arrow path. Large noise reduction is possible at low pump rates where the phase-amplitude correlation is high. An enhancement of the amplitude squeezing around $R = 1$ is also produced.

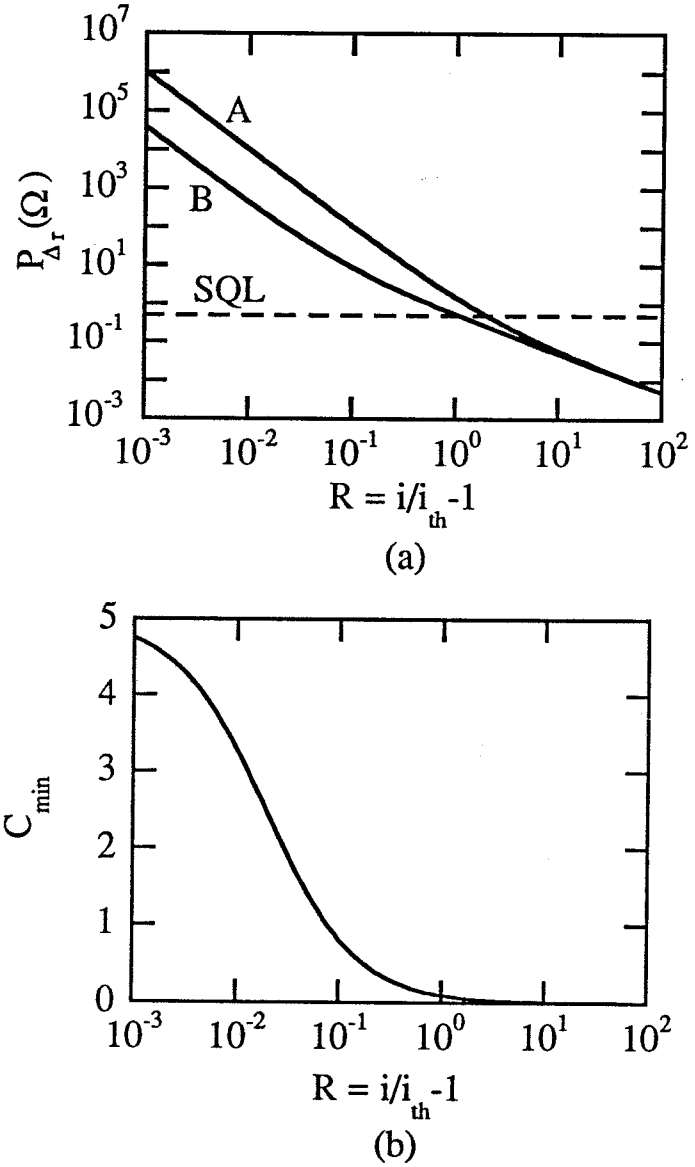

Figure 4-12: (a) The maximum of the low frequency amplitude noise reduction under optimal feedback conditions. Trace A indicates the noise under free-running conditions and trace B indicates the minimum noise attainable using optical feedback. (b) The value of C corresponding to this maximum reduction.

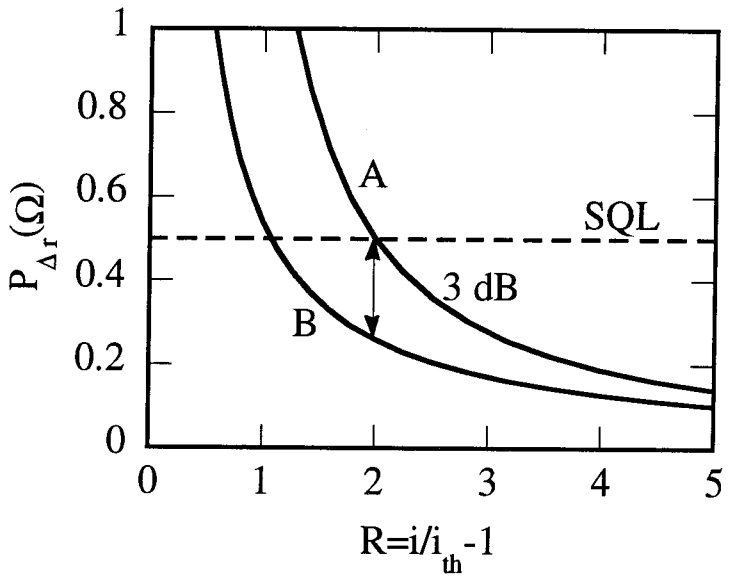

Figure 4-13: An expanded portion of Figure 4-12 showing $\approx$ 3 dB of squeezing enhancement at $R = 2$. Trace A is for free-running conditions and trace B is with optimal optical feedback.

This enhancement of the amplitude squeezing at moderate pump rates is potentially important for room temperature generation of squeezed light as mentioned in Section 4.2.4. Most experiments to date have required cryogenic operation of the laser in order to observe substantial squeezing, the largest being 8.3 dB below the SQL. By contrast, to the author's knowledge, the only room temperature experiment for a free-running laser has observed only 0.33 dB. The use of optical feedback, which can also improve the side mode suppression, could possibly add at least 1-2 dB to the squeezing under such conditions. A significant improvement in the degree of squeezing under strong feedback conditions has already been reported [92] although the role of phase-to-amplitude coupling in this experiment is unclear.

If pump-suppression is not used, then the laser approaches the shot noise limit at high pump rates which is a result of the unsuppressed pump fluctuations. Since the pump noise cannot be reduced by optical feedback, the shot noise barrier cannot be broken using this method, although considerable noise reduction near threshold is still possible. The amplitude noise for the non-pump-suppressed case is plotted in Figure 4-14.

It is also instructive to examine how the laser noise depends on feedback parameters at a fixed pump rate. Figures 4-15 and 4-16 show the noise spectra and amplitude-phase correlation as a function of feedback power at constant feedback phase for several pump rates. As the pump rate increases, the minimum noise occurs at decreasing values of C. The reason that the noise reduction decreases with increasing pump rate is that the noise due to spontaneous emission into non-lasing modes which dominates at high pump rates does not produce correlated amplitude and phase noise. This can be seen explicitly if at the low frequency phase-amplitude correlation without feedback is considered. This is (with $n_{sp} = 1$ and $\tau_p = \tau_{pe}$)

$$|P_{\Delta\hat{r}\Delta\hat{\psi}}| = \frac{\alpha}{\sqrt{(1+\alpha^2)(1+R/2)}}. \tag{4.49}$$

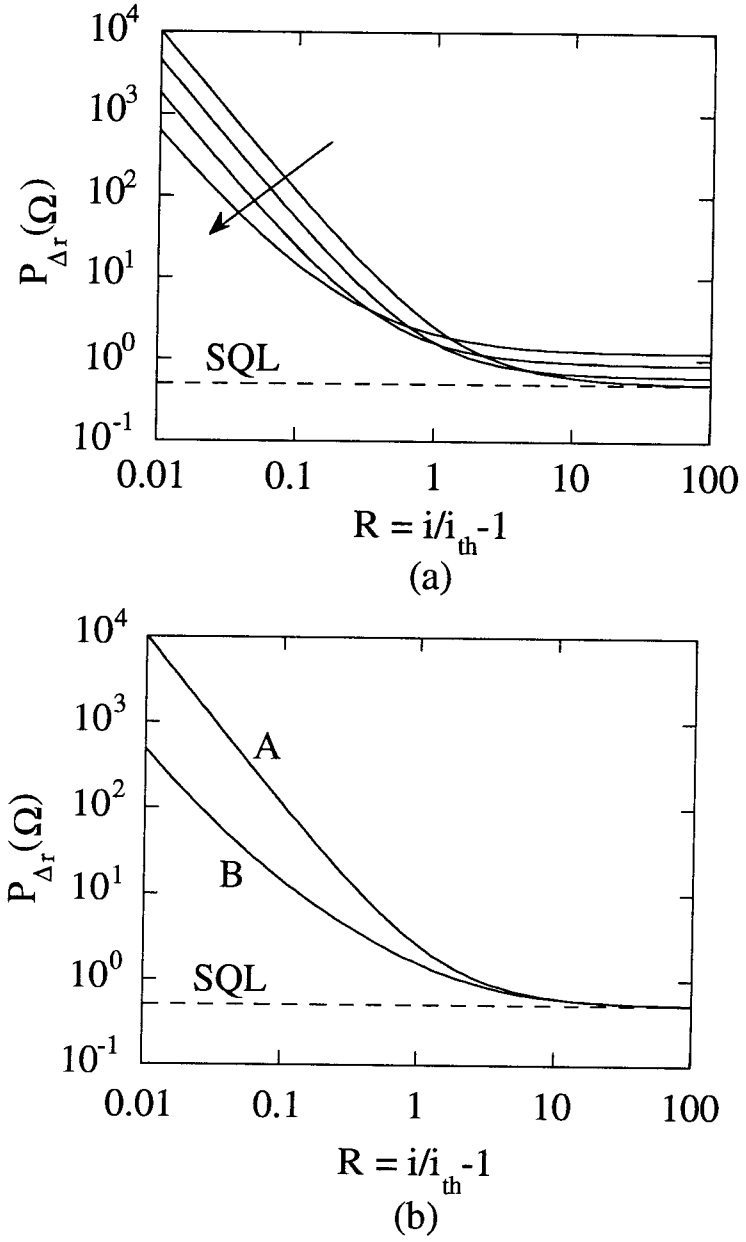

Figure 4-14: (a) Low frequency noise reduction in a laser featuring Poissonian pump noise. Here $C = 0, 0.1, 0.3, 1$ increasing along the arrow path. (b) The maximum noise reduction in this case. Trace A is with no feedback while trace B is with optimal feedback.

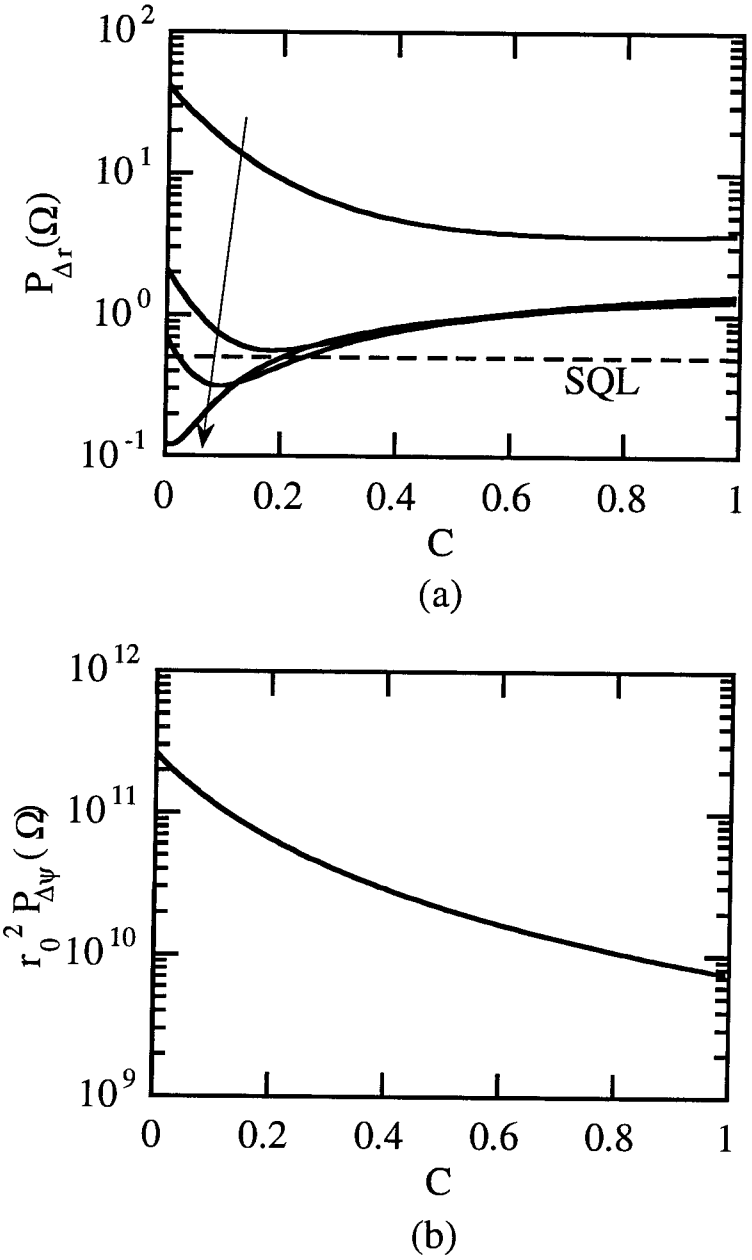

Figure 4-15: (a) Low frequency amplitude noise dependence on feedback for $R = 0.1, 0.5, 1, 10$ increasing along the arrow path. (b) The corresponding phase noise.

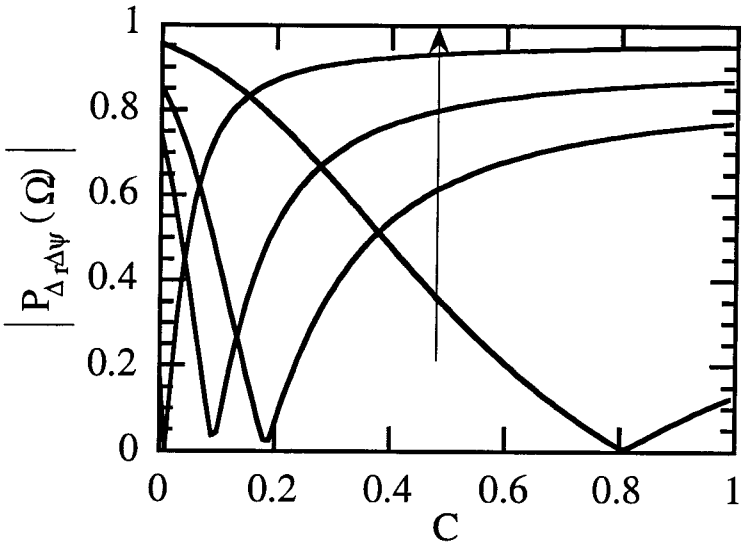

Figure 4-16: Low frequency amplitude-phase correlation dependence on feedback for $R = 0.1, 0.5, 1, 10$ increasing along the arrow path.

As R increases, the amplitude-phase correlation decreases to zero indicating that the optical feedback will be ineffective at reducing the amplitude noise far above threshold as mentioned above.

If instead the feedback amplitude is kept constant and the feedback phase is varied, the noise reduction is considerably altered as shown in Figures 4-17 and 4-18. Here $R = 1$, $n_{sp} = 2$, $\alpha = 5$ and the various traces are for different values of $\kappa_0 \tau$. Sharp increases in the noise occur when the feedback phase is such that $1 + C_i + \alpha C_r \approx 0$ and in fact, for $1 + C_i + \alpha C_r < 0$, the laser mode is not stable and mode hopping is likely to occur. Thus, careful control of the feedback phase is necessary in order to take full advantage of the potential for reducing the noise with optical feedback.

Finally, the semiclassical result can be recovered in the limit $R \rightarrow 0$ when the amplitude noise rises far above the shot noise level. In this case the noise due to the quantum nature of the field is negligible compared to the vacuum and dipole noise.

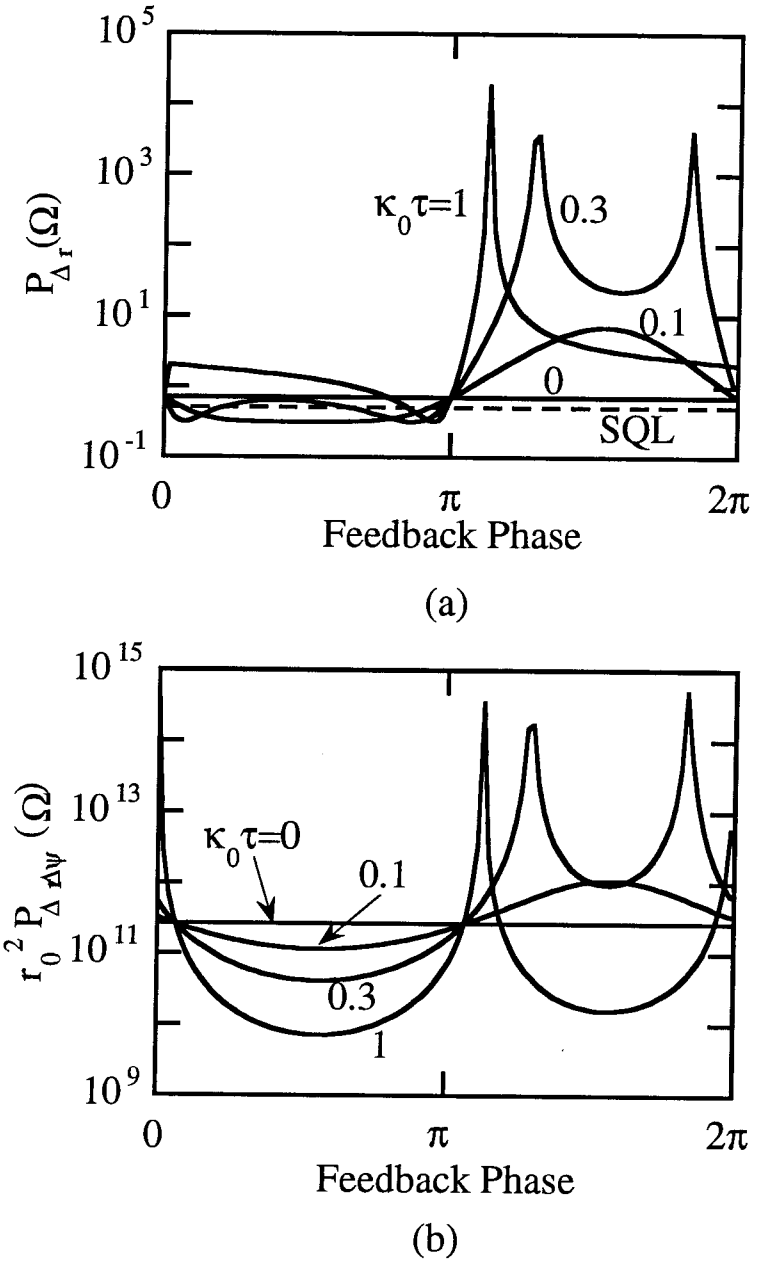

Figure 4-17: The low frequency noise spectra dependence on feedback phase ϕ_0. (a) Amplitude noise and (b) phase noise.

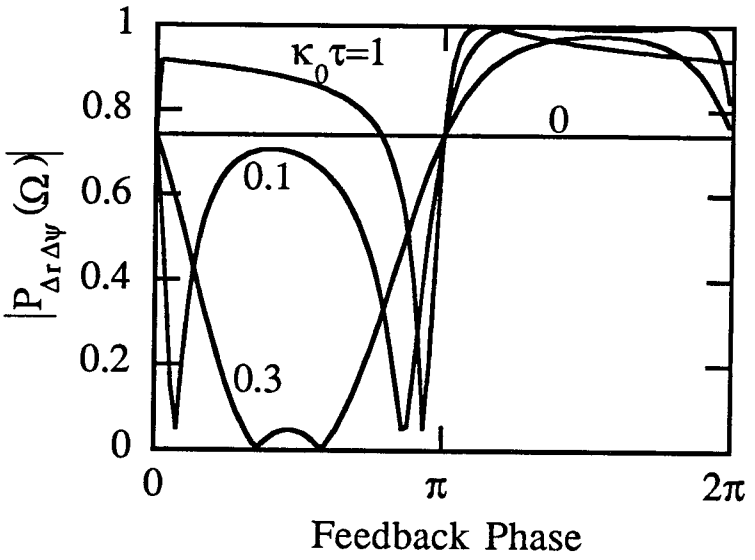

Figure 4-18: The low frequency amplitude-phase correlation dependence on feedback phase ϕ_0.

The low frequency amplitude noise, (4.46), then reduces to

$$P_{\Delta r}(0) = \frac{\eta}{n_{sp}R^2}\frac{1+C^2}{(1+\alpha C)^2}. \tag{4.50}$$

This corresponds to the result derived in a semiclassical analysis for the amplitude noise reduction using dispersive loss [7]. However, we see that this result is only valid near threshold and that as the pump rate is increased, other noise sources not present in the semiclassical model dominate the laser amplitude noise. Due to the absence of a restoring force for the field phase, the phase diffusion noise is far above the SQL even at high pump rates, however, and the fully quantum mechanical result for the phase noise (and hence the laser spectral linewidth) (4.47) corresponds to the semiclassical result. This indicates that even at high pump rates, the semiclassical predictions of linewidth reduction with optical feedback are valid.

4.7 Spectral uncertainty product

Since large simultaneous reductions in the amplitude and phase noise of the laser external field are possible, it is important to verify that the spectral uncertainty relation implied by the Heisenberg Uncertainty Principle is not violated. This relation can be expressed [107,108,10]

$$P_{\Delta\hat{r}}(\Omega)P_{\Delta\hat{\psi}}(\Omega) \geq \frac{1}{4r_0^2} \tag{4.51}$$

where r_0^2 is the output photon flux in photons/second. For a conventionally pumped laser at a moderate pump rate, the large amount of phase diffusion noise below the cavity bandwidth generates a spectral uncertainty product far in excess of this fundamental limit. In the infinite pump rate limit in a pump-suppressed laser, this phase diffusion noise is what compensates for the large degree of amplitude squeezing at low frequencies [10]. While the amplitude noise drops below the SQL by a factor proportional to Ω^2 (as $\Omega \rightarrow 0$), the phase noise increases above the SQL by a factor of $1/\Omega^2$ satisfying (4.51).

Any changes in the phase noise spectrum caused by optical feedback will thus have significant effects on the squeezing bandwidth. We examine the case of optical feedback producing phase noise reduction ($C_i > 0$) but no amplitude noise reduction ($C_r = 0$) since this is where the most dramatic changes in the phase noise spectra occur. Figure 4-19 shows the phase noise, amplitude noise and spectral uncertainty product $4r_0^2 P_{\Delta\hat{r}}(\Omega)P_{\Delta\hat{\psi}}(\Omega)$ as a function of frequency at $R = 10^5$ and at several values of C_i. It can be seen that as the phase noise drops due to the feedback, the amplitude squeezing bandwidth is reduced to compensate. All of the spectral characteristics are shifted uniformly to lower frequencies by a factor of $1 + C_i$.

The results of Figure 4-19 also determine the quantum limits to the amount of phase noise reduction (and therefore linewidth reduction) that can be obtained using optical feedback. This limit is clearly set by the SQL, which, in the case of the phase

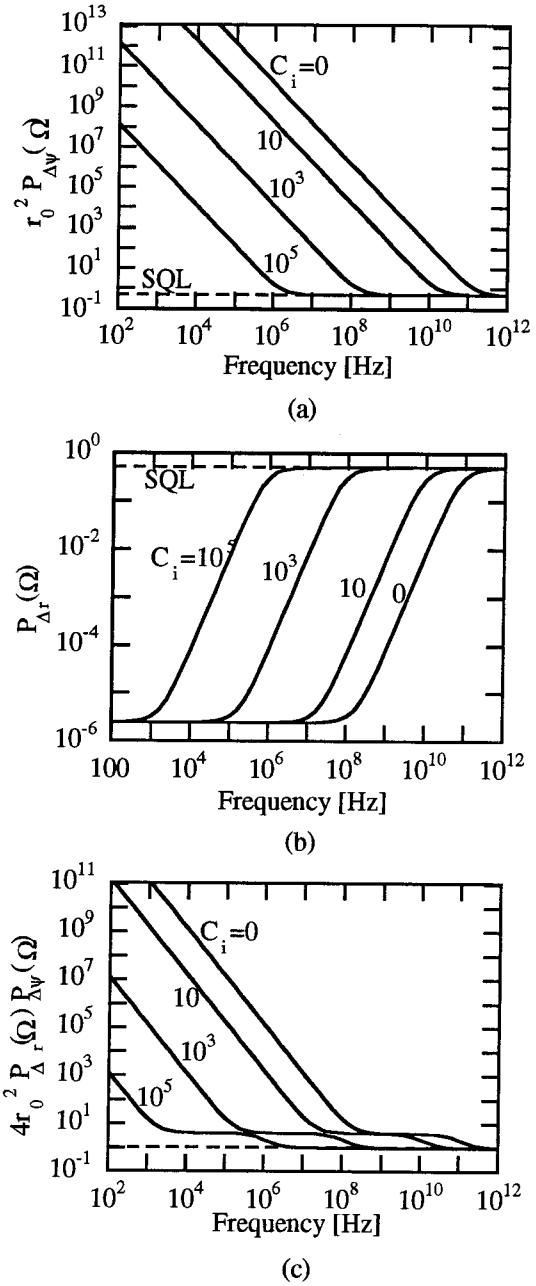

Figure 4-19: Noise spectra dependence on feedback parameter C_i in the high pump rate limit ($R = 10^5$). (a) Phase noise, (b) amplitude noise and (c) spectral uncertainty product.

noise, is caused by the vacuum fluctuations reflected from the front facet of the laser. Since there exists no restoring force for the phase of the internal optical field, the cancellation of the vacuum phase noise in the external field does not occur and the full shot noise is present in addition to the phase diffusion noise from the internal laser field. In addition, this vacuum phase noise is not affected at all by the external cavity.

4.8 Discussion

It is interesting to compare the quantum noise reduction which can be obtained using optical feedback with the reductions obtained using other methods such as junction voltage feedforward [11] and amplitude-phase decorrelation [11,102]. It has been found that the laser junction voltage is also correlated with the output intensity noise [109]. The junction voltage correlation with output field intensity, $P_{\Delta r \Delta v}$, is given in the low-frequency limit with $n_{sp} = 1$ by [110]

$$P_{\Delta r \Delta v} = -\sqrt{\frac{1}{1 + R/2}}. \tag{4.52}$$

It is, of course, precisely this correlation which gives rise to the amplitude-phase correlation since the lasing medium refractive index depends on the carrier density and hence the junction voltage. However, the additional phase fluctuations which arise from spontaneous emission into the lasing mode dilute the correlation slightly. Thus, the amplitude-phase correlation given by (4.49) can be rewritten as

$$|P_{\Delta r \Delta \phi}| = \sqrt{\frac{\alpha^2}{1 + \alpha^2}} |P_{\Delta r \Delta v}| = \sqrt{\frac{\alpha^2}{1 + \alpha^2}} \sqrt{\frac{1}{1 + R/2}} \tag{4.53}$$

which separates out the degradation in the correlation caused by the uncorrelated component of the phase noise (due to spontaneous emission into the lasing mode) from the degradation caused by the uncorrelated component of the amplitude noise (due to

spontaneous emission into *non-lasing* modes). Thus we find that the amplitude-phase correlation is only slightly smaller than the amplitude-junction voltage correlation for typical values of $\alpha \approx 3 - 5$.

The fact that the amplitude-phase correlation is slightly smaller than the amplitude-junction voltage correlation changes the amount by which the amplitude noise can be reduced. At low pump rates ($R \rightarrow 0$), $P_{\Delta r \Delta v} \rightarrow -1$ and the perfect anti-correlation implies that it is possible to reduce the amplitude noise by a large amount. In this same limit, $|P_{\Delta r \Delta \phi}| \rightarrow \alpha/\sqrt{1+\alpha^2}$ which means that the amplitude noise can be reduced at most by a factor of $1 + \alpha^2$ using either feedforward, amplitude-phase decorrelation or feedback. On the other hand, when the laser is significantly above threshold ($R \geq 1$), then the uncorrelated amplitude noise plays the major role in reducing the amplitude-phase decorrelation. In this case, $P_{\Delta r \Delta \phi} \approx P_{\Delta r \Delta v}$ and thus the noise reduction obtained by junction voltage feedforward is roughly equal to the reduction obtained using optical feedback. This can be seen by comparing Figure 4-12 with the results obtained in Ref. [11]. Thus, it is found that at moderate pump rates, optical feedback is almost as effective as junction voltage feedforward in enhancing the squeezing of a pump-suppressed semiconductor laser. In addition, the maximum amplitude noise reduction obtainable using optical feedback is identical to that for amplitude-phase decorrelation at all pump rates since both methods rely on the same correlation property for the noise reduction.

One advantage that optical feedback may have over junction voltage feedforward is that parasitics often make a clean measurement of the actual junction voltage difficult, especially at room temperature. In addition, feedforward at high frequencies can be limited by the speed of electronic components. Optical feedback suffers from neither of these problems, and therefore this technique may be somewhat simpler to implement.

In conclusion, optical feedback can significantly improve the quantum noise properties of pump-suppressed semiconductor lasers. The potential for noise reduction

is due to the quantum correlation between the amplitude and phase of the external optical field emitted from such devices. At low frequencies and moderate pump rates, an enhancement of the amplitude squeezing by up to 3 dB is possible. This enhancement could find application in room-temperature generation of squeezed light when the high pump rates needed to obtain more complete squeezing are not practical. Other aspects of quantum noise reduction using optical feedback have also been investigated including the effects of finite cavity delay and feedback phase.

Chapter 5

Amplitude noise reduction using dispersive optical feedback

5.1 Introduction

In this section, the theoretical predictions obtained in Chapter 4 are tested experimentally in the classical regime with the laser biased close to threshold. Near threshold the theory predicted that substantial reductions in the amplitude noise could be obtained since it is in this regime that the noise due to vacuum and dipole moment fluctuations dominates. These sources produce correlated noise in both the field amplitude and phase which can be exploited with optical feedback to reduce the amplitude noise. Reductions in the amplitude noise of up to $1 + \alpha^2$ (about 10 dB) should be possible, the main fundamental limitation very close to threshold being the imperfect correlation between amplitude and phase caused by the uncorrelated component of the phase noise.

Compared with linewidth reduction, the volume of previous experimental work on amplitude noise reduction with optical feedback has been relatively small. A reduction in the amplitude noise has been observed by Dahmani et al. [5], but the dependence of this reduction on feedback level and injection current were not measured and the role of phase-amplitude coupling was not clear. Newkirk and Vahala [102,105] have also measured substantial reductions in the laser amplitude noise using amplitude-

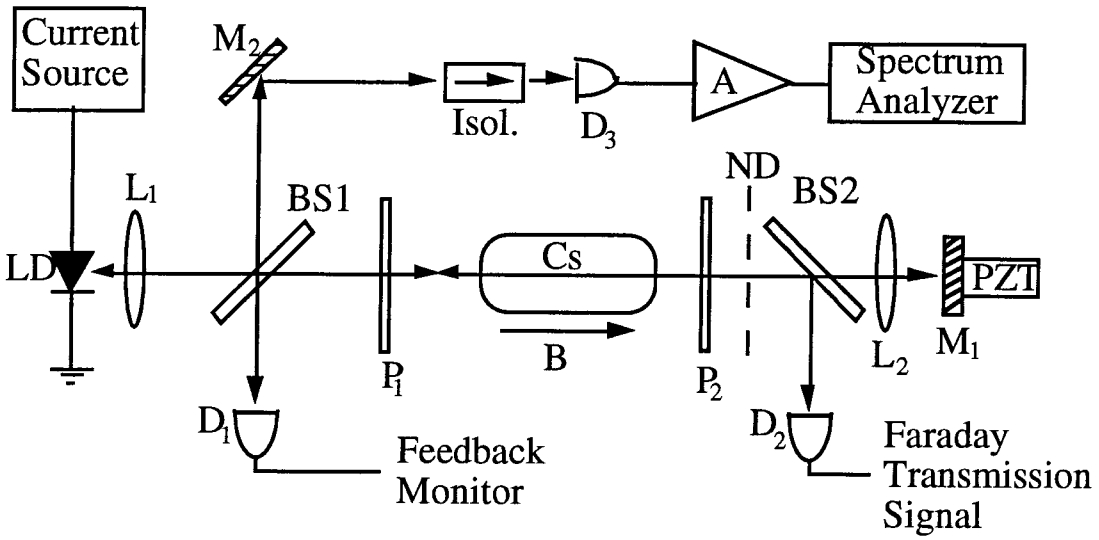

Figure 5-1: Experimental Setup: LD, laser diode; L, lens; BS, beam splitter; M, mirror; P, polarizer; D, detector; ND, neutral density filter. The amplitude noise power is measured at D_3, and the feedback power is monitored at D_1.

phase decorrelation and in doing so demonstrated the feasibility of using the phase-amplitude correlation to reduce the amplitude noise.

5.2 Low frequency amplitude noise

The experimental setup, shown in Figure 5-1, was described in Section 2.2.3. In this particular experiment, a single-mode GaAs semiconductor laser (STC LT50A-03U) lasing at 852 nm and with a threshold current of 51.4 mA was used. The Cs was heated to $\approx 90°C$ resulting in a feedback power $\approx 10^{-6}$ of the output power when the laser was tuned to near the Doppler-broadened Cs transition at 852 nm. Due to the wavelength selectivity of the Cs, the feedback affected the dynamics of only a single longitudinal mode. Most of the light (98%) was coupled out of the external cavity (at BS1) and was then passed through a pair of optical isolators which provided 60 dB of isolation. For measurement of the low-frequency noise ($f < 150$ MHz), the beam was

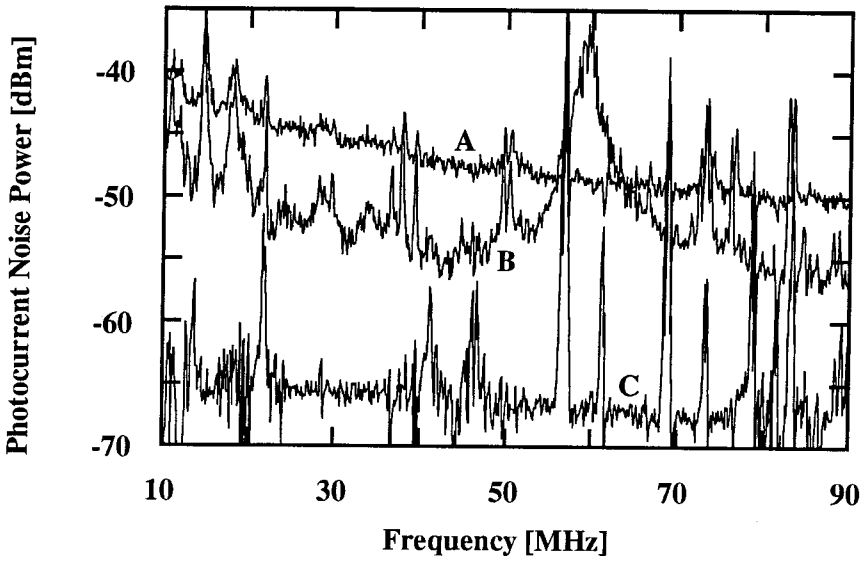

Figure 5-2: Frequency dependence of the detector photocurrent noise power at an injection current of 76 mA. Free running (trace A), with $P_{fb}/P_{out} = 4 \times 10^{-7}$ (trace B). Trace C indicates the SQL.

focused onto a large area, high-efficiency photodiode (Hamamatsu 1722-01) and the resulting photocurrent amplified and sent to an electronic spectrum analyzer. The net current-to-current differential efficiency above threshold between the laser and the detector was 36%. The detector was found to be linear at DC up to photocurrents of 20 mA but showed some weak saturation at frequencies above 100 MHz at the higher photocurrents.

The laser was tuned to the top of the Doppler-broadened Cs Faraday line, the feedback was applied and the amplitude noise spectrum was measured. A portion of this spectrum is shown in Figure 5-2, taken at an injection current of 76 mA. Trace A is the noise under free-running conditions and trace B is the noise with a feedback power of 4×10^{-7} of the output power. Trace C is the shot noise level calibrated by shining a filtered incandescent lamp onto the detectors to produce the

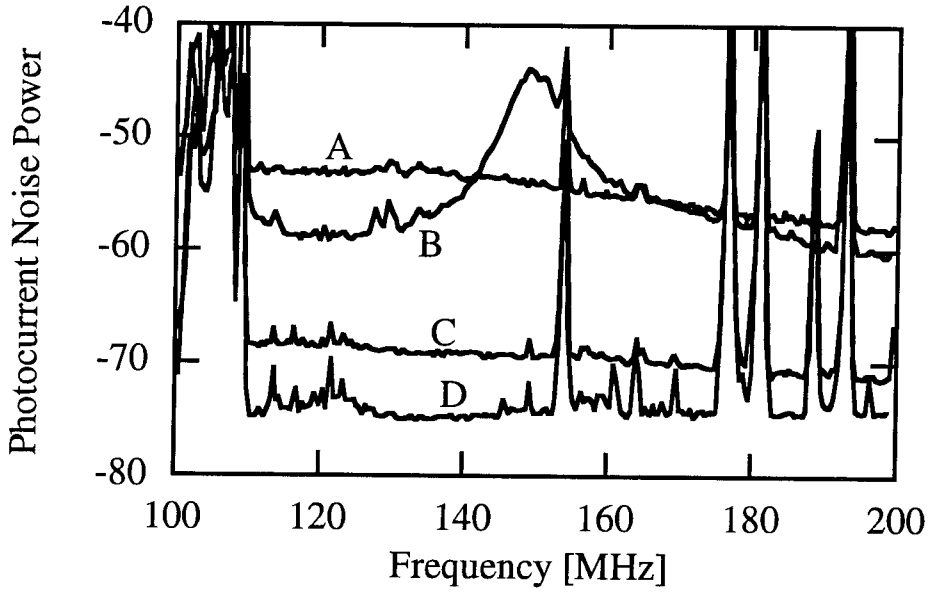

Figure 5-3: Raw data showing the frequency dependence of the photocurrent noise power spectrum taken at an injection current of 76 mA. Data are shown with no feedback (trace A) and $P_{fb}/P_{out} = 1.7 \times 10^{-6}$ (trace B). Traces C and D indicate the SQL and background amplifier noise respectively.

same photocurrent as the laser did.

Under feedback conditions, the amplitude noise is seen to be reduced at most frequencies with a peak occurring at 60 MHz, a frequency corresponding to the external cavity free spectral range modified from its empty cavity value of 200 MHz by the dispersion of the Cs. Reductions by as much as 7 dB were observed under optimal optical feedback conditions at an injection current of 76 mA. Larger reductions of the noise are expected closer to threshold, but the inability to tune the laser to the Cs line at lower injection currents prevented these from being observed.

It can be seen from Figure 5-2 that the noise is not flat but decreases with increasing frequency: a 7 dB decrease in the noise occurs over roughly one order of magnitude in frequency. Because of this unusual behavior at lower frequencies, the amplitude noise power was measured as a function of the feedback power at a frequency of 116

MHz in an attempt to obtain a better agreement with theory; a sample of raw data between 100 MHz and 200 MHz taken at an injection current of 76 mA is shown in Figure 5-3. Trace A in this figure shows the laser noise with no feedback; trace B, the noise with feedback; trace C, the SQL; and trace D, the background amplifier noise level. The results of the measurement at 116 MHz are plotted in Figure 5-4 at two different pump rates. It is assumed in this plot that the coupling of feedback light back into to laser is 80%. For each measurement, the feedback phase was adjusted so that the laser frequency with feedback was the same as the unperturbed laser frequency (zero-frequency pulling [6]) thereby fixing the phase to a constant, known value. Each measurement was normalized to the SQL after subtracting the background amplifier noise. At an injection current of 76 mA (trace A), the maximum noise reduction was found to be 7 dB; at higher injection currents this maximum reduction decreased (trace B). The theoretical predictions are also plotted (solid lines) using (4.43) and parameter values of $\tau_p = \tau_{pe} = 9.1 \times 10^{-12}s$, $\tau_{sp} = 4.3 \times 10^{-9}s$, $n_{sp} = 1$ (76mA), $n_{sp} = 1.25$ (97mA), $\beta = 10^{-5}$, $\alpha = -4.5$ (76 mA), $\alpha = -3.4$ (97 mA), $\tau = 1.4 \times 10^{-8}s$, $\eta_{int} = 0.85$ and $\eta_{ext} = 0.42$. The laser is assumed to have an uncoated facet ($R = 0.31$), refractive index of 3.5, a length of $200\mu m$ and 80% feedback coupling. A reasonable agreement between theory and experiment is found at the higher injection current, although it is emphasized that many of the laser parameters assumed in the fit are not known precisely and are adjusted to obtain a good agreement with the experiment. However, all parameters are in roughly the right range for a laser of this type. At the lower injection current, the laser noise increased if the feedback power was increased above about 1.4×10^{-6} causing a deviation from the theoretical prediction.

As mentioned above, the difficulty of tuning the laser to the Cs line and the danger of thermal damage to the laser at high output powers limited the range of injection currents at which these measurements could be made. Due to the high threshold current of this particular laser, the maximum pump rate obtainable was

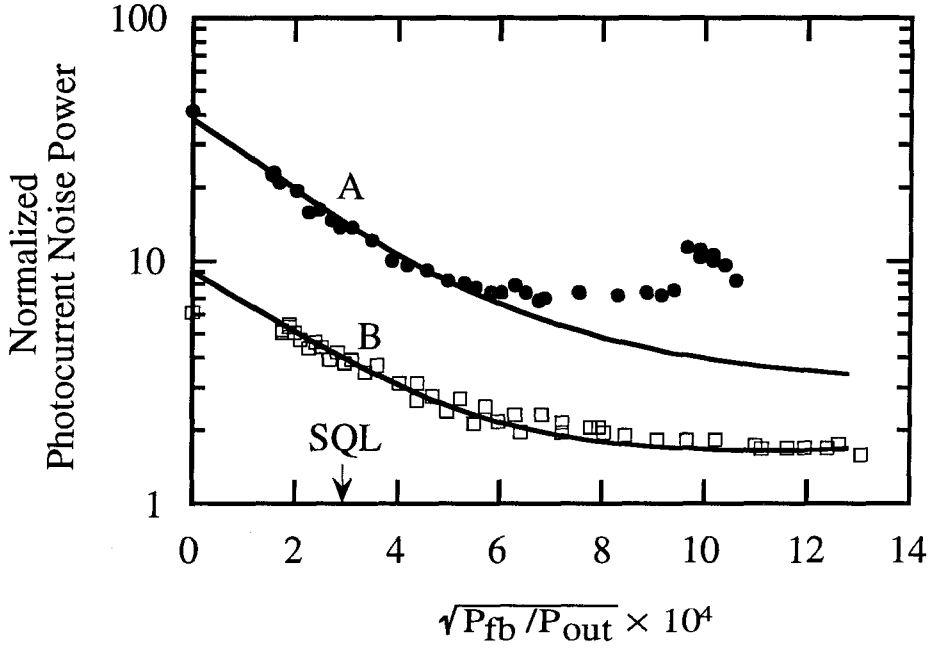

Figure 5-4: Amplitude noise power at 116 MHz, normalized to the SQL, as a function of feedback power at injection currents of 76 mA (trace A) and 97 mA (trace B). The solid lines are the theoretical predictions based on (4.43).

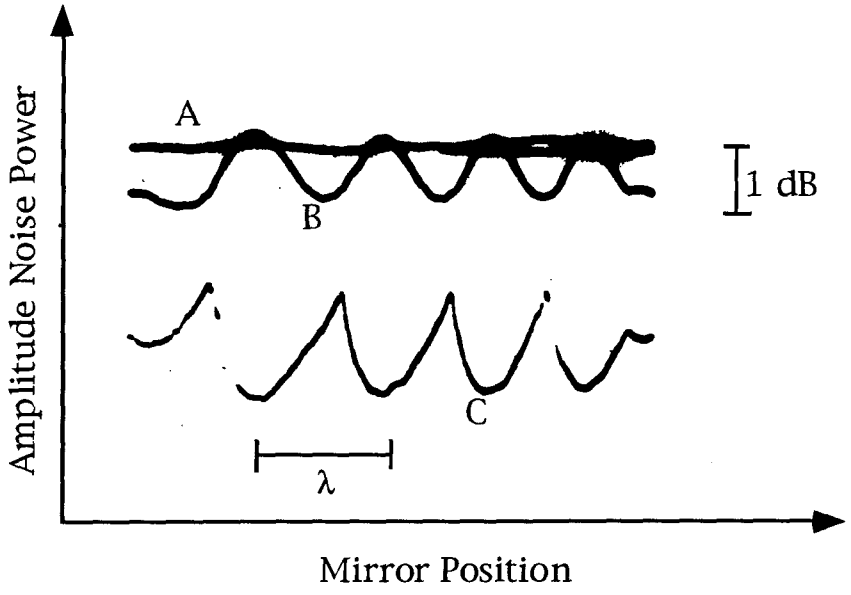

Figure 5-5: Amplitude noise reduction dependence on feedback phase. The noise at a single frequency of 130 MHz is measured as the end mirror position is scanned over several wavelengths. Trace A is with no feedback, trace B is with $P_{fb}/P_{out} \approx 1 \times 10^{-8}$ and trace C is with $P_{fb}/P_{out} \approx 5 \times 10^{-7}$.

$R = i/i_{th} - 1 = 1.4$ which permitted a noise reduction to within 2.3 dB of the SQL but which was not enough to produce squeezed light. As can be seen in Figure 4-13, a pump rate of about R=2 is required before significant low-frequency squeezing should be observable. An extension of this experiment into the quantum regime, performed with a different laser, is discussed in Chapter 6.

The dependence of the noise reduction on the feedback phase is illustrated in Figure 5-5. Here the noise power at a single frequency (130 MHz) is plotted as the external cavity end mirror position is scanned over several wavelengths. The noise is measured at three different feedback levels: trace A is with no feedback, trace B is with very weak feedback ($P_{fb}/P_{out} \approx 1 \times 10^{-8}$) and trace C is with somewhat stronger feedback ($P_{fb}/P_{out} \approx 5 \times 10^{-7}$). In trace B a smooth oscillation is seen: the very weak feedback perturbs the lasing frequency and amplitude noise, but the

frequency is continuous as the mirror position is changed. In trace C, sharp changes in the amplitude noise can be seen where the noise is maximum. This is due to the laser frequency jumping discontinuously as the mirror position is scanned.

5.3 Amplitude noise at higher frequencies

The amplitude noise at higher frequencies (100-600 MHz) is shown in Figure 5-6(a). These measurements were made by focusing the light onto a high-speed photodiode (Ortel PD050-OM). Data at five different feedback powers are shown with the feedback phase the same for all curves (determined by enforcing the zero-frequency-pulling condition). A smooth reduction in the noise at certain frequencies (116 MHz, 170 MHz, 280 MHz, 340 MHz, etc.) is clearly visible. The peaks are created by positive feedback at frequencies corresponding to the inverse of the external cavity round-trip time (at 320 MHz, for example) become narrower and increase in size as the feedback power is increased. The expanded lower frequency portion of this plot is shown in Figure 5-6(b). The narrowing of the peak at 140 MHz is seen clearly here.

Finally, the dependence of the high-frequency noise on end mirror position was measured. Changing the end mirror position effectively changes the phase of the optical feedback. Figure 5-7 shows the noise spectrum at a constant feedback power of $P_{fb}/P_{out} = 1.3 \times 10^{-6}$ but at three different phases (traces B, C and D). The spectrum with no feedback is also shown in trace A. It can be seen that the width and frequency of the peaks change significantly as the phase changes.

A theoretical plot using (4.43) of the expected dependence of the amplitude noise power spectrum structure under feedback conditions is shown in Figure 5-8. The parameter values used were: $\tau_{sp} = 3.8 \times 10^{-9}s$, $\tau_{ph} = 9.1 \times 10^{-12}s$, $n_{sp} = 1$, $R = 0.94$, $\beta = 10^{-5}$, $\alpha = -6$, $\tau = 14 \times 10^{-9}s$, $\eta_{int} = 0.85$, $\eta_{ext} = 0.17$ and $R_s = 1k\Omega$. Figure 5-8(a) shows how the spectrum changes as the feedback power [which varies between 0 (trace A) and $\kappa = 0.2$ GHz (trace B)] is changed while Figure 5-8(b) shows

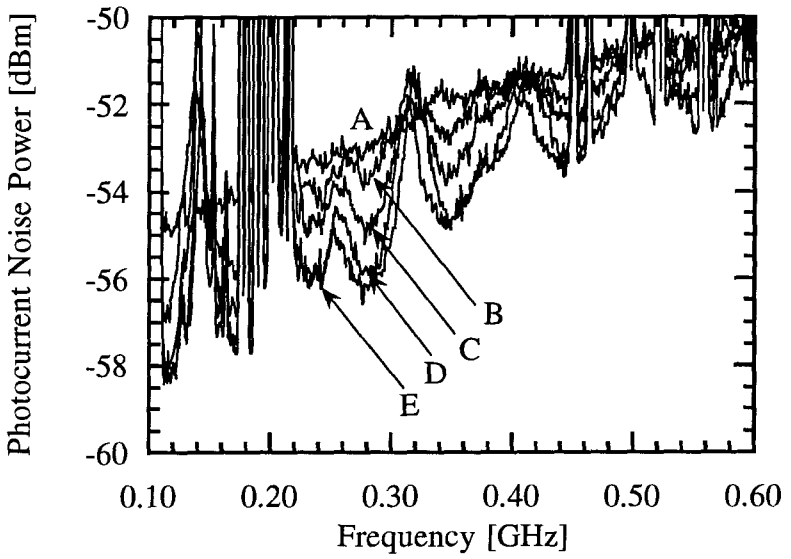

(a)

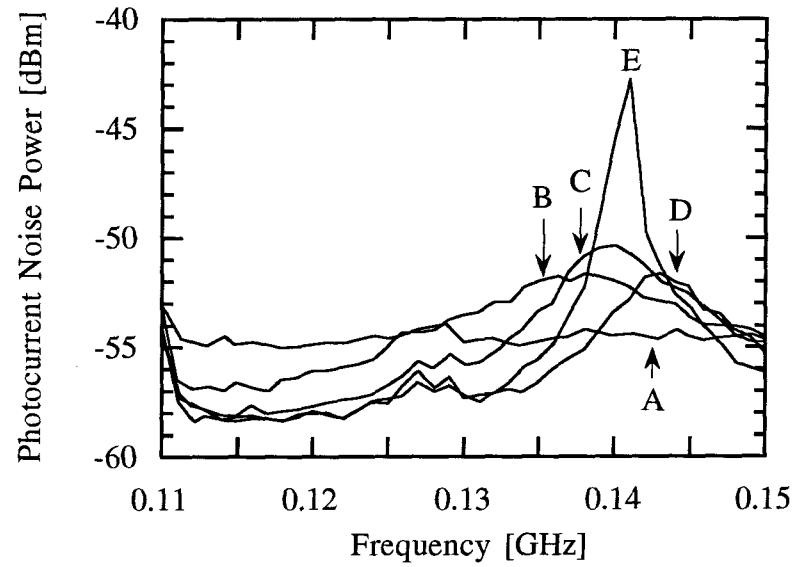

(b)

Figure 5-6: (a) High-frequency amplitude noise power as a function of feedback power. The laser injection current was 98.12 mA and $P_{fb}/P_{out} = 0$ (trace A), 1.1×10^{-7} (trace B), 5.4×10^{-7} (trace C), 9.6×10^{-7} (trace D) and 1.3×10^{-6} (trace E). Plot (b) shows the expanded low frequency portion of the upper plot.

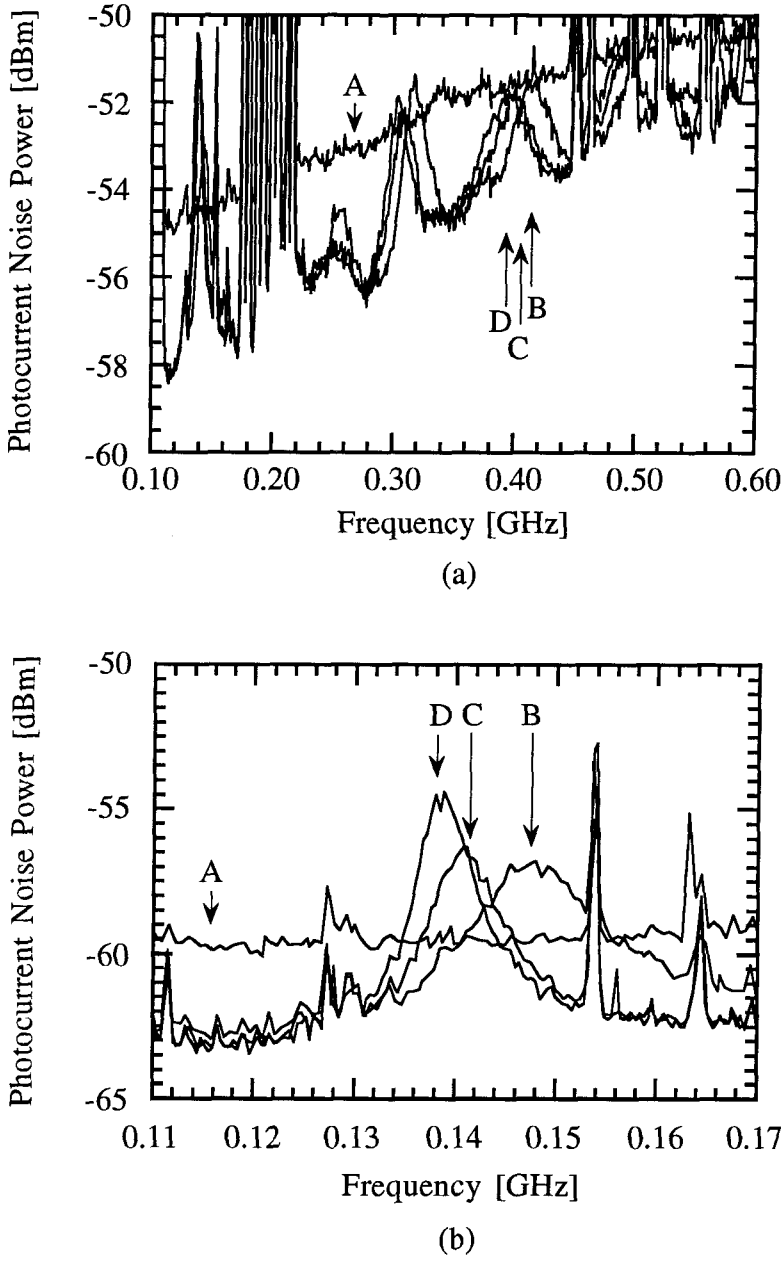

Figure 5-7: (a) High-frequency amplitude noise power as a function of external cavity end mirror position. The laser injection current was 98.1 mA and $P_{fb}/P_{out} = 1.3 \times 10^{-6}$ for traces B, C and D. Trace A is without feedback at the same injection current. Plot (b) shows the expanded low frequency portion of the upper plot.

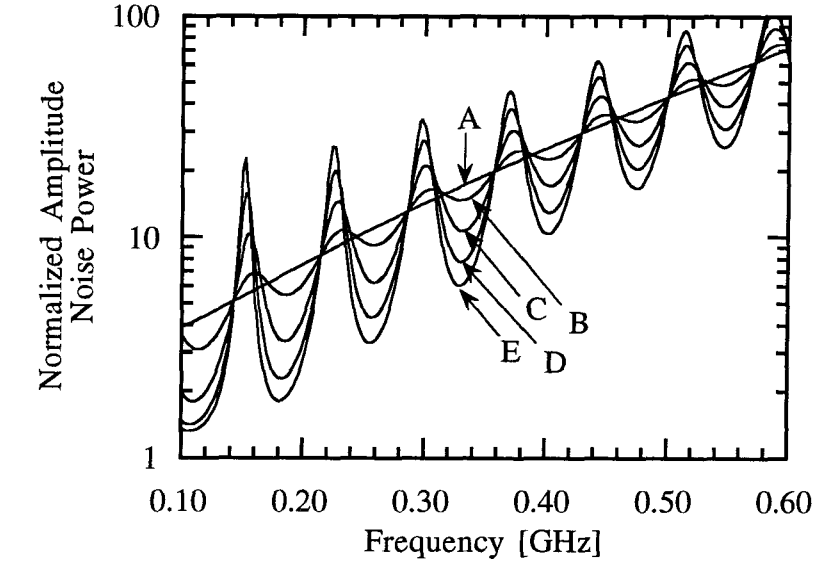

(a)

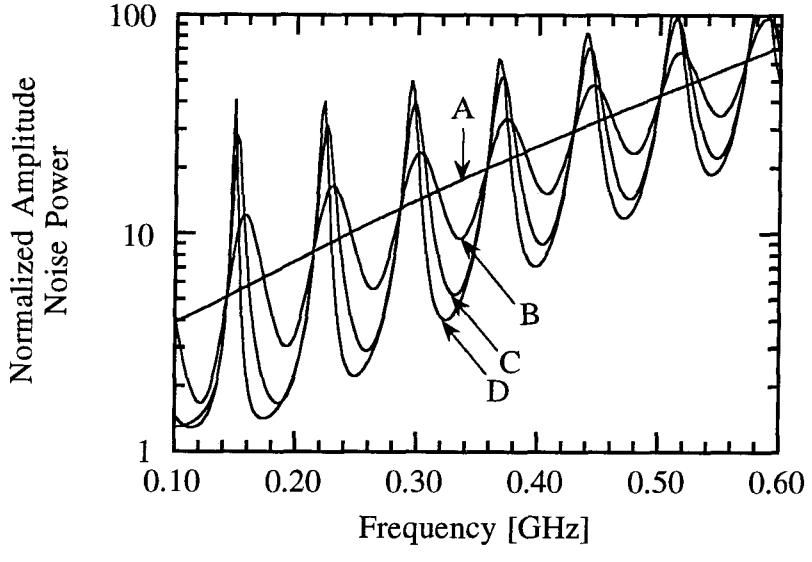

(b)

Figure 5-8: High-frequency structure of the amplitude noise spectrum under feedback conditions as predicted by the theory in Chapter 4. (a) The changes in the spectrum as the feedback power is varied at constant phase and (b) the changes when the feedback phase is varied at constant power. The results are in qualitative agreement with the experimental data of Figures 5-6 and 5-7.

the spectrum dependence on the feedback phase (with $\kappa = 0.2$ GHz). The theory appears to agree with the measured data in a qualitative sense, although the details of the two spectra do differ significantly. The agreement is not expected to be too close, however, since the model of Chapter 4 is fairly simple and lacks many of the details present in the experiment such as the frequency dependence of the Cs transmission.

5.4 Conclusion

The effects of optical feedback on the amplitude noise spectrum of a semiconductor laser have been examined experimentally. Under weak feedback conditions ($P_{fb}/P_{out} \approx 10^{-6}$), the low-frequency amplitude noise is reduced by up to 7 dB at moderate injection currents. The dependence of this reduction on the feedback power compares favorably to theoretical predictions based on a quantum mechanical model of the laser noise.

The dependence of the high-frequency (100 MHz - 600 MHz) amplitude noise spectrum on feedback power and phase was measured. Peaks occur at frequencies corresponding to the inverse of the external cavity round-trip time while the noise is reduced below the free-running level at intervening frequencies. The peak amplitude, frequency and width are found to depend on the feedback parameters in a way qualitatively explained by the theoretical model described in Chapter 4.

Chapter 6

Enhancement of amplitude-squeezing with dispersive optical feedback

6.1 Introduction

This chapter extends the experimental investigations of amplitude noise reduction using optical feedback into the quantum regime. The quantum theory of amplitude noise reduction using optical feedback was discussed in Chapter 4 and predicts the enhancement in the low-frequency squeezing that can be obtained from an already pump-suppressed semiconductor laser at moderate pump rates. The experimental setup and results are described in Section 6.2: squeezing of 19% below the SQL is obtained from a room temperature semiconductor laser with a combination of pump-suppression and weak optical feedback. The experimental data deviate significantly from theoretical predictions, however, and some discussion is presented concerning possible excess noise processes in semiconductor lasers. In Chapter 7, a multi-mode theory incorporating asymmetrical cross-mode non-linear gain is proposed to explain the discrepancy between the experimental results and the single-mode theory. Reasonable agreement is found between the multi-mode theory and the experimental data.

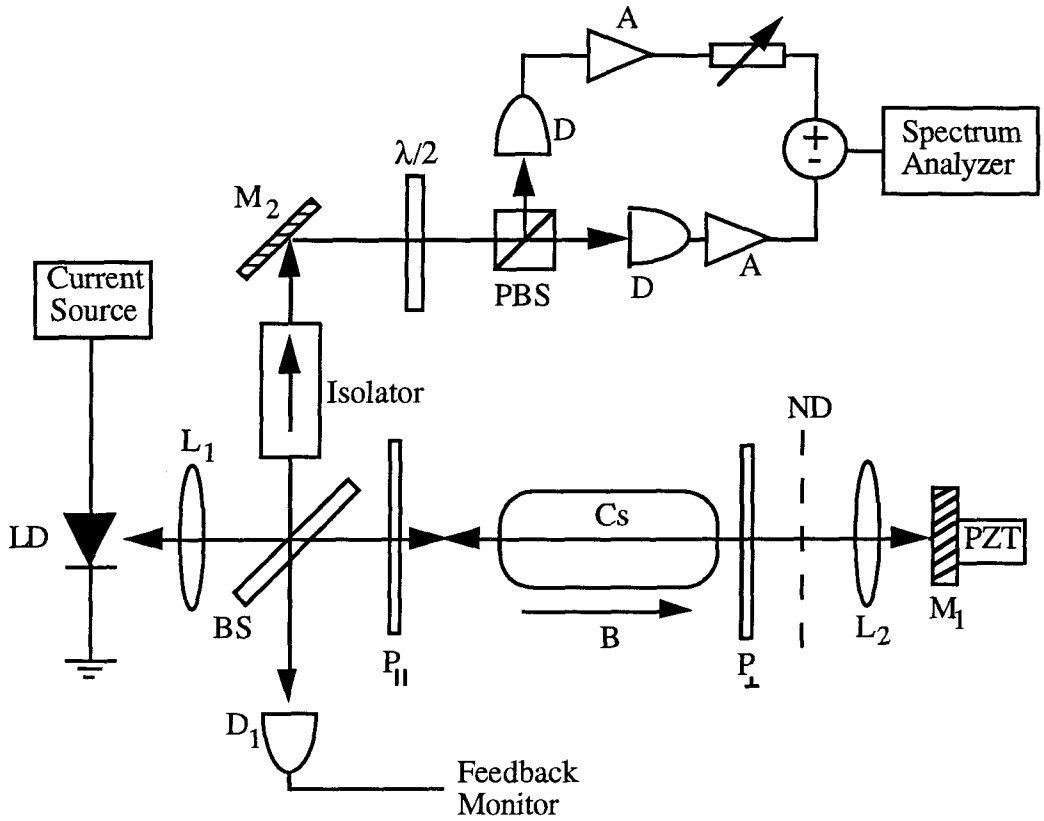

Figure 6-1: Experimental setup: LD, laser diode; BS, beamsplitter; P, polarizer; D, detector; ND, neutral density filter; L, lens; M, mirror; $\lambda/2$, half-wave plate; PBS, polarizing beamsplitter; A, amplifier.

6.2 Measurements of squeezing

The experimental setup is shown in Figure 6-1 and was described in Section 2.2.3. An unmodified commercial, Fabry-Perot quantum well semiconductor laser (SDL-5412) lasing single mode at 852nm was used in the experiment. It was mounted inside a sealed TO-3 package and was high reflectivity coated on the rear facet ($>$ 98% power reflectivity, according to the manufacturer) and anti-reflection coated on the front facet ($<$ 5%). The threshold current was 17 mA at room temperature and the differential quantum efficiency, 69%. The laser was driven with a home-built constant current source [111] and was carefully temperature stabilized to prevent both

frequency drifts and temperature-induced changes in the mode structure. The entire laser mount was placed inside two foam-lined containers which provided thermal and acoustical isolation from the rest of the room. Pump suppression was achieved at high frequencies while allowing DC current to pass uninhibited by placing an inductor in series with the laser.

Most (99%) of the light emitted from the laser was reflected out of the external cavity by a beamsplitter (BS) while the remaining 1% was transmitted in order to provide weak feedback. As in Section 2.2.3, feedback was applied to the laser via Faraday rotation on the Doppler broadened transition only when the laser was tuned to the Cs D_2 transition at 852 nm. The transmitted field was then reflected off the end mirror (M_1) and retraced its path back to the laser providing weak optical feedback. A neutral density filter placed in the beam path and a piezoelectric transducer (PZT) attached to the end mirror allowed careful control of the feedback intensity and phase. Part of the returning field was reflected into a detector (D_1) for measurement of the feedback strength: typical feedback powers were about 10^{-7} of the output power. In this way, dispersive, wavelength-selective optical feedback could be applied to the laser diode.

The output from the external cavity was passed through an isolator which provided 60 dB of isolation before being sent to a balanced receiver [88] for measurement of the amplitude noise with respect to the SQL. The balanced receiver consisted of a half-wave plate, polarizing beam splitter and high quantum efficiency (97%) photodetectors (Hamamatsu S3994, 30 MHz bandwidth). The current-to-current differential efficiency from laser to detectors was 43%. The laser light was centered on the detectors and expanded to fill the available detector area (1 cm^2), a procedure which was found to be important in keeping the detectors from saturating under the high incident powers. The electronic signals from the photodetectors were amplified, sent through a variable delay and variable attenuators, and transmitted finally to a differential amplifier (Techtronix 7A24) which could either add or subtract the

two photocurrents. The output from the differential amplifier was then sent to an electronic spectrum analyzer for measurement of the noise. The noise was measured at a single frequency of 30 MHz with a resolution bandwidth of 300 kHz. A 1 Hz video bandwidth was used resulting in a measurement error of about 0.1 dB.

The receiver was balanced in the following way. First, the half-wave plate was adjusted so that the DC photocurrents from the two photodetectors (D) were equal. A small sinusoidal modulation was then applied to the laser injection current at the frequency at which the noise was measured. The output signal from the differential amplifier in the subtraction mode at the modulation frequency was minimized by adjusting the electronic attenuation and delay in one arm of the receiver. Common mode rejection of greater than 40 dB was achieved in this way. The modulation was then turned off, and the noise at the same frequency measured in both addition and subtraction modes of the differential amplifier. The addition mode gave the amplitude noise on the laser light while the subtraction mode gave the SQL. Thus the laser noise could be measured with respect to the SQL without any physical changes in the experimental setup. The background amplifier noise was subtracted from all measured signals.

The longitudinal mode spectrum of the laser was also monitored simultaneously with the amplitude noise using a grating spectrometer. The mode spectrum was found to be a strong function of the injection current and temperature: at most combinations of these two parameters the laser was strongly multi-mode (side mode suppression < 10 dB) and the amplitude noise was usually tens of dB above the SQL. However, at any fixed injection current, the laser could usually be made to operate with fairly good side mode suppression (> 20 dB) without too much effort. Considerably more effort was required to obtain squeezing. The laser appeared to produce squeezed light only in a very limited range of temperatures, where the side mode suppression was particularly good (see Section 6.3 for a more complete discussion of the role of side mode suppression). For all of the results presented in the remainder of this chapter,

the laser was operated in this quasi-single-mode state.

The laser noise under free-running conditions was found to be extremely sensitive to spurious optical feedback. Feedback powers as small as 10^{-8} of the output power were found to affect the measured noise level by up to several dB. To reduce the effects of this feedback, most of the optics in the beam path were slightly misaligned so that the reflected beam would not return to the laser. However, even scattered light from the input polarizer of the isolator caused significant variation in the noise level. This was measured by placing the isolator on a translation stage and then varying its position with a PZT causing the phase of the feedback field to change thereby producing oscillations in the measured amplitude noise level. The position of the beam on the isolator could then be adjusted to minimize the effect of the spurious feedback on the laser noise. Even under the best conditions, the variation in the noise level with isolator position could not be reduced below about 0.5 dB for the free-running laser. When intentional feedback from the external cavity was applied, the noise was found to be much less sensitive to the isolator position, presumably because the stronger intentional feedback drowned out the effects of the weaker spurious feedback. In addition, several other sources of spurious feedback such as reflections from the collimating lens and scattered light off the monitor photodiode (contained inside the TO-3 package opposite the rear facet of the laser) could not be easily controlled and the effects of these sources on the laser noise remain unclear. The fact that the reflecting surfaces of these two sources were so close to the laser should have made their effects on the noise minimal, however.

A useful technique for estimating the amount of spurious feedback being applied to the laser was to measure the dependence of the lasing frequency on the injection current. Under free-running conditions, the lasing frequency decreases smoothly as the injection current is increased. When feedback is present, however, the lasing frequency is "pulled" slightly from its free-running value by an amount which depends on the amplitude and phase of the feedback (see Section 2.2.3). Thus, as the injection

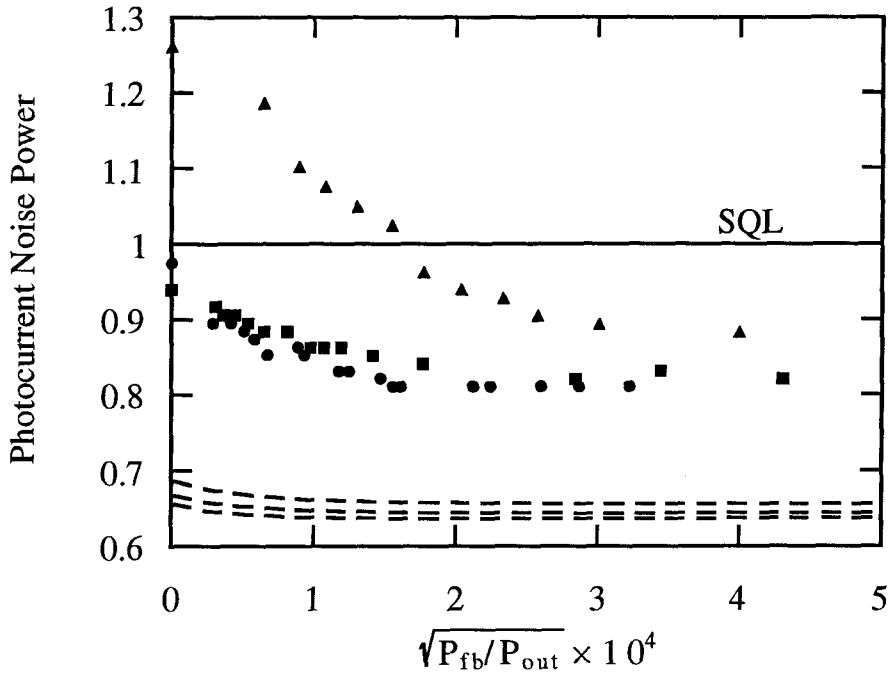

Figure 6-2: Photocurrent noise power, normalized to the SQL, as a function of the feedback coupling rate for the case of wavelength-selective feedback. The data were taken at three different injection currents corresponding to 5.8 i_{th} (triangles), 6.4 i_{th} (squares) and 6.8 i_{th} (circles). The prediction of the single-mode theory is given by the dashed lines.

current is scanned, the lasing frequency changes in a step-like manner, staying nearly constant over a small range of injection currents and then jumping suddenly to a different frequency. In our case the lasing frequency was measured by blocking the feedback from the external cavity at the mirror and then measuring the transmission through the Cs cell as the lasing frequency was scanned over the Cs line by changing the injection current. When spurious feedback was present, a step-like structure appeared on the transmission signal (similar to that in Figure 2-5b) allowing an estimation of the feedback power. Under optimal alignment conditions, the feedback power was estimated to be below $10^{-8}P_{out}$.

The laser noise was measured relative to the SQL as a function of the feedback

power and is plotted in Figure 6-2. For each data point, the noise of the free-running laser was first minimized with respect to the spurious feedback by adjusting the position of the optical isolator. The feedback from the external cavity was then applied and the noise reminimized by adjusting the position of the end mirror. The data were taken at three different injection currents, corresponding to 5.8 i_{th}, 6.4 i_{th} and 6.8 i_{th}. At the lowest injection current used, the laser noise is clearly reduced from above the SQL to well below due to the optical feedback. At higher injection currents, although the ultimate noise level at high feedback is lower, the feedback-induced reduction in the noise is somewhat less. A maximum squeezing of 19% below the SQL is measured under optimal feedback conditions which is an improvement by over a factor of three from the best previous room temperature result from a free-running laser (6% squeezing [87]). This 19% squeezing measured at the detector translates into 29% squeezing at the output facet of the laser when the effects of the optical attenuation in the detection system are taken into account. Also shown in the plot is the prediction of the single-mode theory, (4.46), (dashed lines) using the parameter values $n_{sp} = 1.5$, $\alpha = -2.5$ and with ϕ_0 adjusted to produce the minimum noise. The laser is assumed to have a length of 200 μm, refractive index of 3.5, facet power reflectivity of 5% and a value of 70% is taken for the coupling efficiency of the feedback back into the laser. Clearly the agreement is not particularly good, an issue discussed further below.

The experiment was also repeated with the laser tuned off the Cs line and the polarizers opened to allow partial transmission of the light through the external cavity. In this case the wavelength selectivity of the feedback was lost and the feedback applied to all semiconductor cavity modes simultaneously. Such an arrangement produced controlled conditions similar to those which occur when unintentional feedback from optical components or detectors is present. Qualitatively similar results to the wavelength-selective case were obtained and are shown in Figure 6-3. The difference in the noise power measured under free-running conditions between Figure 6-2 and

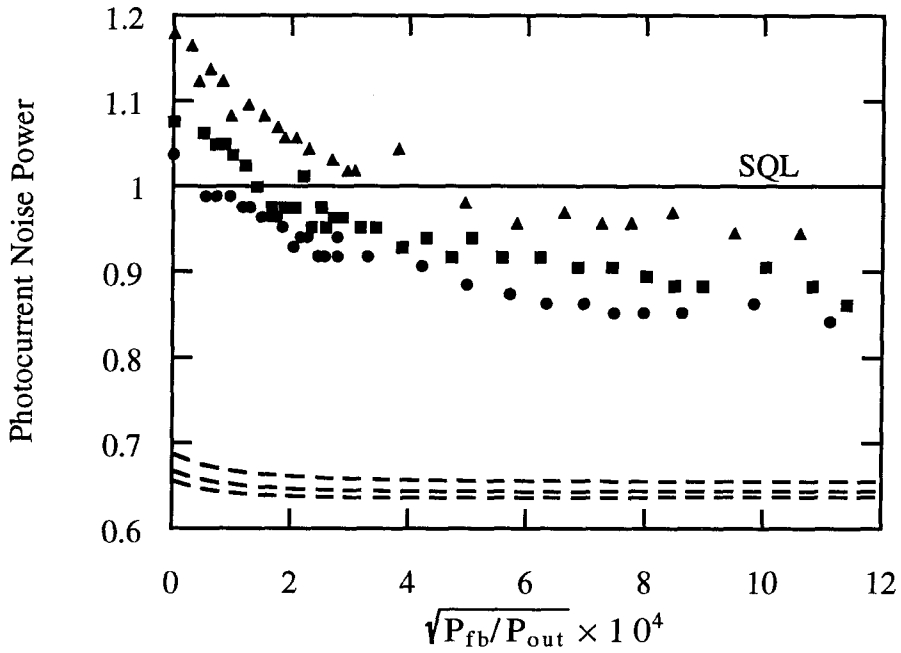

Figure 6-3: Photocurrent noise power, normalized to the SQL, as a function of the feedback level for non-wavelength-selective feedback (empty cavity).

Figure 6-3 is believed to be due to changes in the side mode structure induced by the small temperature change required to bring the laser frequency off the Cs line. The single-mode theory is again shown (dashed lines).

Two experimental checks were performed in order to verify the measured level of squeezing. First, high power LED's with peak wavelength of 890 nm were shone into the two detectors and the resulting photocurrent noise power measured at the same DC photocurrent as produced by the laser. The noise level was found to agree with the shot noise level measured with the laser (by subtracting the photocurrents) to within 2%. Second, an optical attenuator was placed in the beam path and the squeezing measured as function of the optical attenuation as shown in Figure 6-4. Figure 6-4(a) shows the photocurrent noise power, normalized to the SQL, as a function of the optical attenuation. The squeezing is reduced linearly towards the SQL as

the attenuation is increased in exactly the manner predicted by theory (solid line). As a further check on the detector response linearity, the raw photocurrent noise power was plotted (Figure 6-4(b)) as a function of the DC detector current (optical attenuation) for the laser, SQL as measured with the laser light and SQL as measured with the LED. The SQL is found to be linear with the detector current, as expected, while the laser noise drops under the SQL in a non-linear fashion as the attenuation is reduced. From the measurement error of 0.1 dB on the noise and these checks, it is believed that the measurements of the squeezing are accurate to within 3%.

6.3 Discussion

There are a number of possible mechanisms which could be responsible for the excess noise measured in the previous section. The most likely candidate would appear to be effects due to imperfect side mode suppression in the laser. Because of non-linear effects due to spatial and spectral hole burning, a Fabry-Perot semiconductor laser does not oscillate in a perfectly single longitudinal mode. Weak side modes are always present to some degree, and can contribute to the noise in a number of different ways. Several of these possibilities are discussed below and an attempt to evaluate the relative importance of each is made.

The existence of side modes leading to excess noise in semiconductor lasers has been mentioned by several authors [90,93,94,101], and evidence for this was presented in the previous section (since when the laser was strongly multi-mode, the noise tended to be high). The effect of longitudinal side modes on the laser noise depends crucially on the broadening mechanism. If the laser is assumed to be completely homogeneously broadened, then the presence of side modes does not alter the photocurrent noise significantly when the total field power is detected [112]. Although the amplitude noise on each individual mode can be quite high, anti-correlations between the modes produce a cancellation of the noise when all the modes are detected together. This

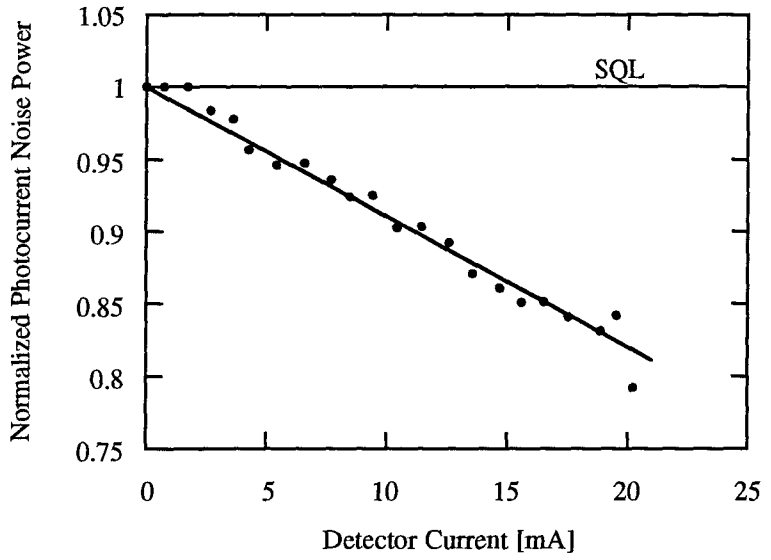

(a)

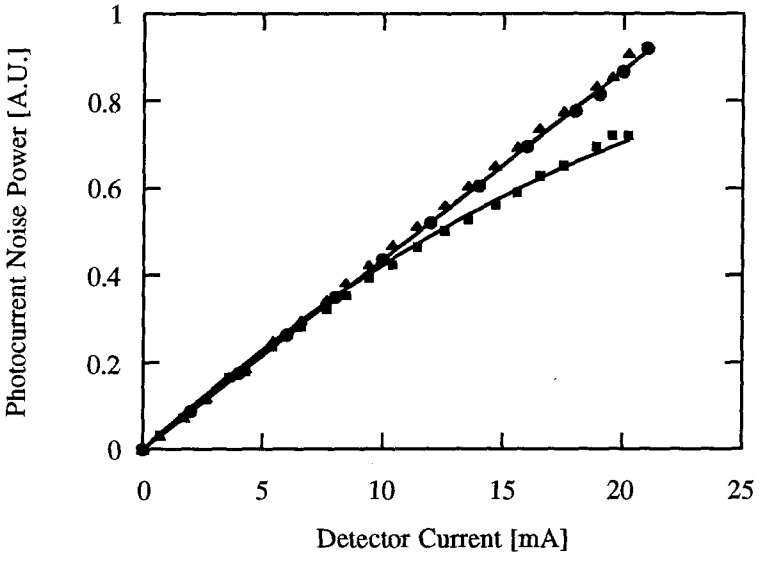

(b)

Figure 6-4: Dependence of the squeezing on the optical attenuation. (a) The photocurrent noise power, normalized to the SQL, as a function of the attenuation. The squeezing is reduced in a linear fashion towards the SQL. (b) The raw noise power for the laser (squares) and the SQL measured using the laser (circles) and LED (triangles). The SQL is seen to be linear with the DC photocurrent while the laser noise drops below the SQL indicating squeezing.

anti-correlation is generated because all modes couple to the same carrier population; fluctuations in the intensity of one mode get coupled through the carrier density into the noise in the intensity of the other modes. If, on the other hand, the laser is assumed to be inhomogeneously broadened, then all of the longitudinal modes couple to independent carrier populations. As a result, no correlations exist between the noise on the individual modes and the photocurrent noise powers generated by each mode add incoherently. If the mode structure is that of a strong main mode and weak side modes, then although the side modes have significantly less power, they are much closer to threshold and therefore have a much larger noise relative to their SQL. As a result they can contribute a significant amount of noise to the total photocurrent noise power.

Optical feedback, when applied to the laser, has the potential to change the mode structure since it changes the photon lifetime of the cavity in a mode-selective way. As a result, it was initially thought that perhaps the measured noise reduction could have been entirely due to a change in the side mode power induced by the optical feedback rather than the phase-amplitude coupling mechanism described in Chapter 4. In order to test this hypothesis, the longitudinal mode spectrum of the laser was monitored simultaneously with the amplitude noise using an optical spectrum analyzer. The power in six of the side modes closest to the laser was measured under the presumed free-running conditions and again with the feedback applied. The change in the average side mode power was almost imperceptible, but was measured to decrease by 6 ± 4 % as the laser amplitude noise changed from 1 dB above the SQL to 0.9 dB below. This 1.9 dB change corresponds to a change in the total noise power from $1.26P_{SQL}$ to $0.81P_{SQL}$ where P_{SQL} is the photocurrent noise power corresponding to the standard quantum limit. Since the main mode noise should account for about $0.65P_{SQL}$ according to the single mode theory, the net excess noise under feedback conditions is reduced from $0.6P_{SQL}$ to $0.18P_{SQL}$. This represents a 70% decrease in the excess noise, and it is hard to see how a 6% change in the side mode power could

be responsible. The combined power in all the side modes was estimated to be about 1-2% of the total output power.

Mode partition noise is another important source of noise in homogeneously broadened lasers. Although the strong anti-correlations between the individual modes cancel out when the total power from all modes is detected, if some of those modes are blocked or attenuated, then the noise on the remaining transmitted power can increase significantly. Variations in mode transmission can occur in a number of ways. As mentioned by Freeman et al. [94], if the laser facet reflectivity has some wavelength dependence (created, perhaps, by the AR coating), then as the power fluctuates between the different longitudinal modes, the varying reflectivity could cause the total output power to vary substantially. Such an effect would be expected to be more pronounced at room temperature where the gain bandwidth of the laser is larger and where the power is therefore distributed over a larger range of wavelengths. This effect could perhaps explain why amplitude squeezing has been significantly more successful at cryogenic temperatures than at room temperature. If this source of noise were in fact the cause of the excess noise measured in Section 6.2, however, one would expect that as the noise was reduced with the optical feedback, the side mode suppression would change. Such an effect was not observed as discussed above.

Longitudinal mode partition noise was also a potential source of error in the calibration of the SQL. Because the polarization rotation caused by the half-wave plate has some wavelength dependence (even though a zero-order wave plate was used), partition of power among modes of different wavelengths could have caused fluctuations in the polarization of the field incident on the polarizing beamsplitter. Such polarization fluctuations would in turn cause an anti-correlation between the detector photocurrents generating excess noise when the photocurrents were subtracted by the differential amplifier. Since such excess noise would result in a mis-calibration of the SQL, care must be taken to ensure that this process was not occurring. Since all measurements were performed with the laser predominantly single-mode, the re-

sulting polarization fluctuations are expected to be small. The check of the SQL calibration with the LED's confirmed this expectation. In the next section, a polarizer was added immediately after the half-wave plate to reduce any possible error from this process.

Another source of mode partition noise is power fluctuation between different transverse or polarization modes. Here again the laser facet reflectivity could be the source of the mode-dependent attenuation, but the detection system would probably have had a much stronger effect. The optical isolator has a linear polarizer at the input which would attenuate any orthogonal polarization strongly and therefore generate excess noise due to any power fluctuations between polarization modes. No check was performed to rule out polarization mode partition noise, and it remains as a possible source of excess noise.

In addition, although an attempt was made to preserve the spatial intensity distribution throughout the detection system, it is possible that parts of the beam were attenuated more strongly than others leading to mode partition noise due to power fluctuations among transverse modes. One experimental check done to test this hypothesis was to pass the beam through a pinhole placed close to the balanced receiver which transmitted only part of the beam. The pinhole size and position in the beam were varied, and no change in the noise power was measured except the expected effect due to the attenuation of the light.

A final way in which multi-mode effects could generate excess noise is through asymmetrical cross-mode non-linear gain. This possibility is discussed in Chapter 7 and a quantitative model is developed which explains the measurements of the previous section fairly well.

Aside from excess noise generated by the side modes, there are several other possible noise sources which may have contributed to the amplitude noise power. Noise on the injection current due to RF pickup or current source oscillation may have been present. Although this could have generated excess amplitude noise, a

large reduction due to the optical feedback would not be expected according to the analysis in Chapter 4.

Another possibility arises from the fact that since the laser front facet was AR coated, the model used in Chapter 4 does not really apply. In fact, due to the low Q of the semiconductor laser cold cavity, the longitudinal modes of the structure are not orthogonal, a situation which makes the quantization of the cavity optical field difficult in the conventional manner. However, a recent analysis by Tromborg [81] using travelling-wave fields has shown that for the case of a Fabry-Perot laser with one facet HR coated ($R \approx 1$) and the other AR coated, the quantum mechanical amplitude noise in the external optical field should not differ significantly from the model outlined in Section 4.2.1. Therefore, although the *feedback* model of Section 4.4 might not be particularly applicable to the experimental setup here (due to the low front facet reflectivity), the deviation from the conventional theory under free-running conditions should not be large. The non-orthogonality of transverse modes in gain guided structures has also been found to lead to substantial increases in the spontaneous emission noise [113,114,115] into the lasing mode. However, the particular laser used in the experiment was predominantly index guided which should have made this effect small.

Finally, it is entirely possible that there may be some other mechanism causing the excess noise in the laser which is not well understood. For example, the process causing the 1/f noise in the frequency noise power spectrum could also be generating noise in the field amplitude. This situation cannot be ruled out at present, and further investigation is thought to be necessary before more detailed conclusions about the exact origin of the excess noise can be made.

6.4 Conclusion

In summary, the effects of optical feedback on the amplitude noise and squeezing of semiconductor lasers have been investigated experimentally. It was found that extremely weak feedback, on the order of $10^{-8}P_{out}$, can change the amplitude noise power by several dB at frequencies up to 50 MHz. Depending on the phase of the optical feedback, the noise is found to either increase or decrease indicating that careful control of the feedback phase is required in order to generate an enhancement in the squeezing. The squeezing in a pump-suppressed room-temperature laser is enhanced from 2% below the SQL under presumed free-running conditions to 19% below the SQL under optimal feedback conditions corresponding to 29% squeezing at the laser facet. Agreement with the single-mode theory of Chapter 4 is not particularly good indicating that additional mechanisms may play a role in determining the laser noise. The mode structure of the laser was measured simultaneously with the amplitude noise and the feedback-induced changes in the mode structure are thought to be inadequate in accounting for the measured noise reduction in a simple way.

A number of possible reasons for the excess noise were outlined and discussed in light of the experimental results. Among these, effects due to imperfect side mode suppression seem to be the most likely although other possibilities cannot be ruled out with confidence. One possible reason for the discrepancy between experiment and theory is the existence of side modes in conjunction with asymmetrical cross-mode non-linear gain. This issue will be discussed in the next section. A quantitative model is developed for a multi-mode laser incorporating asymmetrical cross-mode non-linear gain. This model is found to give substantially better agreement with the experimental results than does the single-mode model.

Chapter 7

Asymmetrical cross-mode non-linear gain

7.1 Introduction

In Chapter 6 a substantial discrepancy between the experimental data and the simple single-mode theory was found: the measured amplitude noise was found to be as much as double the theoretically predicted value and the feedback-induced noise reduction was substantially larger than expected. Excess amplitude noise when the laser is operating near the SQL has been found in several other attempts to generate amplitude squeezing from free-running semiconductor lasers [87,86,90,92,93,94], and the source of this noise is not well understood. A number of possible reasons were proposed in Section 6.3 to explain the discrepancy. In this section, one possible mechanism is considered in detail: asymmetrical cross-mode non-linear gain. This mechanism has been used previously to explain the enhanced low-frequency noise in semiconductor lasers [101]. It is emphasized that although this explanation seems reasonable and accounts for the experimental data fairly well, there is no direct evidence supporting this alternative over other possibilities. Further experimental investigation is required before a firm conclusion can be drawn.

Asymmetrical cross-mode non-linear gain is a phenomenon in which the gain of one mode can be affected by the intensity of another mode in an asymmetrical manner. In a nearly single-mode semiconductor laser, this results in an enhancement of the gain

at frequencies above the lasing mode and a reduction of the gain at frequencies below. The basic mechanism, described in papers by Bogatov et al. [100] and Ishikawa et al. [116], can be understood as follows. Consider a semiconductor laser in which two modes are oscillating, one strong main mode and a much weaker side mode. The stimulated emission rate of carriers depends on the square of the internal optical field which in this case contains not only DC terms due to each mode individually, but also a term representing the beating between the two modes. This beating leads to a modulation of the carrier density in the active region at the difference frequency between the two longitudinal modes.

We now consider how this modulation of the carrier density affects the main mode optical field. Modulation of the carrier density modulates the gain of the active region which in turn generates amplitude modulation of the main mode and therefore AM sidebands on either side of the lasing frequency at the difference frequency between longitudinal modes. However, due to the detuned nature of the semiconductor laser oscillator, the refractive index is also modulated thereby generating FM sidebands, one of which is in phase with the AM modulation and the other of which is out of phase. Since the FM modulation index can be as large as or even larger than the AM index, a strong asymmetry in the sidebands can occur. Thus, part of the main mode intensity is coupled into the side modes in an asymmetrical fashion.

The effect of this asymmetrical inter-mode coupling on the amplitude noise of semiconductor lasers has been analyzed by Su et al. [101,117]. They find that the coupling between the strong mode and side modes leads to a renormalization of the side mode relaxation resonance, moving it to very low frequencies (essentially to DC) and substantially enhancing the amplitude noise at low frequencies. Though the model of Su et al. could explain qualitatively the reduction of the squeezing under free-running conditions observed in Chapter 6, theirs is a purely semiclassical model and includes only noise due to spontaneous emission into the lasing mode. In addition, they do not treat the effects of optical feedback on this excess noise. In this chapter,

the model of Ref. [101] has been extended to include both of these issues in order to attempt to explain the excess noise present in the measurements of the amplitude noise in Chapter 6.

7.2 Two-mode model including asymmetrical cross-mode non-linear gain

The model presented here is an extension of the single-mode model of Chapter 4 to include multi-mode effects and asymmetrical cross-mode non-linear gain. Only two modes are assumed, one strong main mode and one weak side mode. Following Ref. [101], the equations of motion for the carrier density, $\hat{N}_c(t)$, the main mode field, $\hat{A}_1(t)$, and side mode field, $\hat{A}_2(t)$, are written as

$$\frac{d\hat{N}_c(t)}{dt} = P - \frac{\hat{N}_c(t)}{\tau_{sp}} - \frac{\omega}{\mu^2}\hat{\chi}_{i1}\hat{A}_1{}^{\dagger}\hat{A}_1 - \frac{\omega}{\mu^2}\hat{\chi}_{i2}\hat{A}_2{}^{\dagger}\hat{A}_2 + \hat{\Gamma}_p(t) + \hat{\Gamma}_{sp}(t) + \hat{\Gamma}(t) \tag{7.1}$$

$$\frac{d\hat{A}_1(t)}{dt} = -\frac{1}{2}\left[\frac{1}{\tau_p} + 2i(\omega_{L1} - \omega_{01}) - \frac{\omega}{\mu^2}(\hat{\chi_{i1}} - i\hat{\chi_{r1}}) + \frac{v_g\epsilon_0}{V}|A_1|^2 + \frac{v_g\epsilon_{12}}{V}|A_2|^2\right]\hat{A}_1(t) + \hat{G}_1(t) + \hat{g}_1(t) + \sqrt{\frac{1}{\tau_{pe}}}\hat{f_{e1}}(t) + \kappa e^{i\phi_0}\sqrt{\tau_{pe}}\,\hat{r_1}(t-\tau) \tag{7.2}$$

$$\frac{d\hat{A}_2(t)}{dt} = -\frac{1}{2}\left[\frac{1}{\tau_p} + 2i(\omega_{L2} - \omega_{02}) - \frac{\omega}{\mu^2}(\hat{\chi_{i2}} - i\hat{\chi_{r2}}) + \frac{v_g\epsilon_0}{V}|A_2|^2 + \frac{v_g\epsilon_{21}}{V}|A_1|^2\right]\hat{A}_2(t) + \hat{G}_2(t) + \hat{g}_2(t) + \sqrt{\frac{1}{\tau_{pe}}}\hat{f_{e2}}(t) \tag{7.3}$$

where v_g is the group velocity, V is the mode volume and

$$\epsilon_{ij} = \epsilon_0 \frac{1 + \alpha\prime\tau\prime(\omega_i - \omega_j)}{1 + [\tau\prime(\omega_i - \omega_j)]^2} \tag{7.4}$$

is the non-linear gain coefficient. Here $\tau\prime$ is the relaxation time and $\alpha\prime$ is the phase-amplitude coupling constant associated with the physical process responsible for the non-linear gain.

These equations are linearized as in Section 4.4 and the resulting small-signal equations Fourier transformed and solved for the external field amplitudes. The fluctuation in the total emitted photon flux, $\Delta S_T(t)$, is then calculated using the relations

$$\Delta\hat{S}_T(t) = 2r_{10}\Delta\hat{r}_1(t) + 2r_{20}\Delta\hat{r}_2(t) \tag{7.5}$$

$$\Delta\hat{r}_1(t) = \frac{1}{\sqrt{\tau_{pe}}}\Delta\hat{A}_1(t) - \hat{f}_{e1r}(t) \tag{7.6}$$

$$\Delta\hat{r}_2(t) = \frac{1}{\sqrt{\tau_{pe}}}\Delta\hat{A}_2(t) - \hat{f}_{e2r}(t). \tag{7.7}$$

Under the assumption that the power in the side mode is much less that the main mode power, the power spectral density for the total intensity fluctuation, normalized to the SQL, is calculated to be

$$P_{\Delta\hat{S}_T}(\Omega) = P^{(0)}_{\Delta\hat{S}_T}(\Omega) + P^{(ex)}_{\Delta\hat{S}_T}(\Omega)\left|\frac{1 + C_i}{1 + C_i + \alpha C_r}\right|^2 \tag{7.8}$$

where $P^{(0)}_{\Delta\hat{S}_T}(\Omega)$ is the amplitude noise power with feedback for a single mode laser, given by (4.43) multiplied by $4r_{10}^2$,

$$P^{(ex)}_{\Delta S_T}(\Omega) = 2\eta\frac{\beta n_{sp}}{\tau_p\tau_{pe}}\left(\frac{A_{20}}{A_{10}}\right)^2 \frac{\Omega^2 + \left(\frac{1+n_{sp}R}{\tau_{sp}}\right)^2}{(\omega_2^2 - \Omega^2)^2 + \gamma_2^2\Omega^2}, \tag{7.9}$$

and

$$\beta = \left[\frac{v_g(\epsilon_0 - \epsilon_{21})A_{10}^2}{V}\tau_p\left(1 + \frac{1}{n_{sp}R}\right)\right]^2 \tag{7.10}$$

$$\omega_2^2 = \left(\frac{R_{sp}}{A_{20}} + v_g \epsilon_0 A_{20}^2\right)\left(\frac{1}{\tau_{sp}} + \frac{1}{\tau_{st}}\right) \tag{7.11}$$

$$\gamma_2 = \left(\frac{1}{\tau_{sp}} + \frac{1}{\tau_{st}}\right) + v_g \epsilon_0 A_{20}^2 + \frac{R_{sp}}{A_{20}^2} \tag{7.12}$$

η is the optical efficiency and R_{sp} is the spontaneous emission rate into a single mode of the field.

It can be seen from (7.8) that since $P_{\Delta\hat{S}_T}^{(ex)}$ is independent of the feedback parameters, the presence of the side modes adds noise for which the feedback dependence is very simple. The physical process which generates this reduction of the multi-mode noise through optical feedback is the following. The existence of the side mode generates excess amplitude noise under free-running conditions because of the non-linear inter-mode coupling and renormalization of the weak mode relaxation resonance frequency. However, this process also generates fluctuations in the carrier density which are strongly correlated with the excess intensity noise. The carrier density noise generates excess phase noise in the main-mode field through the phase-amplitude coupling process which is then coupled back into the main-mode amplitude by the optical feedback. The main-mode amplitude is thus corrected to compensate for the *total* intensity fluctuation of all modes resulting in a reduction of the excess noise.

Equation (7.8) is shown in the low-frequency limit by the solid lines in Figure 7-1 and Figure 7-2. The value of $P_{\Delta\hat{S}_T}^{(ex)}$ is taken as a fitting parameter and the feedback phase (ϕ_0 in Equations (4.33) and (4.34)) in the theory is again adjusted to minimize the noise. The other parameters are the same as those used in the single-mode fits. The single-mode theory is also shown (dashed lines) in the figures. Clearly substantially better agreement with experiment is obtained with the multi-mode theory indicating that incomplete side mode suppression and cross-mode non-linear gain can at least explain the observed behavior of the noise on feedback intensity. It is recognized that while the agreement of experimental results with this theory is fairly good, the possibility of other processes also contributing to the excess noise is not ruled out and the relative importance of the various noise sources remains unclear.

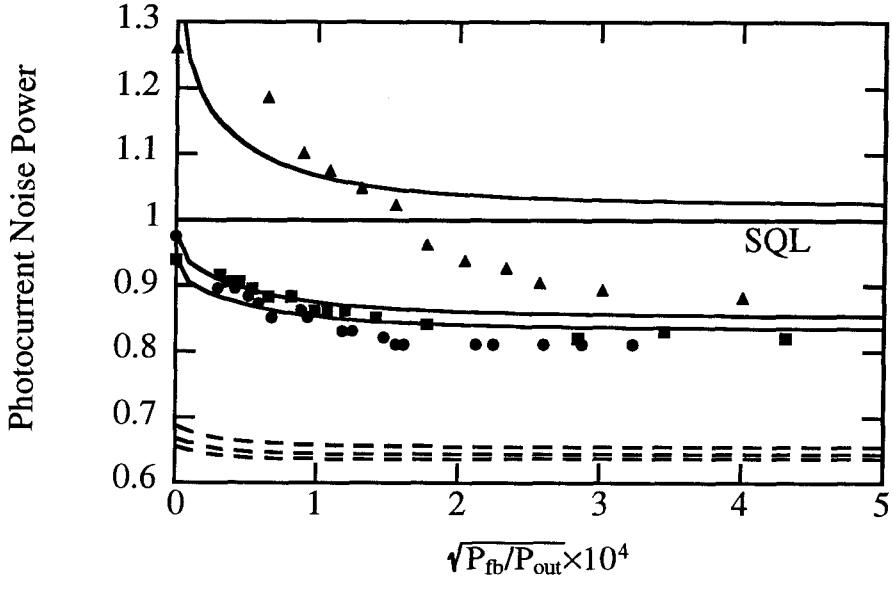

Figure 7-1: Photocurrent noise power, normalized to the SQL, as a function of the feedback coupling rate for the case of wavelength-selective feedback. The data were taken at three different injection currents corresponding to 5.8 i_{th} (triangles), 6.4 i_{th} (squares) and 6.8 i_{th} (circles). The prediction of the single-mode theory is given by the dashed lines and the multi-mode theory by the solid lines. Much better agreement is found with the multi-mode theory.

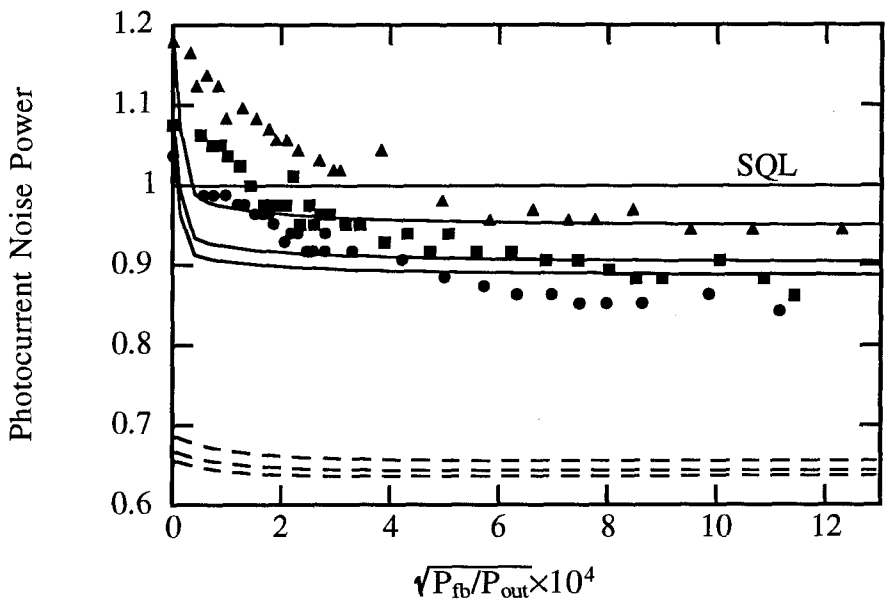

Figure 7-2: Photocurrent noise power, normalized to the SQL, as a function of the feedback level for non-wavelength-selective feedback (empty cavity). The prediction of the single-mode theory is given by the dashed lines and the multi-mode theory by the solid lines. Much better agreement is found with the multi-mode theory.

7.3 Conclusion

In summary, it is proposed that the excess noise found under free-running conditions and the larger-than-expected feedback induced reduction are caused by the existence of weak side modes in combination with asymmetrical cross-mode non-linear gain. This process causes additional amplitude noise under free-running conditions in the low-frequency part of the spectrum as a result of the inter-mode coupling. It also generates an additional correlation between the total intensity of all modes and the main mode phase. This correlation allows a reduction of the excess noise by the optical feedback in addition to the reduction obtained for the single-mode noise. A quantitative two-mode model is outlined to evaluate the effects of optical feedback on this excess noise source. With the non-linear gain coefficient taken as a fitting parameter, much better agreement is found between experiment and the multi-mode theory than is found with the single-mode theory.

While cross-mode non-linear gain certainly explains the measured results, it is not claimed that this process has been confirmed to be responsible entirely for the excess noise. The origin of this excess noise is perhaps an important area for further investigation since it would appear to be the main limitation to the generation of amplitude squeezed light from room temperature semiconductor lasers. In addition, methods of reducing the excess noise such as injection locking, optical feedback or other mode-stabilizing techniques could play an important role in facilitating the generation of amplitude squeezed light from semiconductor lasers.

Chapter 8

Amplitude squeezing from a room temperature semiconductor laser

8.1 Introduction

In the previous chapter, amplitude squeezing was obtained from a semiconductor laser which was subjected to weak optical feedback from an external cavity. When the optical feedback was removed, squeezing of only 2% below the SQL was observed. This chapter describes an experiment in which amplitude squeezing was obtained from a room temperature semiconductor laser with no intentional optical feedback. Squeezing as large as 1.5 dB (29% below the SQL corresponding to 41% below the SQL at the facet of the laser) is measured from the device using a balanced homodyne detector. This measurement is important in that it demonstrates that significant amplitude squeezing can be obtained from a commercial laser operating at room temperature with essentially no modifications. Until now, to the knowledge of the author, the largest amount of amplitude squeezing obtained from a room temperature device without any external feedback or mode control has been 0.33 dB [87]. All other reported measurements have either been performed either with the laser cooled to cryogenic temperatures [90] or with some sort of extensive mode control such as optical feedback [94,95] or injection locking [93].

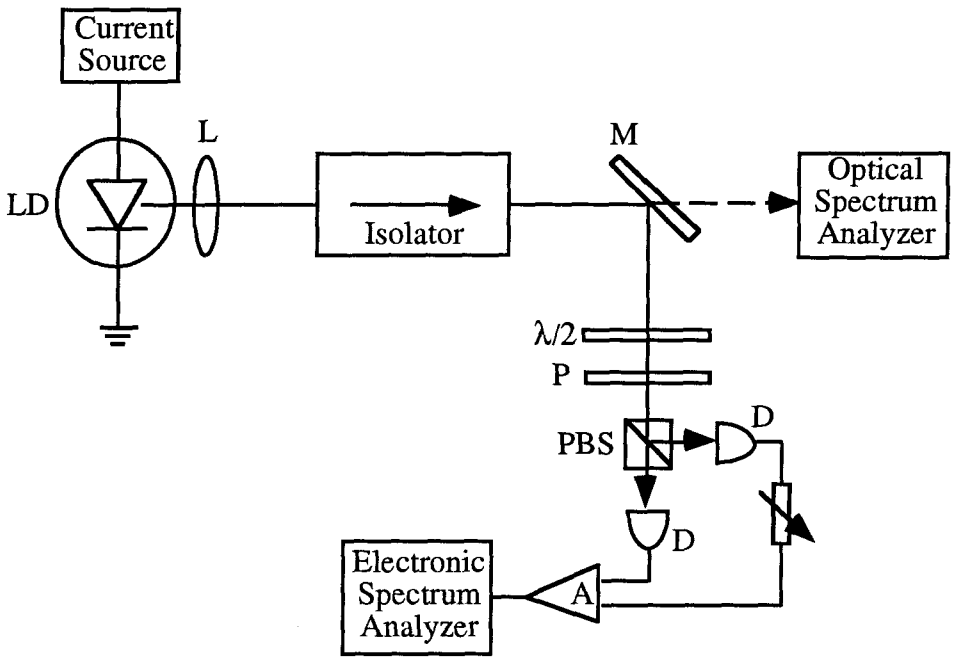

Figure 8-1: Experimental setup: LD, laser diode; L, lens; M, mirror; $\lambda/2$, half-wave plate; P, polarizer; PBS, polarizing beam splitter; D, detector; A, differential amplifier.

8.2 Measurements of amplitude squeezing

The experimental setup is shown in Figure 8-1. The semiconductor laser used (SDL-5402-H1) was a quantum-well index-guided structure with a threshold current of 10.2 mA and a maximum rated operating current of 60 mA resulting in 50 mW of output power. The differential quantum efficiency was 68% at room temperature. The device was mounted by the manufacturer inside a TO-4 package which included a thermistor, thermoelectric (TE) cooler and monitor photodiode. The laser temperature was stabilized using a home built temperature controller, and a precision current source provided the injection current which passed through an inductor before going to the laser. The inductor allowed DC current to pass through unimpeded while suppressing the pump fluctuations at higher frequencies where the noise was

measured.

The output light from the laser was collimated using an AR coated collimating lens (Newport F-L40B) before being sent through an optical isolator to the detection system. The amplitude noise was measured using the balanced receiver described in Chapter 6 but with the addition of a polarizer between the half-wave plate and polarizing beam splitter (see Figure 8-1). The polarizer was adjusted so that the DC photocurrents into the two detectors (D) were equal (i.e., the light incident on the polarizing beam splitter was polarized at 45°). The half-wave plate was then adjusted to maximize the transmission through the polarizer. The polarizer was present in order to reduce the effects of polarization mode partition noise which could interfere with the SQL calibration as discussed in Section 6.3. Although most measurements were made when the laser was predominantly single-mode and the measured level of squeezing was checked with two other independent methods, the addition of the polarizer provided added security in the calibration of the SQL.

The beams incident on the photodiodes were again expanded to fill the entire detector area and the AC photocurrents were amplified and sent to a differential amplifier which could either add or subtract the photocurrents. The output from the differential amplifier was then sent to an electronic spectrum analyzer for measurement of the noise. In one electronic arm of the balanced receiver, an attenuator and delay unit were present. The detector was balanced using the method in Chapter 6 and common mode rejection of 40 dB was obtained at a frequency of 28 MHz.

The SQL calibration was checked by shining the light from high-power LED's onto the detectors to produce the same photocurrent as did the laser. Figure 8-2 shows the measured photocurrent noise power spectrum for the LED's (trace A) and laser (trace B). Figure 8-2a shows the noise when the photocurrents at DC were added while Figure 8-2b shows the noise when the photocurrents were subtracted. The delay introduced into one arm of the detector caused a frequency-dependent phase shift between the two signals entering the differential amplifier which resulted in the

photocurrent noise power varying as a function of frequency between the laser noise level and the SQL [88]. In Figure 8-2b, it can be seen that at a frequency of 7 MHz the laser photocurrent noise power is at 1.4 dB below the SQL (determined by the LED) indicating that the laser noise was amplitude squeezed by this amount. For this measurement, the laser injection current was 64 mA, resulting in a detector photocurrent of 12.9 mA/detector (current-current differential efficiency of 48%) and the laser was cooled to about 10° C with the TE cooler. The resolution bandwidth for this measurement was 100 kHz and the background amplifier noise level was subtracted off all measured signals.

The detection system was balanced at a frequency of 28 MHz and the photocurrent noise at this frequency was then measured as a function of the laser injection current. The results, normalized to the SQL, are plotted against the pump rate $R = i/i_{th} - 1$ in Figure 8-3. It can be seen that the noise does increase as the laser gets closer to threshold, crossing over the SQL at an injection current of about 3.5 times the threshold current. Also shown in the figure is the prediction of the single-mode theory of Chapter 4 in the low frequency limit with $n_{sp} = 1.2$. Although the general features of the data seem to be in rough agreement with the theory, there is still a roughly 10-20% discrepancy over the entire range of injection currents at which the measurements were made. The origin of this excess noise is unclear, but one of the noise sources discussed in Section 6.3 may have been responsible.

As an additional check that the squeezing was indeed real, the amplitude noise was then measured as a function of the optical attenuation as in Chapter 6; the results are shown in Figure 8-4. The noise power normalized to the SQL is again found to be reduced in a linear fashion towards unity as the attenuation is increased verifying that the squeezing was indeed as large as 29% below the SQL.

As with the measurements presented in Chapter 6, the squeezing was only obtained in a narrow range of laser temperatures and injection currents. At most combinations of the two parameters, the laser operated multi-mode and the amplitude noise was

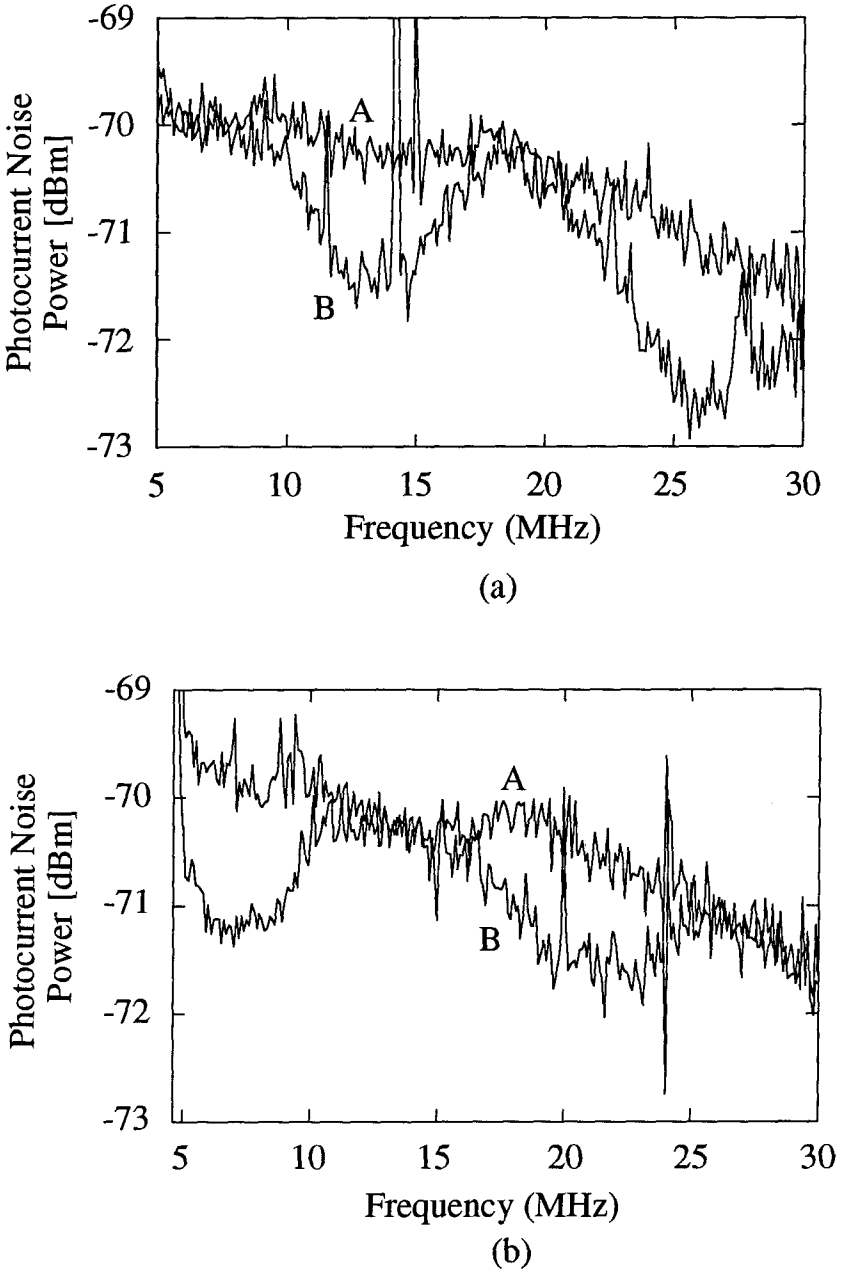

Figure 8-2: Photocurrent noise power spectrum from the LED (trace A) and laser (trace B) when the differential amplifier (a) added the detector photocurrents at 28 MHz and (b) subtracted them. Squeezing is indicated by the laser noise dropping below the LED noise (SQL) at certain frequencies.

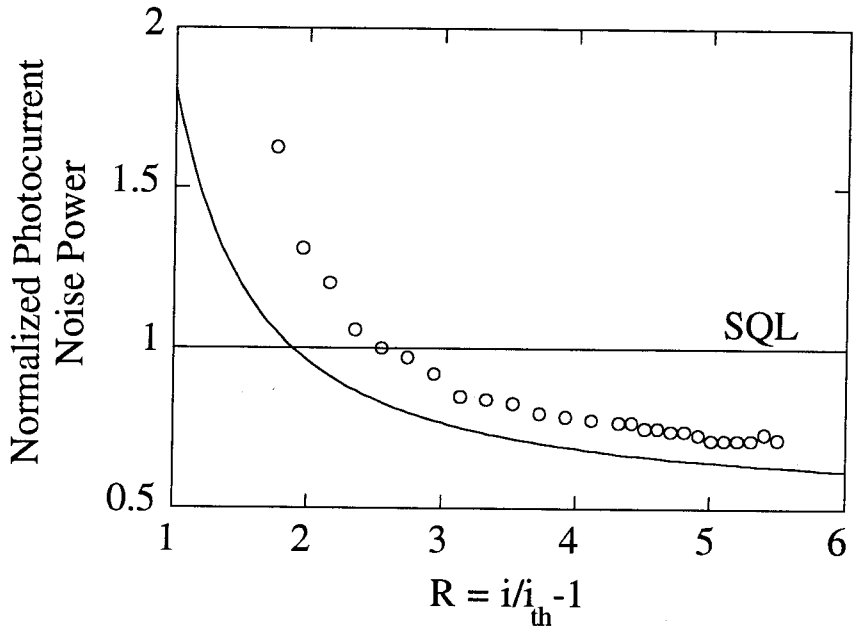

Figure 8-3: Photocurrent noise power spectrum dependence on injection current. The solid line is the prediction of the single mode theory of Chapter 4.

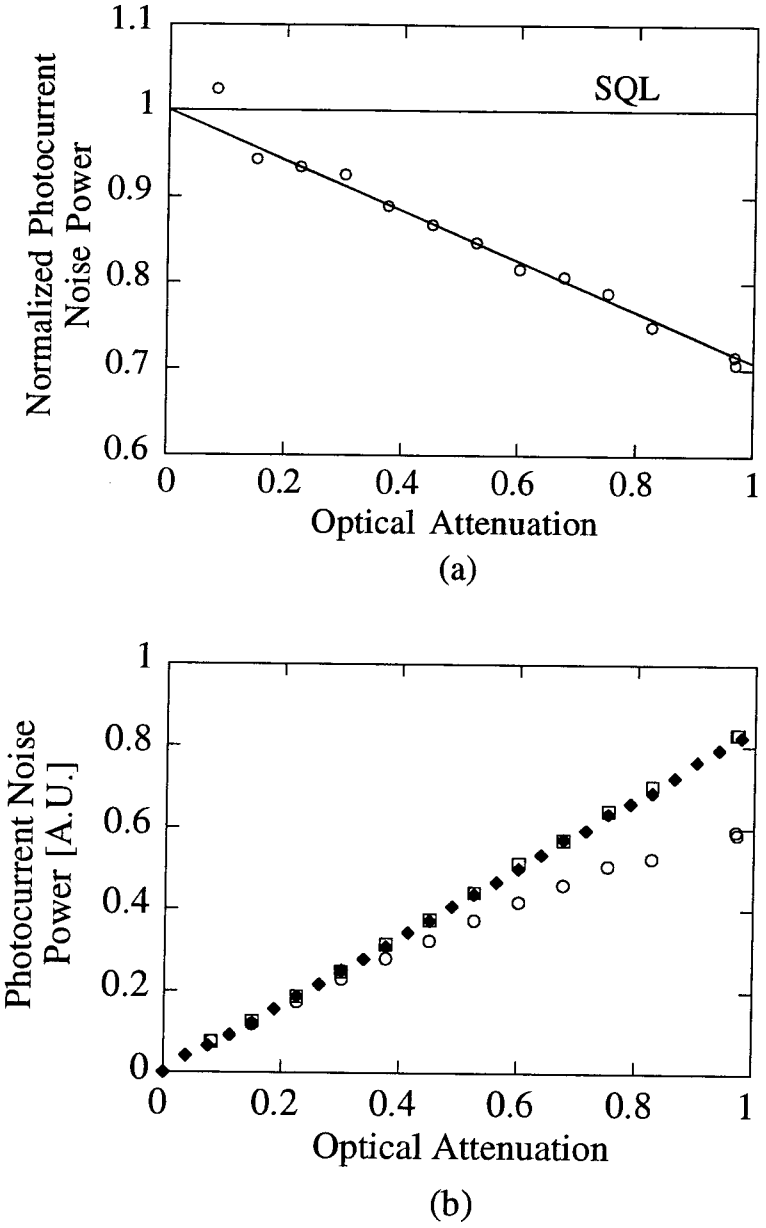

Figure 8-4: Dependence of the squeezing on the optical attenuation. (a) The photocurrent noise power, normalized to the SQL, as a function of the attenuation. The squeezing is reduced in a linear fashion towards the SQL. (b) The raw noise power for the laser (open circles) and the SQL measured using the laser (open squares) and LED (solid diamonds). The SQL is seen to be linear with the DC photocurrent while the laser noise drops below the SQL indicating squeezing.

far above the SQL. It appeared that particularly good side mode suppression was required in order generate squeezed light from the laser.

Several checks were performed in order to determine if spurious optical feedback was present and, if so, was influencing the laser noise. First of all the laser temperature was varied by an amount not large enough to cause a significant change in the side mode suppression but large enough to vary the laser frequency by a few GHz. The idea here was that if optical feedback were present with an intensity large enough to change the amplitude noise, then changing the laser frequency would change the phase of the feedback thereby generating oscillations in the amplitude noise (similar to those in Figure 5-5). The amplitude noise was found to vary by less than the measurement error of 0.1 dB, however. In addition, the position of the optical isolator (which was the offending component in Chapter 6) was varied by several wavelengths by placing its translation stage on a PZT, and again no significant change in the amplitude noise was observed. Finally, the position of the collimating lens was also varied by several wavelengths and no change in the measured squeezing was observed.

The above checks seem to indicate that optical feedback from the tested components was not playing a significant role in reducing the amplitude noise. It is possible, however, that weak optical feedback from some other source may have been present but that the side mode suppression was so good that the noise generated by the side modes was very small compared to the other noise sources. In this case the optical feedback, while changing the side mode noise in a way outlined in Chapter 7, would not have affected the total noise of the laser by a measurable amount since the side mode noise would have been so small.

8.3 Conclusion

In conclusion, amplitude noise 29% below the SQL was measured from a room temperature semiconductor laser without any external modifications aside from those

necessary to perform the detection (such as a collimating lens, optical isolator, etc.). The side mode suppression is found to be around 35 dB for most modes of the laser which may be the reason for the large degree of squeezing observed in this experiment. The effects of optical feedback on the amplitude noise in this configuration do not appear to produce a significant enhancement or reduction of the amplitude squeezing.

Appendix A

Vacuum Field Cancellation

The purpose of this appendix is to explain in a simple manner the cancellation of the vacuum field in the output of a semiconductor laser pumped high above threshold as discussed qualitatively in Section 4.2.2. The basic idea can be understood as follows.

Consider the arrangement in Figure A-1 which shows a semiconductor laser with a fully reflecting rear facet and a partially (but minimally) transmitting front facet. This front facet couples a single lasing mode of the internal field, represented by the slowly varying quantum mechanical annihilation operator $\hat{A}(t)$, to an incoming and outgoing mode outside the laser cavity which oscillate at the same optical frequency and are represented by the slowly varying operators $\hat{f}(t)$ and $\hat{r}(t)$ respectively. The incoming mode, $\hat{f}(t)$, is either a vacuum field or some applied optical field (in the

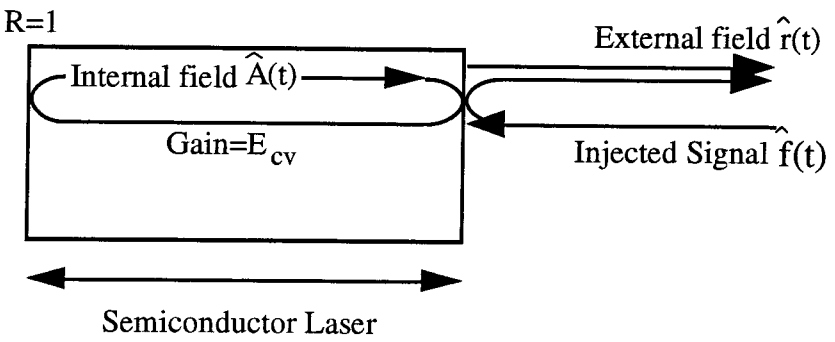

Figure A-1: Cancellation of the incident vacuum field in a semiconductor laser.

case of injection locking). It is assumed that the amplitude and phase of $\hat{f}(t)$ vary more slowly than any other process in the laser so that we can effectively treat the fluctuations as occurring at DC.

The mechanism for the field cancellation is as follows. When $\hat{f}(t)$ hits the front facet of the laser, most of it is reflected back (with a phase shift of π) while part is transmitted into the laser. Assume for the moment that the phase of $\hat{f}(t)$ is such that it interferes constructively with the internal field $\hat{A}(t)$ (an arbitrary phase shift will be analyzed more quantitatively below). This transmitted portion changes the instantaneous photon lifetime (cavity decay rate) of the laser: the internal field sees a momentarily reduced facet reflectivity due to the incoming field. This reduced loss rate must be balanced by a reduced gain (to satisfy the gain=loss condition) and therefore the carrier density drops somewhat. This reduced carrier density causes a smaller total spontaneous emission rate and therefore a lower instantaneous threshold current. Since the injection current of the laser has not changed, there must be a corresponding change in the stimulated emission rate and internal field amplitude. This then leads to a slightly increased output field. But this output field, which has been transmitted through the front facet, must interfere with the portion of the vacuum fluctuations which has been reflected from the facet. Since the fields are out of phase, they interfere destructively and in fact completely cancel out the effect of the incident field altogether.

A somewhat more quantitative description is now presented. The equation of motion for the slowly-varying internal field of the laser in the presence of a slowly varying incident field $\hat{f}(t)$ is

$$\frac{d\hat{A}(t)}{dt} = -\frac{1}{2}\left[\frac{1}{\tau_p} + 2i(\omega_L - \omega_0) - \frac{\omega}{\mu^2}(\chi_i - i\chi_r)\right]\hat{A}(t) + \sqrt{\frac{1}{\tau_p}}\hat{f}(t) \qquad \text{(A.1)}$$

where τ_p is the cavity photon lifetime, ω_0 is the cold cavity resonant frequency, μ is the non-resonant refractive index, and χ is the resonant optical susceptibility. Under

the assumption that $\hat{f}(t)$ is a small and slowly-varying fluctuation, we can rewrite (A.1) as

$$\frac{d\hat{A}(t)}{dt} = -\frac{1}{2}\left[\frac{1}{\tau_p} + 2i(\omega_L - \omega_0) - \frac{\omega}{\mu^2}(\chi_i - i\chi_r) - 2\sqrt{\frac{1}{\tau_p}}\frac{\hat{f}(t)}{A_0}\right]\hat{A}(t) \tag{A.2}$$

where $\hat{A}(t) = A_0 + \Delta\hat{A}(t)$, i.e., the reference phase will be that of $\hat{A}(t)$.

The injected field, $\hat{f}(t)$, is now written as a slowly varying (DC) fluctuation with some phase, ϕ_0, with respect to $\hat{a}(t)$,

$$\hat{f}(t) = F_0 e^{i\phi_0} \tag{A.3}$$

and (A.2) is solved for the steady state solution which gives

$$\frac{1}{\tau_p} + 2i(\omega_L - \omega_0) - E_{CV}(1 - i\alpha) - 2\sqrt{\frac{1}{\tau_p}}\frac{F_0}{A_0}e^{i\phi_0} = 0. \tag{A.4}$$

where $E_{CV} = (\omega/\mu^2)\chi_i$ is the gain per photon and α is the linewidth enhancement factor. It has been assumed here that the transparency density is small compared to the inversion density and also that the inversion is perfect (no stimulated absorption). Relaxing these constraints does not qualitatively alter the final result. The imaginary part of (A.4) just gives a shift of the laser frequency. The real part corresponds to a change in the gain=loss condition, the new gain given by

$$E_{CV} = \frac{1}{\tau_p} - 2\sqrt{\frac{1}{\tau_p}}\frac{F_0}{A_0}\cos\phi_0 \tag{A.5}$$

which implies that the change in E_{CV} due to the injected signal is

$$\Delta E_{CV} = -2\sqrt{\frac{1}{\tau_p}}\frac{F_0}{A_0}\cos\phi_0. \tag{A.6}$$

The change in the carrier density which corresponds to this change in gain can now be calculated using $E_{CV} = \beta N_{c0}/\tau_{sp}$ where β is the spontaneous emission factor, N_{c0}

is the carrier density and τ_{sp} is the spontaneous emission lifetime of the carriers. It is found that

$$\frac{\Delta N_{c0}}{\tau_{sp}} = -\frac{2}{\beta}\sqrt{\frac{1}{\tau_p}\frac{F_0}{A_0}}\cos\phi_0 \tag{A.7}$$

and that the threshold current therefore changes (instantaneously) by

$$\frac{\Delta i_{th}}{e} = \frac{\Delta N_{c0}}{\tau_{sp}} = -\frac{2}{\beta}\sqrt{\frac{1}{\tau_p}\frac{F_0}{A_0}}\cos\phi_0 \tag{A.8}$$

To find the change in the internal photon number corresponding to the above changes (at constant injection current), the expression relating the total photon emission rate with the carrier loss rate is used:

$$\frac{i - i_{th}}{e} = (A_0^2 + 1)E_{CV} \approx A_0^2 E_{CV}. \tag{A.9}$$

Therefore, the fluctuations in the above quantities are related at a constant injection current i by

$$-\frac{\Delta i_{th}}{e} = A_0^2 \Delta E_{CV} + 2A_0 E_{CV}\Delta A. \tag{A.10}$$

Substituting (A.6) and (A.8) into (A.10) and solving for the internal field fluctuation $\Delta\hat{A}$ we find

$$\Delta\hat{A} = F_0\sqrt{\tau_p}\cos\phi_0\left(1 + \frac{1}{\beta A_0^2}\right) \tag{A.11}$$

Thus it can be seen that an incident field, F_0, produces a corresponding change in the real part of $\hat{a}(t)$ equal to ΔA. It remains to calculate the external field, $\hat{r}(t)$, using the relation

$$\hat{r}(t) = -\hat{f}(t) + \sqrt{\frac{1}{\tau_p}}\hat{A}(t). \tag{A.12}$$

It is found that

$$\Delta\hat{r} \;=\; -F_0 e^{i\phi_0} + \sqrt{\frac{1}{\tau_p}}\Delta\hat{A} \tag{A.13}$$

$$= -F_0 \cos\phi_0 - iF_0 \sin\phi_0 + F_0 \cos\phi_0 \left(1 + \frac{1}{\beta A_0^2}\right) \quad \text{(A.14)}$$

$$= \frac{F_0}{\beta A_0^2} \cos\phi_0 - iF_0 \sin\phi_0 \quad \text{(A.15)}$$

Then, using $\hat{r}(t) = (r_0 + \Delta\hat{r})e^{i\Delta\hat{\psi}} \approx r_0 + \Delta\hat{r} + i\Delta\hat{\psi}$ and $\beta A_0^2 = R = i/i_{th} - 1$ it is found that

$$\langle \Delta\hat{r}^2 \rangle = \frac{\langle F_0^2 \cos^2\phi_0 \rangle}{R^2} \quad \text{(A.16)}$$

which clearly shows that the fluctuation in the external field falls like $1/R^2$ above threshold and that it can be reduced to an arbitrarily small number by pumping hard enough. The key cancellation occurs in (A.14) where the reflected portion of the incident field interferes with the added noise on the internal field.

References

[1] A. L. Schawlow and C. H. Townes, "Infrared and optical masers," *Phys. Rev.*, vol. 112, pp. 1940–1949, 1958.

[2] J. P. Gordon, H. J. Zeiger, and C. H. Townes, "The maser — new type of microwave amplifier, frequency standard and spectrometer," *Phys. Rev.*, vol. 99, pp. 1264–1274, 1955.

[3] C. H. Henry, "Theory of the linewidth of semiconductor lasers," *IEEE J. Quantum Electron.*, vol. QE-18, pp. 259–264, 1982.

[4] K. Vahala and A. Yariv, "Semiclassical theory of noise in semiconductor lasers — part I and II," *IEEE J. Quantum Electron.*, vol. QE-19, pp. 1096–1109, 1983.

[5] B. Dahmani, L. Hollberg, and R. Drullinger, "Frequency stabilization of semiconductor lasers by resonant optical feedback," *Opt. Lett.*, vol. 12, pp. 876–878, 1987.

[6] Y. Shevy, J. Iannelli, J. Kitching, and A. Yariv, "Self-quenching of the semiconductor laser linewidth below the Schawlow–Townes limit by using optical feedback," *Opt. Lett.*, vol. 17, pp. 661–663, 1992.

[7] A. Yariv, R. Nabiev, and K. Vahala, "Self-quenching of the fundamental phase and amplitude noise in semiconductor lasers with dispersive loss," *Opt. Lett.*, vol. 15, pp. 1359–1361, 1990.

[8] J. Kitching, R. Boyd, A. Yariv, and Y. Shevy, "Amplitude noise reduction in semiconductor lasers with weak, dispersive optical feedback," *Opt. Lett.*, vol. 19, pp. 1331–1333, 1994.

[9] H. Haug, "Quantum-mechanical rate equations for semiconductor lasers," *Phys. Rev.*, vol. 184, pp. 338–348, 1969.

[10] Y. Yamamoto, S. Machida, and O. Nilsson, "Amplitude squeezing in a pump-noise-suppressed laser oscillator," *Phys. Rev. A*, vol. 34, pp. 4025–4042, 1986.

[11] A. Karlsson and G. Björk, "Use of quantum-noise correlation for noise reduction in semiconductor lasers," *Phys. Rev. A*, vol. 44, pp. 7669–7683, 1991.

[12] J. Kitching, A. Yariv, and Y. Shevy, "Room temperature generation of amplitude squeezed light from a semiconductor laser with weak optical feedback," *Phys. Rev. Lett.*, vol. 74, pp. 3372–3375, 1995.

[13] C. E. Wieman and L. Hollberg, "Using diode lasers for atomic physics," *Rev. Sci. Instrum.*, vol. 62, pp. 1–20, 1991.

[14] A. S. Zibrov, R. W. Fox, R. Ellingsen, C. S. Weimer, V. L. Velichansky, G. M. Tino, and L. Hollberg, "High-resolution diode-laser spectroscopy of calcium," *Appl. Phys. B*, vol. 59, pp. 327–331, 1994.

[15] M. T. Jaekel and S. Reynaud, "Quantum limits in interferometric measurements," *Europhys. Lett.*, vol. 13, pp. 301–306, 1990.

[16] B. E. A. Saleh and M. C. Teich, "Information transmission with photon-number-squeezed light," *Proc. IEEE*, vol. 80, pp. 451–460, 1992.

[17] J. G. Rarity and P. R. Tapster, "Quantum communications," *Appl. Phys. B*, vol. 55, pp. 298–303, 1992.

[18] M. Ohtsu, K. Nakagawa, M. Kourogi, and W. Wang, "Frequency control of semiconductor lasers," *J. Appl. Phys.*, vol. 73, pp. R1–R17, 1993.

[19] M. Kourogi, C. Shin, and M. Ohtsu, "A 250 Hz spectral linewidth 1.5 μm MQW-DFB laser diode with negative-electrical-feedback," *IEEE Phot. Tech. Lett.*, vol. 3, pp. 496–498, 1991.

[20] C. Shin and M. Ohtsu, "Stable semiconductor laser with a 7-Hz linewidth by an optical-electrical double-feedback technique," *Opt. Lett.*, vol. 15, pp. 1455–1457, 1990.

[21] A. Yariv, *Optical Electronics.* Philadelphia: Saunders College Pub., 4 ed., 1991.

[22] A. Yariv, *Quantum Electronics.* New York: John Wiley and Sons, 3 ed., 1989.

[23] M. W. Fleming and A. Mooradian, "Fundamental line broadening of single-mode (GaAl)As diode lasers," *Appl. Phys. Lett.*, vol. 38, pp. 511–513, 1981.

[24] M. Lax, "Classical noise V. Noise in self-sustained oscillators," *Phys. Rev.*, vol. 160, pp. 290–307, 1967.

[25] H. Haug and H. Haken, "Theory of noise in semiconductor laser emission," *Z. Phys.*, vol. 204, pp. 262–275, 1967.

[26] C. Harder, K. Vahala, and A. Yariv, "Measurement of the linewidth enhancement factor α of semiconductor lasers," *Appl. Phys. Lett.*, vol. 42, pp. 328–330, 1983.

[27] N. Ogasawara, R. Ito, and R. Morita, "Linewidth enhancement factor in GaAs/AlGaAs multi-quantum-well lasers," *Jap. J. Appl. Phys.*, vol. 24, pp. L519–L521, 1985.

[28] J. Kitching, Y. Shevy, and A. Yariv, "Quantum mechanical analysis of amplitude and phase noise in a semiconductor laser with optical feedback," 1995. To be published.

[29] S. Saito and Y. Yamamoto, "Direct observation of Lorentzian lineshape of semiconductor laser and linewidth reduction with external grating feedback," *Electron. Lett.*, vol. 17, pp. 325–327, 1981.

[30] R. Wyatt and W. J. Devlin, "10 kHz linewidth 1.5 μm InGaAsP external cavity laser with 55 nm tuning range," *Electron. Lett.*, vol. 19, pp. 110–112, 1983.

[31] E. Patzak, A. Sugimura, S. Saito, T. Mukai, and H. Olesen, "Semiconductor laser linewidth in optical feedback configurations," *Electron. Lett.*, vol. 19, pp. 1026–1027, 1983.

[32] R. Lang and K. Kobayashi, "External optical feedback effects on semiconductor injection laser properties," *IEEE J. Quantum Electron.*, vol. QE-16, pp. 347–355, 1980.

[33] E. Patzak, H. Olesen, A. Sugimura, S. Saito, and T. Mukai, "Spectral linewidth reduction in semiconductor lasers by an external cavity with weak optical feedback," *Electron. Lett.*, vol. 19, pp. 938–940, 1983.

[34] K. Vahala and A. Yariv, "Detuned loading in coupled cavity semiconductor lasers — Effect on quantum noise and dynamics," *Appl. Phys. Lett.*, vol. 45, pp. 501–503, 1984.

[35] P. Spano, S. Piazzolla, and M. Tamburrini, "Theory of noise in semiconductor lasers in the presence of optical feedback," *IEEE J. Quantum Electron.*, vol. QE-20, pp. 350–357, 1984.

[36] H. Li and N. B. Abraham, "Analysis of the noise spectra of a laser diode with optical feedback from a high-finesse resonator," *IEEE J. Quantum Electron.*, vol. 25, pp. 1782–1793, 1989.

[37] D. R. Hjelme, A. R. Mickelson, and R. G. Beausoleil, "Semiconductor laser stabilization by external optical feedback," *IEEE J. Quantum Electron.*, vol. 27, pp. 352–372, 1991.

[38] G. P. Agrawal, "Line narrowing in a single-mode injection laser due to external optical feedback," *IEEE J. Quantum Electron.*, vol. QE-20, pp. 468–471, 1984.

[39] E. M. Belenov, V. L. Velichanskiĭ, A. S. Zibrov, G. T. Pak, T. V. Petrakova, N. V. Senkov, V. A. Sautenkov, A. V. Uskov, and A. K. Chernyshev, "Spectral characteristics of an injection laser with an intracavity absorbtion cell," *Sov. J. Quantum Electron.*, vol. 18, pp. 1076–1080, 1989.

[40] D. R. Hjelme and A. R. Mickelson, "On the theory of external cavity operated single-mode semiconductor lasers," *IEEE J. Quantum Electron.*, vol. QE-23, pp. 1000–1004, 1987.

[41] J. M. Iannelli, Y. Shevy, J. Kitching, and A. Yariv, "Linewidth reduction and frequency stabilization of semiconductor lasers using dispersive losses in an atomic vapor," *IEEE J. Quantum Electron.*, vol. 29, pp. 1253–1261, 1993.

[42] F. Favre, D. L. Guen, and J. C. Simon, "Optical feedback effects upon laser diode oscillation field spectrum," *IEEE J. Quantum Electron.*, vol. QE-18, pp. 1712–1717, 1982.

[43] W. D. Lee and J. C. Campbell, "Narrow-linewidth frequency stabilized $Al_xGa_{1-x}As/GaAs$ laser," *Appl. Phys. Lett.*, vol. 60, pp. 1544–1546, 1992.

[44] W. D. Lee, J. C. Campbell, R. J. Brecha, and H. J. Kimble, "Frequency stabilization of an external-cavity diode laser," *Appl. Phys. Lett.*, vol. 57, pp. 2181–2183, 1990.

[45] N. Cyr and M. Têtu, "Solitary resonance in the velocity-selective magnetic-optical activity spectrum of the Rb^{87} D_2 line," *Opt. Lett.*, vol. 16, pp. 946–948, 1991.

[46] J. Menders, K. Benson, S. H. Bloom, C. S. Liu, and E. Korevaar, "Ultranarrow line filtering using a Cs Faraday filter at 852 nm," *Opt. Lett.*, vol. 16, pp. 846–848, 1991.

[47] Z. D. Liu, D. Bloch, and M. Ducloy, "Absolute active frequency locking of a diode laser with optical feedback generated by Doppler-free collinear polarization spectroscopy," *Appl. Phys. Lett.*, vol. 65, pp. 274–276, 1994.

[48] J. Iannelli, *Coherence and spectral properties of composite-cavity semiconductor lasers.* Ph.D. thesis, California Institute of Technology, 1995.

[49] P. Laurent, A. Clairon, and C. Bréant, "Frequency noise analysis of optically self-locked diode lasers," *IEEE J. Quantum Electron.*, vol. 25, pp. 1131–1142, 1989.

[50] C. M. Van Vliet, "A survey of results and future prospects on quantum 1/f noise and 1/f noise in general," *Solid State Elec.*, vol. 34, pp. 1–21, 1991.

[51] M. S. Keshner, "1/f noise," *Proc. IEEE*, vol. 70, pp. 212–218, 1982.

[52] F. N. Hooge, T. G. M. Kleinpenning, and L. K. J. Vandamme, "Experimental studies on 1/f noise," *Rep. Prog. Phys.*, vol. 44, pp. 479–532, 1981.

[53] M. P. van Exter, S. J. M. Kuppens, and J. P. Woerdman, "Excess phase noise in self-heterodyne detection," *IEEE J. Quantum Electron.*, vol. 28, pp. 580–584, 1992.

[54] R. J. Lang, K. J. Vahala, and A. Yariv, "The effect of spatially dependent temperature and carrier fluctuations on noise in semiconductor lasers," *IEEE J. Quantum Electron.*, vol. QE-21, pp. 443–451, 1985.

[55] H. E. Rowe, *Signals and Noise in Communication Systems.* Princeton: D. van Nostrand, 1965.

[56] K. Petermann, *Laser diode modulation and noise.* Boston: Kluwer Academic, 1991.

[57] L. B. Mercer, "1/f frequency noise effects on self-heterodyne linewidth measurements," *J. Lightwave Technol.*, vol. 9, pp. 485–493, 1991.

[58] D. Halford, "Infra-red microwave frequency synthesis design: some relevant conceptual noise aspects," in *Proc. Frequency Standards and Metrology Seminar*, (Canada), pp. 431–466, 1971.

[59] R. V. Pound, "Electronic frequency stabilization of microwave oscillators," *Rev. Sci. Instrum.*, vol. 17, pp. 490–505, 1946.

[60] R. W. P. Drever, J. L. Hall, F. V. Kowalski, J. Hough, G. M. Ford, A. J. Munley, and H. Ward, "Laser phase and frequency stabilization using an optical resonator," *Appl. Phys. B*, vol. 31, pp. 97–105, 1983.

[61] L. Hollberg and M. Ohtsu, "Modulatable narrow-linewidth semiconductor lasers," *Appl. Phys. Lett.*, vol. 53, pp. 944–946, 1988.

[62] D. W. Allen, "Statistics of atomic frequency standards," *Proc. IEEE*, vol. 54, pp. 221–230, 1966.

[63] J. A. Barnes, A. R. Chi, L. S. Cutler, D. J. Healey, D. B. Leeson, T. E. McGunigal, J. A. Mullen, Jr, W. L. Smith, R. L. Sydnor, R. F. C. Vessot, and G. M. R. Winkler, "Characterization of frequency stability," *IEEE Trans. Instrum. Meas.*, vol. IM-20, pp. 105–120, 1971.

[64] B. E. A. Saleh and M. C. Teich, *Fundamentals of Photonics.* New York: John Wiley & Sons, 1991.

[65] K. Nakagawa, K. Kourogi, and M. Ohtsu, "Frequency noise reduction of a diode laser by using the FM sideband technique," *Opt. Lett.*, vol. 17, pp. 934–936, 1992.

[66] H. Hori, Y. Kitayama, M. Kitano, T. Yabuzaki, and T. Ogawa, "Frequency stabilization of GaAlAs laser using a Doppler-free spectrum of the Cs-D_2 line," *IEEE J. Quantum Electron.*, vol. QE-19, pp. 169–175, 1983.

[67] T. M. Shay and Y. C. Chung, "400 Hz frequency stability of a GaAlAs laser frequency locked to the Rb (D_2) line," *Opt. Eng.*, vol. 29, pp. 681–683, 1990.

[68] M. Ohtsu, M. Murata, and M. Kourogi, "FM noise reduction and subkilohertz linewidth of an AlGaAs laser by negative electrical feedback," *IEEE J. Quantum Electron.*, vol. 26, pp. 231–241, 1990.

[69] D. F. Walls, "Squeezed states of light," *Nature*, vol. 306, pp. 141–146, 1983.

[70] R. E. Slusher, L. W. Hollberg, B. Yurke, J. C. Mertz, and J. F. Valley, "Observation of squeezed states generated by four-wave mixing in an optical cavity," *Phys. Rev. Lett.*, vol. 55, pp. 2409–2412, 1985.

[71] R. M. Shelby, M. D. Levenson, S. H. Perlmutter, R. G. DeVoe, and D. F. Walls, "Broad-band parametric deamplification of quantum noise in an optical fiber," *Phys. Rev. Lett.*, vol. 57, pp. 691–694, 1986.

[72] L. Wu, H. J. Kimble, J. L. Hall, and H. Wu, "Generation of squeezed states by parametric down conversion," *Phys. Rev. Lett.*, vol. 57, pp. 2520–2523, 1986.

[73] E. S. Polzik, J. Carri, and H. J. Kimble, "Spectroscopy with squeezed light," *Phys. Rev. Lett.*, vol. 68, pp. 3020–3023, 1992.

[74] S. Kasapi, S. Lathi, and Y. Yamamoto, "Subshot noise FM spectroscopy with an amplitude squeezed diode laser at room temperature," in *Laser frequency stabi-*

lization and noise reduction, SPIE proceedings 2378, (Y. Shevy, ed.), pp. 108–115, February 1995.

[75] S. Inoue, G. G. Björk, and Y. Yamamoto, "Subshot noise interferometry with amplitude squeezed light from a semiconductor laser," in *Laser frequency stabilization and noise reduction, SPIE proceedings 2378*, (Y. Shevy, ed.), pp. 99–106, February 1995.

[76] Y. Yamamoto and S. Machida, "High-impedance suppression of pump fluctuation and amplitude squeezing in semiconductor lasers," *Phys. Rev. A*, vol. 35, pp. 5114–5130, 1987.

[77] G. P. Agrawal and N. K. Dutta, *Long-wavelength semiconductor lasers.* New York: Van Nostrand Reinhold, 1986.

[78] H. Haken, *Laser Theory.* Berlin; New York: Springer-Verlag, 1984.

[79] D. E. McCumber, "Intensity fluctuations in the output of cw laser oscillators. I," *Phys. Rev.*, vol. 141, pp. 306–322, 1966.

[80] M. Lax, "Quantum noise VII: the rate equations and amplitude noise in lasers," *IEEE J. Quantum Electron.*, vol. QE-3, pp. 37–46, 1967.

[81] B. Tromborg, H. E. Lassen, and H. Olesen, "Traveling wave analysis of semiconductor lasers: modulation responses, mode stability and quantum mechanical treatment of noise spectra," *IEEE J. Quantum Electron.*, vol. 30, pp. 939–956, 1994.

[82] M. Lax and W. H. Louiselle, "Quantum noise IX: quantum Fokker-Planck solution for laser noise," *IEEE J. Quantum Electron.*, vol. QE-3, pp. 47–58, 1967.

[83] L. Susskind and J. Glogower, "Quantum mechanical phase and time operator," *Physics*, vol. 1, pp. 49–61, 1964.

[84] P. Carruthers and M. M. Nieto, "Phase and angle variables in quantum mechanics," *Rev. Mod. Phys.*, vol. 40, pp. 411–440, 1968.

[85] M. Sargent III, M. O. Scully, and W. E. Lamb, Jr., *Laser Physics.* Reading, Massachusetts: Addison-Wesley, 1974.

[86] S. Machida and Y. Yamamoto, "Ultrabroadband amplitude squeezing in a semiconductor laser," *Phys. Rev. Lett.*, vol. 60, pp. 792–794, 1988.

[87] S. Machida, Y. Yamamoto, and Y. Itaya, "Observation of amplitude squeezing in a constant-current–driven semiconductor laser," *Phys. Rev. Lett.*, vol. 58, pp. 1000–1003, 1987.

[88] S. Machida and Y. Yamamoto, "Observation of amplitude squeezing from semiconductor lasers by balanced direct detectors with a delay line," *Opt. Lett.*, vol. 14, pp. 1045–1047, 1989.

[89] W. H. Richardson and R. M. Shelby, "Nonclassical light from a semiconductor laser operating at 4 K," *Phys. Rev. Lett.*, vol. 64, pp. 400–403, 1990.

[90] W. H. Richardson, S. Machida, and Y. Yamamoto, "Squeezed photon-number noise and sub-Poissonian electrical partition noise in a semiconductor laser," *Phys. Rev. Lett.*, vol. 66, pp. 2867–2870, 1991.

[91] H. Bachor, P. Rottengatter, and C. M. Savage, "Correlation effects in light sources with high quantum efficiency," *Appl. Phys. B*, vol. 55, pp. 258–264, 1992.

[92] M. J. Freeman, H. Wang, D. G. Steel, R. Craig, and D. R. Scifres, "Amplitude-squeezed light from quantum-well lasers," *Opt. Lett.*, vol. 18, pp. 379–381, 1993.

[93] H. Wang, M. J. Freeman, and D. G. Steel, "Squeezed light from injection-locked quantum-well lasers," *Phys. Rev. Lett.*, vol. 71, pp. 3951–3954, 1993.

[94] M. J. Freeman, H. Wang, D. G. Steel, R. Craig, and D. R. Scifres, "Wavelength-tunable amplitude-squeezed light from a room-temperature quantum-well laser," *Opt. Lett.*, vol. 18, pp. 2141–2143, 1993.

[95] M. J. Freeman, D. C. Kilper, D. G. Steel, R. Craig, and D. R. Scifres, "Room-temperature amplitude-squeezed light from an injection-locked quantum-well laser with a time-varying drive current," *Opt. Lett.*, vol. 20, pp. 183–185, 1995.

[96] P. R. Tapster, J. G. Rarity, and J. S. Satchell, "Generation of sub-Poissonian light by high-efficiency light-emitting diodes," *Europhys. Lett.*, vol. 4, pp. 293–299, 1987.

[97] P. J. Edwards and G. H. Pollard, "Quantum noise-correlated operation of electrically coupled semiconductor light emitters," *Phys. Rev. Lett.*, vol. 69, pp. 1757–1760, 1992.

[98] S. Machida and Y. Yamamoto, "Quantum-limited operation of balanced mixer homodyne and heterodyne receivers," *IEEE J. Quantum Electron.*, vol. QE-22, pp. 617–624, 1986.

[99] Y. Yamamoto and H. A. Haus, "Effect of electrical partition noise on squeezing in semiconductor lasers," *Phys. Rev. A*, vol. 45, pp. 6596–6604, 1992.

[100] A. P. Bogatov, P. G. Eliseev, and B. N. Sverdlov, "Anomalous interaction of spectral modes in a semiconductor laser," *IEEE J. Quantum Electron.*, vol. QE-11, pp. 510–515, 1975.

[101] C. B. Su, J. Schlafer, and R. B. Lauer, "Explanation of low-frequency relative intensity noise in semiconductor lasers," *Appl. Phys. Lett.*, vol. 57, pp. 849–851, 1990.

[102] M. A. Newkirk and K. J. Vahala, "Amplitude-phase decorrelation: a method for reducing intensity noise in semiconductor lasers," *IEEE J. Quantum Electron.*, vol. 27, pp. 13–22, 1991.

[103] R. Nabiev, Y. Popov, and A. Yariv, "Semiconductor laser with dispersive loss: quantum noises and amplitude squeezing," *J. Phys. III*, vol. 2, pp. 1605–1614, 1992.

[104] J. Kitching, Y. Shevy, and A. Yariv, "Quantum limits to amplitude-noise reduction in semiconductor lasers with weak optical feedback and dispersive loss," in *Proceedings of the annual meeting of the Optical Society of America*, Toronto, 1993. Presentation MH4.

[105] M. A. Newkirk and K. J. Vahala, "Large (14.5 dB) reduction of intensity noise from a semiconductor laser by amplitude-phase decorrelation," *Appl. Phys. Lett.*, vol. 60, pp. 1289–1291, 1992.

[106] G. Björk, A. Karlsson, and Y. Yamamoto, "Definition of a laser threshold," *Phys. Rev. A*, vol. 50, pp. 1675–1680, 1994.

[107] R. Serber and C. H. Townes, "Limits on electromagnetic amplification due to complimentarity," in *Symposium on Quantum Electronics*, pp. 233–255, New York: Columbia University Press, 1960.

[108] W. H. Louiselle, *Quantum statistical properties of radiation.* New York: Wiley, 1973.

[109] W. H. Richardson and Y. Yamamoto, "Quantum correlation between the junction-voltage fluctuation and the photon-number fluctuation in a semiconductor laser," *Phys. Rev. Lett.*, vol. 66, pp. 1963–1966, 1991.

[110] W. H. Richardson and Y. Yamamoto, "Quantum measurement of the photon number via the junction voltage in a semiconductor laser," *Phys. Rev. A*, vol. 44, pp. 7702–7716, 1991.

[111] K. G. Libbrecht and J. L. Hall, "A low-noise high-speed diode laser current controller," *Rev. Sci. Instrum.*, vol. 64, pp. 2133–2135, 1993.

[112] S. Inoue, H. Ohzu, S. Machida, and Y. Yamamoto, "Quantum correlation between longitudinal-mode intensities in a multimode squeezed semiconductor laser," *Phys. Rev. A*, vol. 46, pp. 2757–2765, 1992.

[113] A. E. Siegman, "Lasers without photons — or should it be lasers with too many photons?" *Appl. Phys. B*, vol. 60, pp. 247–257, 1995.

[114] K. Petermann, "Calculated spontaneous emission factor for double-heterostructure injection lasers with gain-induced waveguiding," *IEEE J. Quantum Electron.*, vol. QE-15, pp. 566–570, 1979.

[115] A. Yariv and A. Margalit, "On spontaneous emission into guided modes with curved wavefronts," *IEEE J. Quantum Electron.*, vol. QE-18, pp. 1831–1832, 1982.

[116] H. Ishikawa, M. Yano, and M. Takusagawa, "Mechanism of asymmetric longitudinal mode competition in InGaAsP/InP lasers," *Appl. Phys. Lett.*, vol. 40, pp. 553–555, 1982.

[117] X. L. Lu, C. B. Su, and R. B. Lauer, "Increase in laser RIN due to asymmetric nonlinear gain, fiber dispersion, and modulation," *IEEE Phot. Tech. Lett.*, vol. 4, pp. 774–777, 1992.